Small Signal Analysis of Nonlinear Systems with Periodic Operating Trajectories

by

James O. Groves, Jr.

Dissertation submitted to the Faculty of the
Virginia Polytechnic Institute and State University
in partial fulfillment of the requirements for the degree of
Doctor of Philosophy
in
Electrical Engineering

APPROVED:

Fred C. Lee
Fred C. Lee, Chairman

Borojevic
Dusan Borojevic

William T. Baumann
William T. Baumann

Dan Chen
Dan Y. Chen

John W. Layman
John W. Layman

April, 1995

Blacksburg, Virginia

Key words: Small-Signal, Harmonic-balance, power supply, Analysis, Controls

SMALL SIGNAL ANALYSIS OF NONLINEAR SYSTEMS WITH PERIODIC OPERATING TRAJECTORIES

by

James O. Groves

Fred C. Lee, Chairman

Electrical Engineering

(ABSTRACT)

A new method for small-signal analysis of switching power converters is developed and implemented in a computer program. The method is derived for systems where the nonlinearities can be described by elements that can take on one of two values, based upon a controlling variable. Another requirement is that the system be periodic.

The method is shown by examples to be very accurate, even at high frequencies. It predicts the subharmonic oscillation that can occur in converters with constant-frequency current-mode control. It is implemented using the COSMIR program to solve for the state equations and for steady-state, making a general power supply simulation program.

To Judy, Matt, Todd, and Lauren

Acknowledgements

I would like to thank my advisor, Dr. Fred C. Lee, for his continued support, encouragement, and patience since I have been at Virginia Polytechnic Institute and State University. The two years I spent on campus were the most enjoyable years of my career so far. His patience as I have tried to balance my personal life, my full-time job, and my research has been extraordinary. I have also enjoyed the relationships and friendships of the students of the Virginia Power Electronics Center.

I would like to thank my other committee members, Dr. Dusan Borojevic, Dr. Dan Chen, Dr. William T. Baumann, and Dr. John W. Layman for their comments and suggestions. I would also like to thank Dr. Bo Cho and Dr. Vatché Vorpérian for their comments as past committee members. Tammy Hiner and Loretta Estes provided invaluable help in administrative support, as well as encouragement.

I would also like to thank my colleagues at Celestica and IBM for their continued support and encouragement. Bob Huljak deserves special thanks for his belief in me, and for his sponsoring my leave under the IBM Resident Study Program. Danny Lee deserves thanks for continuing the support of this work. My managers over the last several years deserve recognition for their support: Bill Hemena, Randy Byzet, and Terry Lahr.

I thank the Coleman Housegroup at Dayspring in Blacksburg for their continued prayers and

support. I also thank the Friday night Bible study at the Lord Hill Church in New York for their prayers and support. I also need to thank Don and Lynnie Wilson, Jim and Susan Adams, Dave and Judy Coonce, and Wayne and Betty Coleman.

My family has been wonderful in their support and patience during this time. I thank my very special wife, Judy, and my children, Matt, Todd, and Lauren, for their love and patience, even when it seemed all I ever did was to sit upstairs at the computer.

I also need to thank my mother and stepfather, Nila and Howard Johnson, for their support over the years. My wifes' parents, Jim and Eunice Heise, also deserve thanks for their support.

Most importantly, I thank my God for giving me all that I have.

Contents

Figures

Tables

1.0 Introduction

This work describes a new approach for modelling small-signal transfer functions of a switching power electronics system. The motivation for this work was to have a general-purpose small-signal method which could be implemented as part of a general-purpose power electronics simulation package, with as few restrictions as possible on the circuits to be analyzed. The goal for this method is to have a complete tool set that can be used in a business environment.

The approach taken is to pose the small-signal solution at a particular frequency as the steady-state time-domain solution of the original system under modulation by a small-signal stimulus. A small-signal harmonic-balance technique will be used to give computational efficiency as compared to a brute-force time-domain approach. This approach will compute only the modulation sidebands of the small-signal modulated system, and not the fundamental switching harmonics.

The new method is completely derived, and a program written that implements the new approach. The program works in conjunction with the COSMIR[1] program for switching power supply analysis.

1.1 DISSERTATION OUTLINE

In 2.0, "Small-Signal Measurement and Analysis," the reasons are explored for the need of a new approach. Several important measurements are discussed, including input impedance, output impedance, Audiosusceptibility, and loop-gain measurements. It is shown in this chapter that the small-signal analysis may need to be performed at frequencies exceeding one half the switching frequency, most importantly for measurements other than the loop-gain. The actual hardware measurement process is detailed, so that the relationship between the predicted and the measured response may be understood.

Also contained in 2.0, "Small-Signal Measurement and Analysis" is a discussion of the harmonic content of a switching power converter, both with and without small-signal modulation. It is observed that, in the absence of small-signal modulation, a switching power converter contains harmonics at integer multiples of the switching frequency. With modulation, the converter will still have harmonics at integer multiples of the switching frequency, plus the small-signal modulation will appear as sidebands above and below the switching frequency and its harmonics.

There is a discussion in 2.0, "Small-Signal Measurement and Analysis" concerning the difference between an analytical method and a simulation tool. The need that this new method fills is for a simulation tool that may be used when the circuit complexity may hinder an analytical method. Prior analysis and simulation methods are also covered in this chapter. Finally, all of the above is used to justify the need for a new method for small-signal analysis of switching power converters.

The new method is completely derived in 3.0, "The Derivation of the New Small-Signal Method." The piecewise-linear circuit description is discussed. The large-signal solution is briefly covered. Then, the large-signal solution will be set up as a harmonic balance problem. The large-signal harmonic balance will then be linearized to find the system of small-signal harmonic balance equations. Finally, a solution method for the system of equations wilbe covered.

Several examples using COSMIR and this new method are covered in 4.0, "Examples." In many cases, both predictions and measurements are directly compared.

Conclusions concerning this new method are discussed in 5.0, "Conclusions."

As the COSMIR tool was used, it was apparent that the input netlist syntax was unique. What was desired was a schematic capture front-end that would allow the data entry into simulation to be a schematic. There are many programs available to perform the schematic capture task, but the problem is that the automatic netlist generation is usually in a form compatible with Spice[2]. So, a new front-end program was written for COSMIR to replace the STAEQ program. This new STAEQ program is derived in Appendix C, "Creation of the State Space Matrices," and was written in Turbo Pascal[3].

A users' guide for the new version of STAEQ is in D.2, "Modified Spice2 Input Syntax for COSMIR." The command-line calling syntax for the new small-signal program, ACF, is covered in Appendix E, "The ACF Program User's Guide." The input and output files are also detailed here as well.

All of these programs, the new STAEQ, SIMU, and ACF, may be integrated together into a schematic capture environment to form a powerful working environment. This was done

with the OrCAD™ tool, and is discussed in Appendix F, "The ORCAD/STAEQ/SIMU/ACF Design Environment." Several examples of operation are covered here.

2.0 Small-Signal Measurement and Analysis

2.1 INTRODUCTION

In this chapter, the reasons are explored for the need of a new approach for small-signal analysis. Several important measurements are discussed, including input impedance, output impedance, Audiosusceptibility, and loop-gain measurements. It is shown in this chapter that the small-signal analysis may need to be performed at frequencies exceeding one half the switching frequency, most importantly for measurements other than the loop-gain. The actual hardware measurement process is detailed, so that the relationship between the predicted and the measured response may be understood.

Also contained in this chapter is a discussion of the harmonic content of a switching power converter, both with and without small-signal modulation. It is observed that, in the absence of small-signal modulation, a switching power converter will only contain harmonics at integer multiples of the switching frequency. With modulation, the converter will still have harmonics at integer multiples of the switching frequency, plus the small-signal modulation will appear as sidebands above and below the switching frequency and its harmonics.

There is a discussion in this chapter concerning the difference between an analytical method and a simulation tool. The need that this new method fills is for a simulation tool that may be used when the circuit complexity may hinder an analytical method. Prior analysis and simulation methods are also covered in this chapter. Finally, all of the above is used to justify the need for a new method for small-signal analysis of switching power converters.

2.2 IMPORTANT SMALL-SIGNAL MEASUREMENTS

In switching power converter design, it is necessary to measure several key performance quantities in order to verify the correct functioning of the power converter subsystem with the rest of the overall system. A switching power converter operates as an intermediate stage between an energy source and a load. In the most ideal case, a regulated-voltage power converter should appear to the load as an ideal voltage source with zero output impedance.

As an ideal voltage source, the power converter should isolate the load from any changes in the source supply The zero output impedance attribute indicates that the converter should not change its output voltage as the load current changes. However, this description is true only in an ideal case, and not in a practical converter. Converters do pass signals through from the source supply, as well as slightly changing the output voltage as a result of the output current changing.

DC-DC converters typically use a nominal source supply voltage of 24 to 60 Volts, with some converters fed by inputs as high as 300 to 400 Volts DC, while others are fed from inputs as low as 5 Volts DC. Depending on the application, there may be standards and specifications that determine additional waveforms that may be present on the source supply in addition to the nominal DC value. These waveforms on the input may pass through the power converter and show up on the output in some fashion, which may cause the converter to fail a specification of noise or ripple on the output. At worst-case, these waveforms may cause damage to the power converter or to the load.

It is desirable to predict the output response of the power converter to this additional signal on the input. A small-signal model may be adequate to predict the output response, so

long as the amplitudes of the circuit waveforms are sufficiently small enough so that additional nonlinearities in the circuit are not activated. If nonlinearities are activated, then the small-signal model is not valid and a large-signal transient simulation must be performed to predict the response.

DC-DC converters usually also have specified a transient load response. Certain loads, especially electro-mechanical type loads, have large transient contents. The converter is expected to maintain its regulation through the presence of these large transients. Again, so long as a nonlinearity is not activated somewhere in the power stage and control system, a small-signal model may be used to simulate the response to these transient loads.

Conventional AC-DC converters are really two converters connected together. The first stage is a simple rectifier-capacitor stage that peak detects the input sine wave and creates a bulk voltage of 180 to 360 Volts DC. This is followed with a DC-DC converter that converts the bulk voltage into the desired output voltage. The DC-DC converter must be designed to tolerate a great deal of input ripple voltage at multiples of the power line frequency.

A power converter may be modelled at a block diagram level by a simple two-port network Figure 2-1. From the perspective of making a power converter mimic an ideal battery, two measurements have great importance: the output impedance and the Audiosusceptibility[4] of the power converter. The output impedance, Z_o, is defined as:

$$Z_o = \frac{\Delta V_o}{\Delta I_o} \tag{2.1}$$

while the Audiosusceptibility, A_{io}, is defined as:

$$A_{io} = \frac{\Delta V_o}{\Delta V_i} \tag{2.2}$$

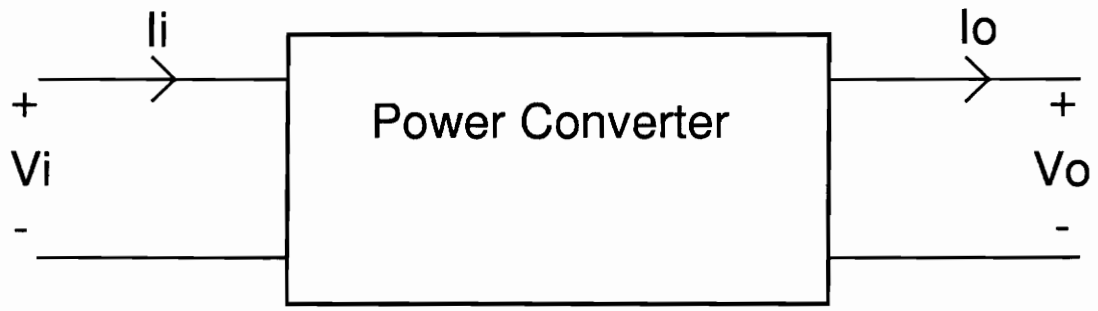

Figure 2-1. Power Converter Terminal Measurements

As can be seen from the definitions, the output impedance is a measure of how stable the output voltage is as the load current changes. The Audiosusceptibility is a measure of how much signal passes through the power converter from the input terminals to the output terminals. Ideally there should be absolutely no signal on the output terminals caused by signals on the input terminals.

The input impedance to the converter, Zi, may be defined as the ratio of the input voltage to the input current:

$$Z_i = \frac{\Delta V_i}{\Delta I_i} \tag{2.3}$$

The input impedance is not usually specified for power converters, but may be an important measurement to know to prevent interactions with the circuits that feed into the converter[5]. Since the input impedance is typically negative while the output impedance of the circuits that source the converter are positive, there is a possibility of instability if the impedances ever cancel each other out. This could happen if an input filter is connected to the input of the power converter. Instability could also arise when many power converters are fed from a single front-end supply.

There is an important measurement that is only directly measurable inside the power converter, and that is loop gain, or T. The loop gain is an important design parameter because it influences all other characteristics of the system, including the output impedance and the Audiosusceptibility. However, the loop gain should not be the prime focus of the design activity since it does not guarantee that the terminal characteristics will be sufficient enough for the power converter to perform well in the system. A high gain, wide-bandwidth loop gain does not necessarily translate to good performance in output impedance and Audiosusceptibility measurements.

2.3 THE CASE FOR A METHOD VALID PAST ONE-HALF f_s

It has been shown in [6] that a switching power converter may be considered a sampled data system, and as such it is meaningless to consider the loop gain at frequencies above one half the switching frequency. In fact, the sampled loop gain was shown to be a periodic function of frequency.

However, it is overly restrictive to limit measurements of output impedance and Audiosusceptibility to an upper limit of one half the switching frequency. It is unreasonable to expect that the load current or input noise will be band-limited.

Using a simulation method having restrictions on its accuracy to frequencies below one half the switching frequency is adequate for loop gain predictions, but is questionable for other measures. The results from such a modelling method can not be trusted at high frequencies.

Ideally what is needed is a method that has no restrictions on frequency, and that may be used freely to compute all quantities with no question.

2.4 SMALL-SIGNAL MEASUREMENT METHODS

It is important to look at small-signal simulation from the perspective of how it is to be measured and compared against. When a switching power converter is built in the lab and measurements are to be made, it is first powered up. The converter will go through large signal transients until it stabilizes out at a periodic steady state operating point.

Once in steady state, a network analyzer will usually be connected and measurements will be taken. The network analyzer is composed of an oscillator and vector voltmeter. The vector voltmeter has two inputs, each input having an internal tracking bandpass filter that tracks the oscillator frequency. The bandpass filter usually has a very narrow bandpass, typically 1 Hertz. The vector voltmeter will display the vector ratio of the two inputs. Thus, the network analyzer will provide a stimulus to a circuit under test, and measure the vector ratio of the frequency component of two signals at precisely the same frequency as the stimulus. This

allows a network analyzer to measure small signal quantities in the presence of very large operating waveforms.

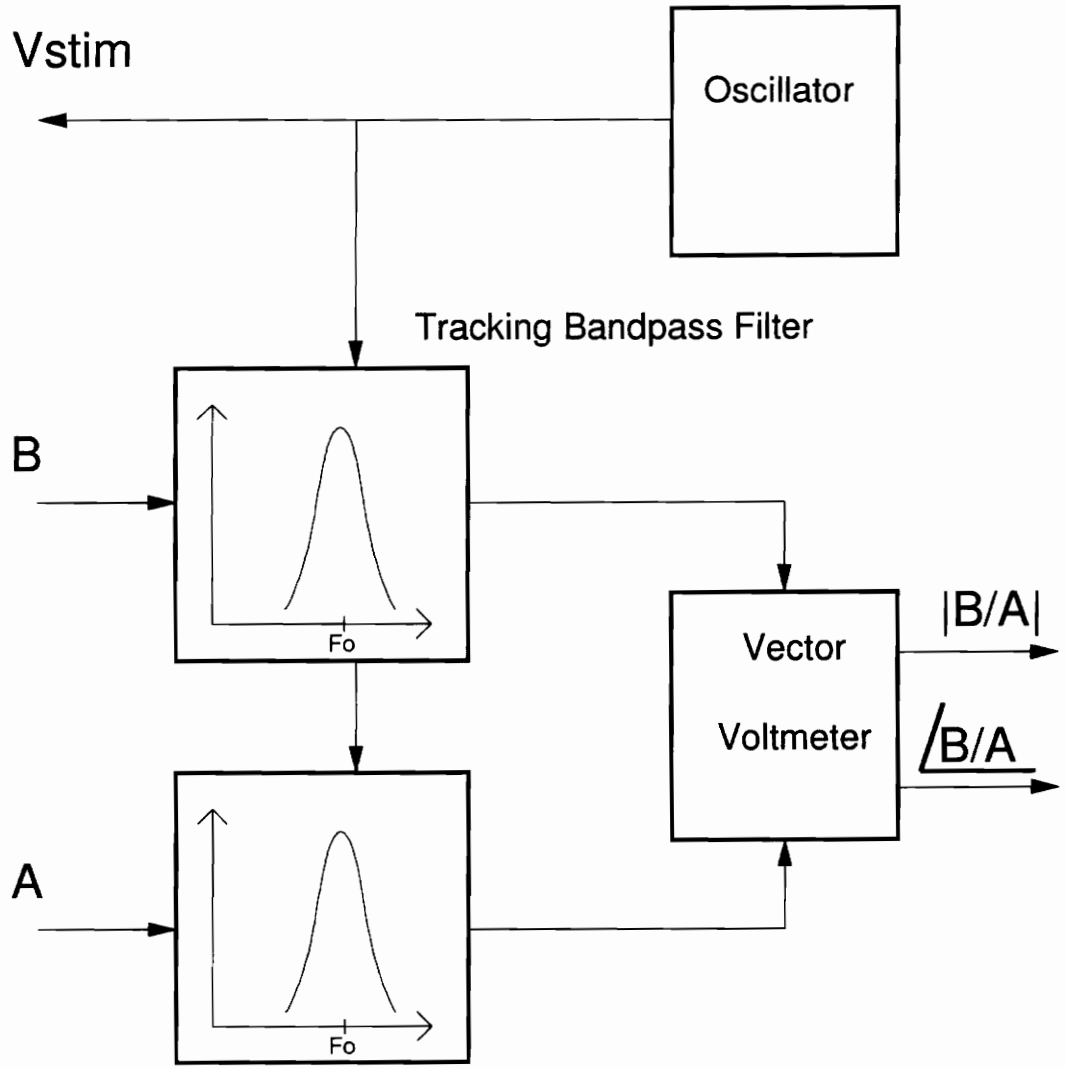

Figure 2-2. Network Analyzer Block Diagram

A sample application of a network analyzer would be the circuit in Figure 2-3. This is a simple RC lowpass filter. It is configured so that it is driven from Vstim, the output of the network analyzer of Figure 2-2. The A and B inputs to the network analyzer are connected at the points marked A and B. This would then give a display of the vector ratio B/A on the network analyzer.

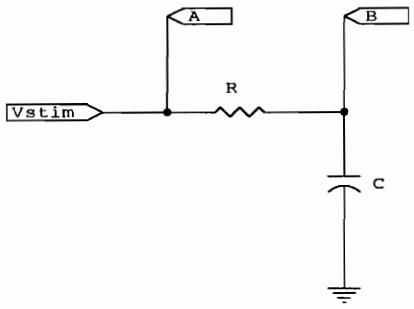

Figure 2-3. Network Analyzer Typical Application

The operating waveforms of a switching power converter have frequency components only at the switching frequency and its integer multiples. In an off-line power converter it is also common to have multiples of the power line frequency included along with the switching harmonics. At precisely these frequencies it is impossible for a small-signal measurement to be made, since the small signal will be overwhelmed by the large signal component. This occurrence shows up as a large discontinuity in the small signal response, typically a spike. Fortunately, since the bandwidth of the network analyzer tracking filters is

so narrow it is possible to get very close to the large signal harmonic frequencies without error. Also, a network analyzer doesn't take a continuous sweep of frequencies, but instead takes a discrete number of samples evenly spaced across the desired frequency range. Depending on the spacing of the samples and the bandwidth of the bandpass filter, it may be possible to miss all or most of the large signal harmonics in any arbitrary sweep.

2.5 EXAMPLE: THE HARMONIC CHARACTERISTICS OF A SIMPLE DC-DC CONVERTER

It is informative to take a look at waveforms and the related harmonic characteristics of a simple DC-DC converter. The converter chosen is a simple boost power stage operated in continuous inductor current mode. This converter is discussed in greater detail in the examples section.

This converter will first be simulated to find the periodic steady state waveforms and the harmonic characteristics. Then, a small-signal sinusoidal voltage will be injected into the circuit, and a new periodic steady state will be computed and the harmonic structure displayed.

The circuit to be simulated is detailed in Figure 2-4. The schematic for this circuit was captured using the OrCAD™ schematic capture package [7], and was simulated using the PSPICE™ simulation package[8], which includes the PROBE waveform analysis tool.

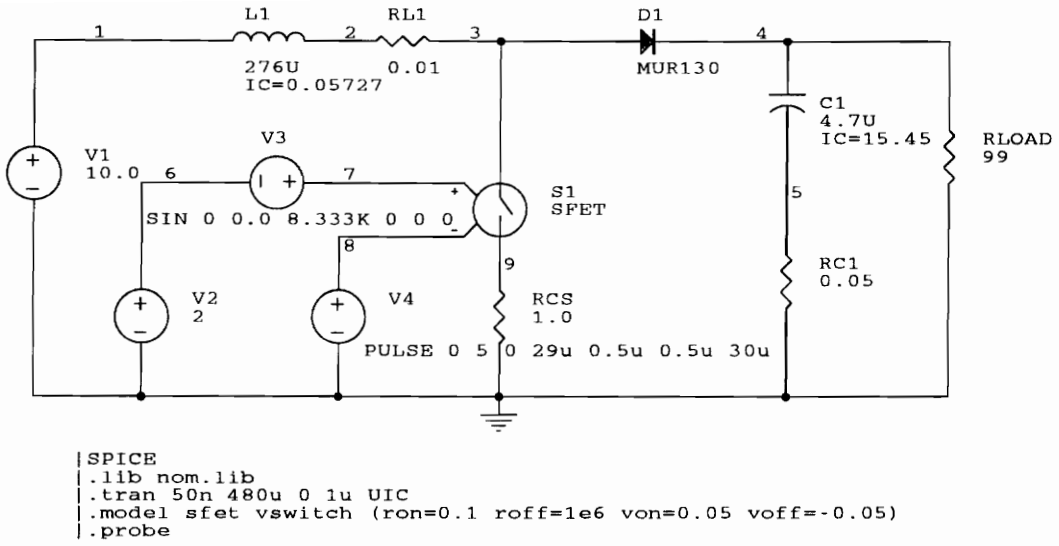

Figure 2-4. Schematic of a Simple Boost Converter

In this circuit, when the ideal switch, S1, turns on, current will build up in inductor L1 and its winding resistance, RL1. When S1 is turned off, current still flows in L1, the voltage at node 3 will increase until diode D1 turns on. The inductor current now charges up the output capacitor, C1, replacing the charge depleted by the current flowing out through the load resistor, R1.

The ideal switch, S1, is really a voltage-controlled resistor. In this case, if the controlling voltage exceeds 50 mV, the resistance of the switch is 0.1Ω. If the controlling voltage is more negative than -50 mV, the resistance of the switch changes to 1 MΩ.

Ignoring the voltage source V3 for the moment, the DC voltage source, V2, is compared against the ramp voltage generated by V4. This ramp is a voltage that linearly rises from 0 to

5V in 29us and then quickly resets back to zero, with a basic repetition rate of 30us. So, when the voltage of V2 is greater than V4, S1 is "on." Similarly, when V2 is less than V4, S1 is "off." These two voltage sources, with the ideal switch, S1, represents the action of a PWM and a power FET.

The floating voltage source, V3, is used to inject small-signal modulation into the circuit. It has a DC value of zero, and so does not effect the average value of the outputs. For this simulation, the amplitude of the small-signal is zero, and so this source has no effect. In the second simulation this source will be set to a nonzero value so as to study the operation of the circuit with the small-signal modulation.

The inductor and capacitor, L1 and C1, have been set up with initial conditions. This is used in conjunction with the UIC control word on the .tran statement so that the circuit will quickly arrive at steady-state. These values were arrived at after many lengthy iterations of simulation.

The netlist generated by the schematic is detailed below. This netlist is the input into the PSPICE™ program.

The inductor current, I(L1), and the output voltage, V(4), are plotted in Figure 2-6. Notice from the schematic that the output voltage, V(4), is composed of both the voltage across capacitor C1 as well as the voltage across the equivalent series resistor, RC1. The spikes in V(4) occur when the switch turns on and the diode, D1, turns off. The nonideal diode, D1, has a reverse recovery current associated with its turn-off, and this current shows up across RC1 as the voltage spike seen shortly after the peak of V(4).

```
* BOOSTAC
*
.LIB NOM.LIB
.TRAN 50N 480U 0 1U UIC
.MODEL SFET VSWITCH (RON=0.1 ROFF=1E6 VON=0.05 VOFF=-0.05)
.PROBE
RL1 2 3 0.01
RC1 5 0 0.05
RCS 9 0 1.0
V1 1 0 10.0
V2 6 0 2
L1 1 2 276U  IC=0.05727
C1 4 5 4.7U  IC=15.45
RLOAD 4 0 99
D1 3 4 MUR130
V4 8 0 PULSE 0 5 0 29U 0.5U 0.5U 30U
S1 3 9 7 8 SFET
V3 7 6 SIN 0 0.0 8.333K 0 0 0
.END
```

Figure 2-5. Simple Boost Converter Netlist

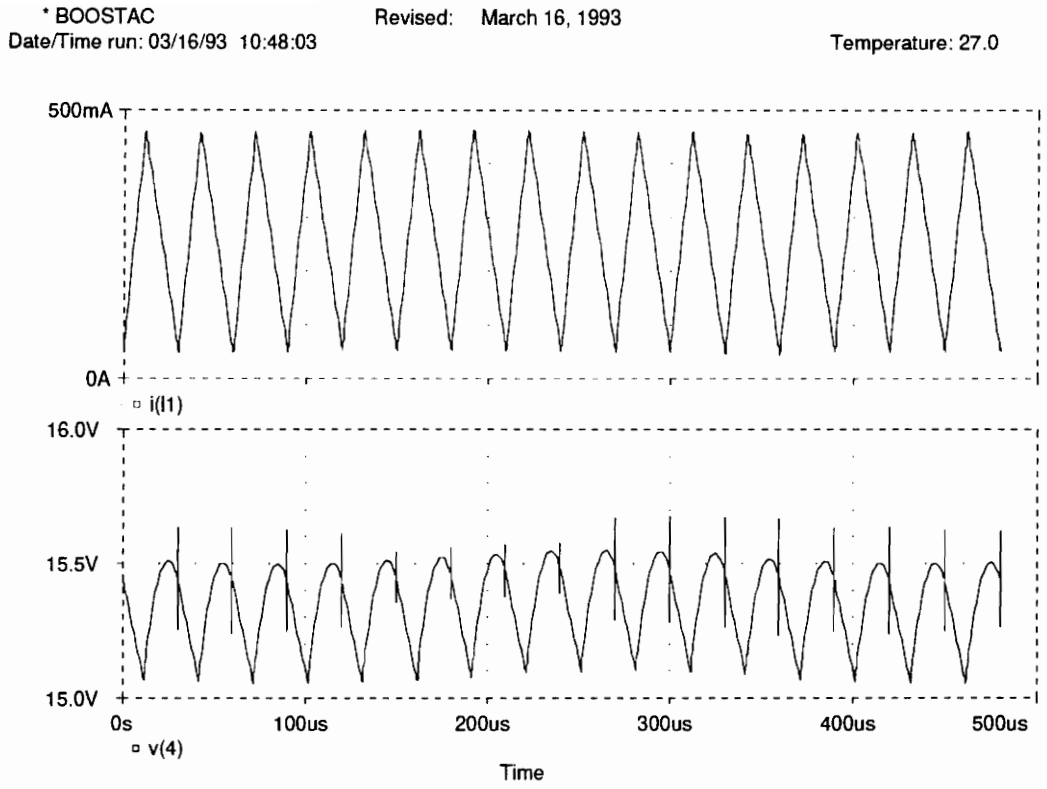

Figure 2-6. Steady-State Inductor Current and Output Voltage

The time-domain waveforms from Figure 2-6 were transformed into the frequency domain using the Fourier transform capabilities of the PROBE™ waveform analysis tool. Notice the strong components at the integer multiples of the switching frequency, 33KHz. The spikes in V(4) that were present in the time-domain plots will show up as very high frequency harmonics, but will not show up in Figure 2-7 since the frequency range has been limited to relatively low frequencies. There is a substantial noise floor caused by numerical

inaccuracies of the simulation. The plot is scaled logarithmically in the vertical axis, so the noise is really about 20-30dB below the main frequency components and thus may be ignored.

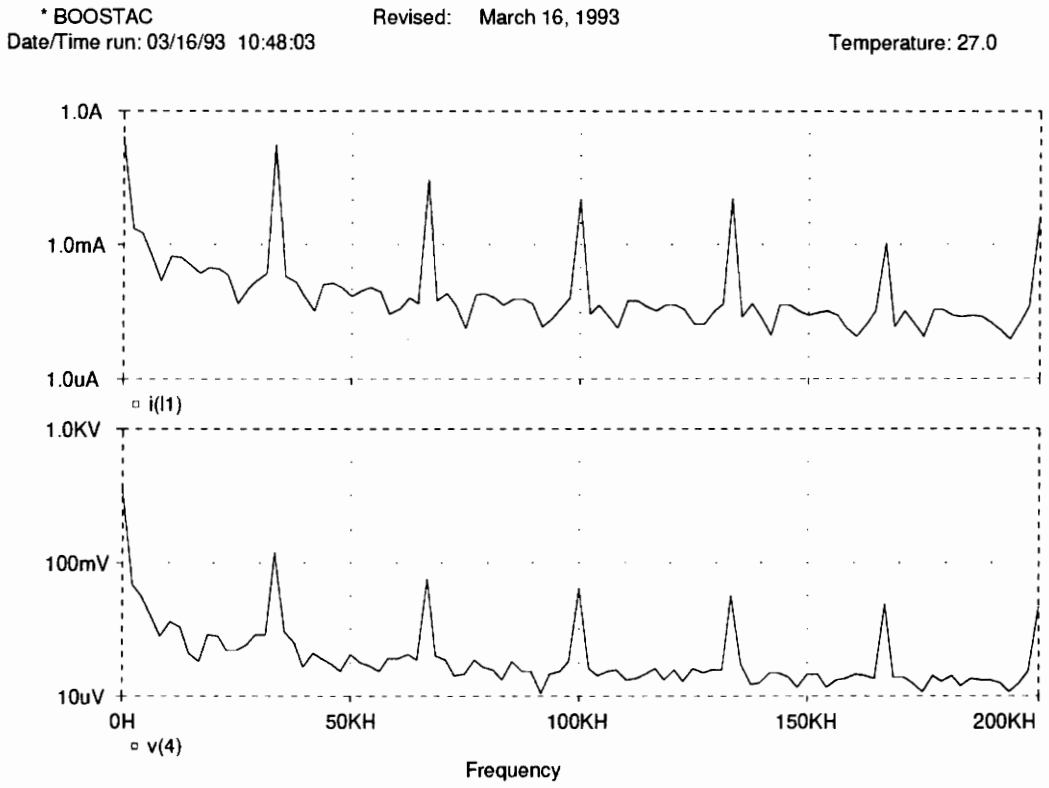

Figure 2-7. Inductor Current and Output Voltage - Frequency Domain

For the next simulation, the magnitude of the floating small-signal source, V3, was set to 0.1V. While this will not effect the average values of the inductor current or the output

capacitor, it does effect the initial conditions used for transient analysis. The addition of this AC small-signal component causes the circuit to settle out at a new periodic steady state operating trajectory that is close to the old steady state, but slightly different. The circuit was run repeatedly until the new steady state was found. The initial conditions were updated with the necessary values for the circuit to start off directly in steady state. The schematic is detailed in Figure 2-8.

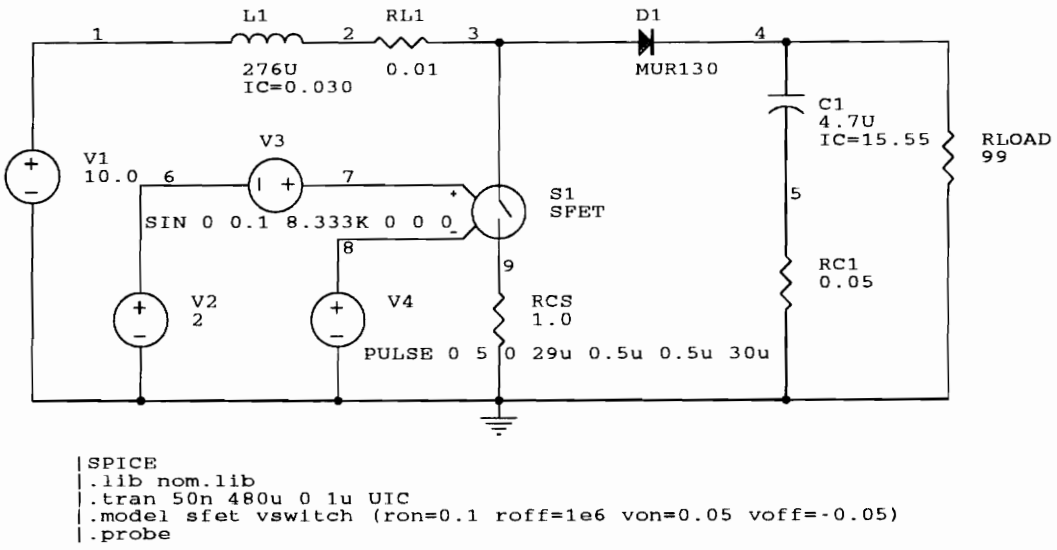

Figure 2-8. Simple Boost Converter Schematic - With Modulation

The inductor current, I(L1), and output voltage, V(4), are plotted in Figure 2-9. Notice how there is a low frequency ripple riding on the waveforms now. This is the frequency of the small-signal stimulus, which is at one-fourth the switching frequency, or about 8.33KHz. Judging from the waveform of V(4), the circuit is still not quite in steady state since every

fourth peak of the ripple should be at the same voltage level, and they're not. But it is close enough for the transformation into the frequency domain in Figure 2-10 where it shows up as a higher noise floor.

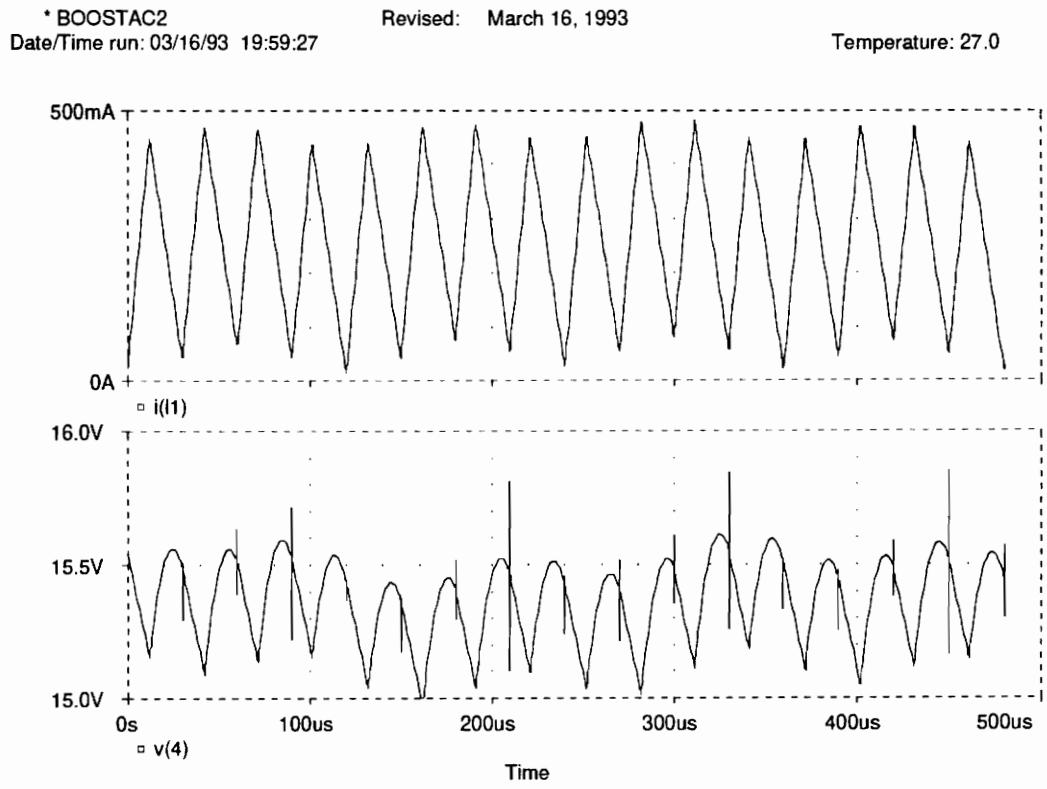

Figure 2-9. Steady-State Inductor Current and Output Voltage - With Modulation

Notice in Figure 2-10 that the strong harmonics of the basic switching frequency of 33KHz now have sidebands at plus and minus the frequency of the small-signal stimulus, which is 8.33KHz. If the small-signal response of this circuit were desired at this frequency,

the magnitude and phase of the desired waveforms would need to be selected at the same frequency as the stimulus, which in this case is 8.33KHz. This selection process is why a network analyzer requires a tracking bandpass filter. Otherwise, other frequency components would be included and invalidate the measurements.

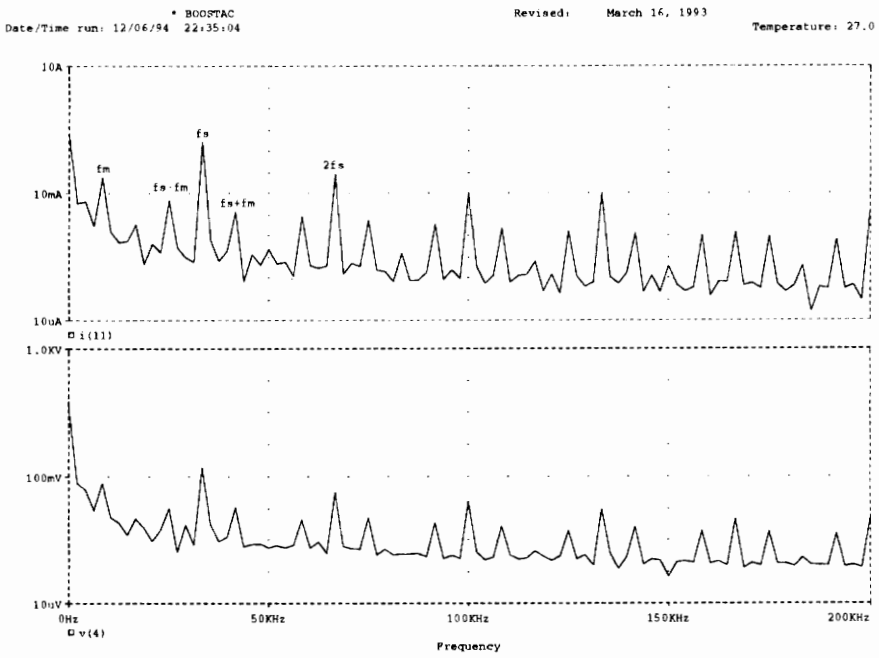

Figure 2-10. Inductor Current and Output Voltage - With Modulation - Frequency Domain

A time-domain approach like this for simulating the small-signal response of a circuit is obviously not a practical approach. The solution of a new steady state at each case of a stimulus frequency is computationally expensive and is quite interactive. The amount of time

necessary to perform a complete frequency sweep would be prohibitively large. This is because this simulator is a general purpose simulator, and uses no information from the original steady state solution, other than the initial conditions, to more quickly solve for new steady state solutions.

2.6 THE GOAL OF MODELLING AND ANALYSIS

Tools and methods that give analytical insight are strongly desired in any problem situation. It is this insight that allows a designer to design the circuit. Once the circuit is designed, it may then be built or simulated in order to verify that the design meets the design objectives.

Analytical methods usually, but not always, use some sort of approximations in their formulation so as to simplify the problem down to a level that is easily comprehended and managed. One general strategy in a circuit design is to "divide and conquer": to break the circuit up into smaller isolated blocks that are themselves easily analyzed. The whole system may then be synthesized out of many of these smaller blocks.

If the circuit is of sufficient complexity that it is not possible to split the circuit up into small, isolated blocks then analytical methods may not offer manageable insight into the circuit operation. An example of this situation is a second-order power stage combined with a second-order input filter and a second-order output filter where the impedances and natural frequencies are all comparable and interact with each other. In this case it may not be possible to split the circuit up into three second-order blocks, but instead the minimum representation may well be a sixth-order system. Analytical methods may not offer manageable insight into such systems.

In cases such as this, a practical recourse is to use simulation as a breadboard mechanism. This way, many component variations may be tried, without smoke or danger, and insight may be gained into the component interactions. This is not very elegant, but is a very practical method.

A parallel may be drawn here between switching power converter analysis and the analysis of simple transistor circuits. Many simple models exist for bipolar transistors[9], and the analysis of simple transistor circuits may easily be performed by hand using these models. Much design insight is given by these models. However, when many transistors are put together, hand analysis may become too laborious. In this case the method usually chosen is to simulate the circuit operation with a program like SPICE[2].

The point to be made here is that there is room for both analytical methods and simulation methods. Analytical methods are useful for many aspects of the design of power converter circuits. However, in practice there may be many parasitic elements that need to be included into the model, and the circuit may get large and complicated. In this case it may make sense to use a simulation approach.

2.7 PREVIOUS MODELLING AND ANALYSIS METHODS

In this section, the analysis of switching converters will be reviewed. Small-signal analysis of switching power converter circuits have generally either used averaging methods, sampled-data methods, or a combination of methods. All three will be discussed.

An averaging method was used in [10], and was given a name of "state-space averaging." In this approach, the switching elements, the diodes and transistors, were assumed to have ideal-switch characteristics. Moreover, a simple switching scheme was assumed, where the

transistor and diode alternated in "on" and "off" states. With this restriction, only two combinations were considered out of the four possible combinations of the two switches.

For an example of ideal switches, refer back to the schematic presented in Figure 2-4. If the Fet and diode are replaced with ideal switches, then the two simplified schematics of Figure 2-11 and Figure 2-12 will result.

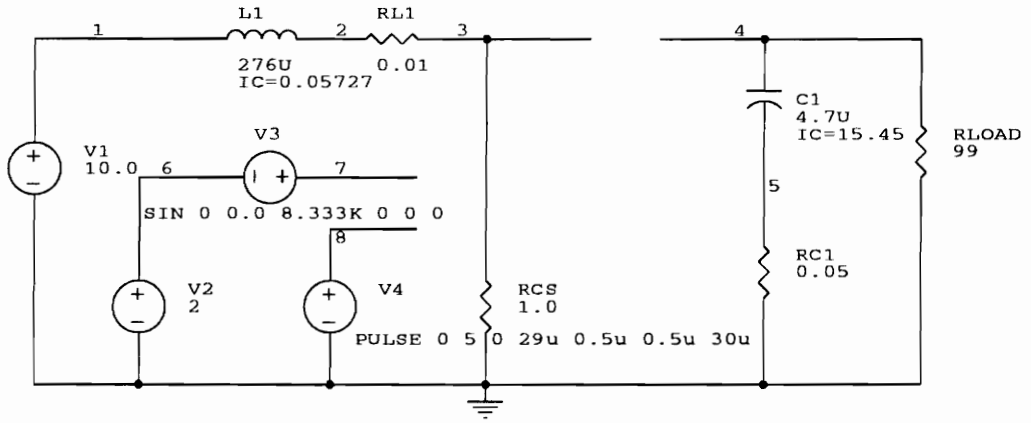

Figure 2-11. Simple Boost Converter - Fet On, Diode Off

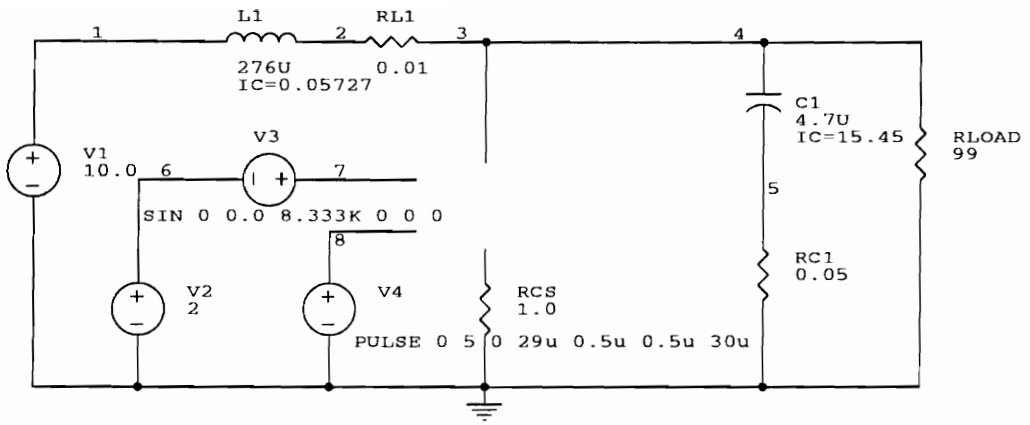

Figure 2-12. Simple Boost Converter - Fet Off, Diode On

In Figure 2-11, the Fet is turned on and the diode is turned off. The opposite is the case in Figure 2-12. In continuous-mode operation, the circuit will alternate between the two topologies. This will give two sets of state-space equations that describe the circuit operation: one for each topology.

$$\dot{x}(t) = a_1 x(t) + b_1 u(t) \tag{2.4a}$$

$$y(t) = c_1 x(t) + d_1 u(t) \tag{2.4b}$$

or

$$\dot{x}(t) = a_2 x(t) + b_2 u(t) \tag{2.5a}$$

$$y(t) = c_2x(t) + d_2u(t) \tag{2.5b}$$

If the system can be described by the first set of equations during the interval $0 < t < kT_s$, where $0 \leq k \leq 1$, and can be described by the second set of equations for the interval $kT_s < t < T_s$, then [10] showed that the small-signal response of the system could be described by:

$$\dot{\hat{x}} = A\hat{x} + B\hat{u} + \{(a_1 - a_2)\bar{x} + (b_1 - b_2)\bar{u}\}\hat{k} \tag{2.6a}$$

and

$$\hat{y} = C\hat{x} + D\hat{u}\{(c_1 - c_2)\bar{x} + (d_1 - d_2)\bar{u}\}\hat{k} \tag{2.6b}$$

where

$$A = ka_1 + (1 - k)a_2 \tag{2.6c}$$

$$B = kb_1 + (1 - k)b_2 \tag{2.6d}$$

$$C = kc_1 + (1 - k)c_2 \tag{2.6e}$$

$$E = ke_1 + (1 - k)e_2 \tag{2.6f}$$

The variables $\bar{x}$ and $\bar{u}$ are the time-averaged values of the state vector and the input vector. The variable k is considered to represent the duty-cycle of the converter. This is not a directly measurable variable in a real converter, but is simply a convenience for analysis.

When equation (2.6a) is transformed into the frequency domain, the result is:

$$(sI - A)\hat{X} = B\hat{U} + \{(a_1 - a_2)\bar{x} + (b_1 - b_2)\bar{u}\}\hat{K} \tag{2.7a}$$

$$\hat{Y} = C\hat{X} + D\hat{U}\{(c_1 - c_2)\bar{x} + (d_1 - d_2)\bar{u}\}\hat{K} \tag{2.7b}$$

To get this set of equations, the two sets of topologies from Figure 2-11 and Figure 2-12 were averaged together to give a single, continuous equation that describes the average behavior of the circuit. Then, this equation was perturbed and linearized to arrive at the small-signal model.

The approximations made to get this equation were a small-signal approximation, and a linear-ripple approximation. The small-signal approximation is fine, and has to be made. The linear-ripple approximation basically requires that the time constants of the LC components of the power stage be much longer than the period of one cycle of the converter. This is overly restrictive when resonant-type power supplies are to be analyzed.

As was pointed out in [11], a subtle error was created in the set-up of the problem. The problem was modelled so that the duty-cycle input, d, controlled the circuit in a continuous

manner instead of being sampled only at the instant of switching. This model is good at low frequencies, but is not adequate at frequencies approaching half the switching frequency. As was shown in [11, 12], this model fails to predict the possible instability at half the switching frequency in current-mode control converters.

Besides predicting possible oscillations at half the switching frequency, another reason to have such good accuracy at very high frequencies is that it ensures that there will be good accuracy at the one-half switching frequency point. Averaging methods may loose accuracy at frequencies well below the one-half switching frequency point. For example, consider Figure 2-13. This is the boost converter discussed later on in the examples section. The details of the circuit may be found there. It is a simple boost power stage, using simple pulse-width modulation. It is an open-loop measurement. The power stage was designed to have a higher resonant frequency than normal, so that the requirements for averaging would be stressed. Notice the large divergence in both magnitude and phase of the state-space averaging response at frequencies well below the one-half switching frequency point.

For simple transfer function measurements such as this, it is common practice to limit the frequency sweep to one-half the switching frequency. Another point Figure 2-13 makes is that it is informative to continue the sweep upwards. In this case, aliasing effects in the pulse-width modulator are causing the magnitude and phase to deviate from their expected behavior. If a designer did not understand this they might waste time looking for some unexpected and unexplained system poles.

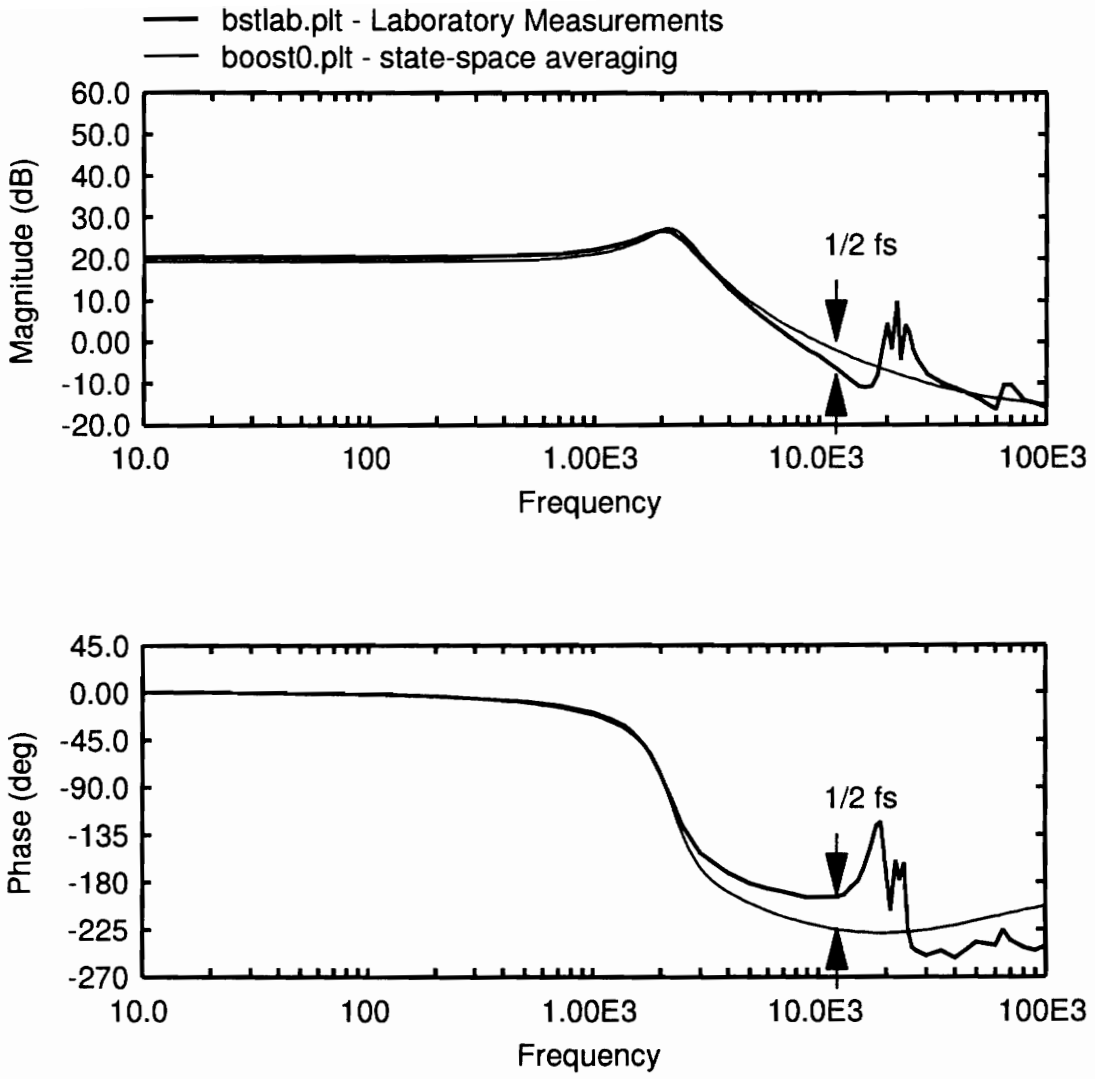

Figure 2-13. Comparison of averaging and real measurements.

In [13], the averaging method was extended to cover the case of discontinuous inductor current operation. In this case, three combinations of the two switches are considered. In this

mode of operation the inductor current stays fixed at zero for some portion of one cycle of operation. In [13], the small-signal response of the inductor current was constrained to be zero, based upon the fact that the large-signal current was zero for a portion of the cycle. When the small-signal inductor current is zero, the order of the system drops by one, and what was a second order system now becomes a first order system. This predicted a response that compared favorably at low frequencies with the observed response of a switching converter operating in the discontinuous conduction mode. The high-frequency response did not match up well, most especially in phase.

In [14], it was pointed out that what was really happening was that the damping of the second order system was increasing so much in discontinuous conduction mode that the complex pair of poles were separating, one going very low while one moves very high in frequency. A simple single-pole model does not accurately predict the response of the system, especially at higher frequencies, but the two-pole model does an adequate job.

The models presented in [10, 13] focused on creating a canonical circuit representation, and generated tables of coefficients for several converter topologies. If a slightly different topology needed to be analyzed, a complete model generation needed to be performed to solve for the coefficients for the canonical model. This was very good for creating an analytical understanding of the converter, but was not good for general purpose simulation.

The failure of the modeling method of [10] to predict the oscillations at half the switch frequency that were observed in current-mode converters led to a sampled-data approach for modelling the system[6, 11]. With this method, the converter system was modelled using the z-transform since the PWM modulator acts as a sampling mechanism. The identity $z = e^{sT}$ is used to map from the z-domain into the s-domain. This gives a loop-gain transfer function

that is a periodic function of frequency. As will be shown later in the examples section, measurements of actual hardware do not indicate such a periodicity of loop-gain transfer functions. However, this approach was the first to give a predictive model for the instability seen in current-mode converters.

Another problem with the method of [6, 11] was that it was not a simple method, nor were there general computer programs that would do all of the hard work. The method spawned many offshoots[12, 15-17], but did not see much general use by practicing design engineers.

One of the hybrid approaches that combined averaging and sampling was the modelling method of [18, 19]. In this approach the power stage was modelled using averaging techniques, but the output variables were created by sampling the average waveforms. This was most useful for loop-gain measurements where the waveform on the input of the PWM was not smooth, but was instead discontinuous. A very good warning was made in [19] about making loop-gain measurements in a system where the input to the PWM is discontinuous. This same problem was discovered in a buck converter and discussed in [20].

One of the restrictions in state-space averaging was the need for the time constants of the power stage to be much longer than the switching period. This was adequate for most PWM converters, but is not adequate for other types of converters, such as resonant or quasi-resonant converters. The averaging method was reexamined and reformulated in [21-25] and found to be adequate for many other types of circuits other than classical PWM circuits.

In a switching power converter, the only nonlinear elements are the switch, diode, and the modulator. The work of [14, 26, 27] gathered these nonlinear elements up into one multi-terminal block, a PWM switch model. The averaging approach was used to find a small-

signal model for this block so that conventional small-signal simulation programs, like Spice, could be used to simulate the small-signal response. In principle, this is similar to replacing a nonlinear model of a transistor with a small-signal one so that the small-signal response of a transistor amplifier might be computed. It is a very powerful approach. Both Continuous and Discontinuous models were created. The only difficulty with this approach is the necessity of manipulating the power converter circuit into a form where the multi-terminal block could be connected. This may be difficult to do in some topologies where the diode and switch are not directly connected together.

In [12], the PWM switch model of [14, 26, 27] was combined with a special simplification of the PWM modulator of [6, 11], thus giving a simple model that would correctly simulate and predict the possible oscillations at half the switching frequency in converters using current-mode control. The models given in [12] combined with the PSPICE™ program give design engineers a good set of tools for working with PWM control systems. Again, the only real problem is the necessity of manipulating the power circuit into a form where the PWM switch may be used. Also, the model is not self contained, but needs circuit parameters filled in as internal variables.

Besides the averaging and the sampled-data approach, there has been an approach based on Fourier analysis and time varying system theory[28]. This approach was derived, and an example was used of a boost converter. The correlation of measurement to prediction was excellent up to several times the switching frequency.

A variation on the sampled-data approach was taken in [16]. In this approach, the z-domain to s-domain transformation was performed using an equivalent hold function, instead of the identity $z = e^{sT}$. This gave good correlation with measurements, but the method

was too complicated for hand analysis, and it is not clear if it was ever implemented in a computer program. It is interesting to note that the author of [16] in a later paper was using a state-space averaging program[17] instead of this method.

2.8 THE NEED FOR A NEW MODELLING AND SIMULATION METHOD

After reviewing the methods for small-signal analysis it is apparent that there is a need for a general purpose small-signal analysis program that is based upon a method that gives good high-frequency response. Design engineers need tools that will take schematics as input, and allow rapid and accurate small-signal analysis so that the control-loop may be designed and verified. The number of assumptions and approximations needs to be minimized.

A brute-force method similar to what was used in an earlier example would be an ideal approach if the computations could be done much faster than is practical today. Simulating the small-signal response in the time-domain is very simple and attractive, and would have none of the restrictions that would prevent it from being a general purpose analysis tool. The problems with this approach is the interactivity needed to increment frequencies, the computation time necessary to solve for the steady-state response, and the computation time needed to perform a Fourier transform on the time-domain output response so that the correct harmonic may be selected.

Ideally, a new small-signal analysis method should be general enough to be included as part of SPICE, but it makes sense to start with a more restrictive approximation of an ideal-switch, piecewise-linear formulation. Based on this, it was decided to look at general small-signal analysis methods that could be used with COSMIR as the front-end program.

COSMIR would be used to take netlist information, build the state-space matrices, and solve for steady-state. The new small-signal program will use all of this information to help solve for the small-signal response.

If the small-signal stimulus to the system is commensurate with the switching frequency of the converter, then the addition of the stimulus to an existing periodic system will cause the system to take on a new steady-state solution with a period commensurate with the stimulus and with switching period. This new steady-state will be closely related to the original steady-state, but with the addition of the response to the small-signal stimulus.

This suggests an approach to the small-signal solution. Since the original steady-state is known, is it possible to solve for just the new steady-state response to the small-signal stimulus? Referring back to Figure 2-10, this could be thought of as solving just for the sidebands, and not the harmonics related to the switching frequency. This is the approach that will be taken in the next chapter.

This method was first published as [29] and [30] in 1988, even though I am only now completing the Dissertation.

3.0 The Derivation of the New Small-Signal Method

3.1 INTRODUCTION

In this chapter, a new small-signal analysis method will be derived from a piecewise-linear time-domain formulation. In this formulation, a switching converter will be represented by a sequence of linear circuits. The state variables in this formulation will be continuous, but the circuit equations are not necessarily continuous. The nonlinear elements are assumed to be adequately represented by either a short or an open circuit.

In addition to the main linear circuit equations, there will be a set of auxiliary equations which will describe the boundary conditions of each linear circuit equation segment. These boundary condition equations will detect when a circuit response will cause one of the non-linearities to change from an open to short circuit, or from short to open.

The piecewise-linear circuit is required to be in periodic, steady-state operation. In this form of steady-state, all of the circuit voltages and currents will be periodic, repeating over and over again. It is not a steady-state in the sense of DC circuits, but is none the less a form of steady state operation. In steady-state, the sequence of linear circuit segments will also be periodic. The sequence will repeat in the same order, and the amount of time spent in each segment will be the same from period to period.

The formulation derived in this chapter parallels the actual measurement process. A circuit analysis program will be used to solve for the sequence of state-space equations and the

periodic steady state response [1]. An additional program will be used to mathmatically perturb the system around the periodic steady state operating point and solve the resulting set of small-signal time-domain equations for the small-signal response. The frequency harmonic that is at the same frequency as the stimulus will be computed, along with the appropriate ratios. This is very similar to the actual lab measurement process.

The problem that is actually solved by this method is a periodic steady-state solution of the switching power system with the addition of a sinusoidal small-signal stimulus. It is assumed that the switching frequency of the power converter and the frequency of the small-signal stimulus are commensurate, and that the resulting system will settle out to a new periodic steady-state that has a frequency related to both the switching frequency and the stimulus frequency by an integer relationship. This solution of a new steady-state will be posed and solved as a harmonic-balance problem.

In the last section of this chapter, it will be shown that this new method is equivalent to averaging when no other harmonics are included in the solution other than the modulation fundamental.

3.2 PIECEWISE-LINEAR FORMULATION

Building upon the concept of ideal switches that was introduced in 2.7, "Previous Modelling and Analysis Methods," we will extend the concept of the series of piecewise-linear segments to include boundary conditions. It is the boundary conditions that determine the instant of transition from one piecewise-linear segment to another.

For instance, consider the well-known rectifier equation[9]:

$$I = f(V) = I_s\left(e^{\frac{qV}{kT}} - 1\right) \tag{3.1}$$

where q is the electron charge, k is Boltzmann's constant, and T is the temperature in degrees Kelvin.

The piecewise-linear model of the rectifier is a simple connection of a voltage source and a resistor:

$$I = f(V) = \left\{ \begin{array}{ll} \frac{(V - V_d)}{R_{off}}, & V < V_d \\ \frac{(V - V_d)}{R_{on}}, & V > V_d \end{array} \right\} \tag{3.2}$$

where $V - V_d = 0$ forms the boundary condition equation that seperates the two segments.

This abrupt characteristic of the nonlinear elements allow us to approximate the continuously nonlinear system equations by a sequence of linear equations. A *mode* will be defined as a unique configuration of saturated elements. In a particular mode, the system may be described by a set of linear equations. The circuit may be described by these equations until a boundary condition is met that causes one, or more, of the nonlinear elements to enter a different saturated region of operation. This will place the circuit into a different mode of operation which will continue until another boundary equation is met. An example of a boundary equation would be the requirement that current in a diode be greater than or equal to zero. Diode current attempting to go negative would switch an "on" diode into an "off" saturated mode.

For instance, during the i-th mode, the circuit equation would be:

$$\dot{x}(t) = a_i\, x(t) + b_i\, u(t) \tag{3.3}$$

$$y(t) = c_i\, x(t) + d_i\, u(t) \tag{3.4}$$

where a_i is a real matrix of dimensions $n_x \times n_x$, b_i is a real matrix of dimensions $n_x \times n_u$, c_i is a real matrix of dimensions $n_y \times n_x$, and d_i is a real matrix of dimensions $n_y \times n_u$.

This representation will be valid between boundary conditions. If the previous boundary condition was met at time t_{i-1}, and the next boundary condition is met at time t_i, then equation (3.3) and equation (3.4) will be valid for $t_{i-1} < t < t_i$.

The boundary between segments i and $i + 1$ occurs at time t_i, and may take on many forms. Since we are using a state-variable formulation, it would make sense for the boundary condition equation to be a linear combination of state variables and the inputs. One such implementation of the boundary condition equation takes the form of:

$$0 = c_i\, x(t) + d_i\, u(t) + \alpha_i\, t \tag{3.5}$$

which is true at $t = t_i$.

Equation (3.5) describes a boundary condition that involves a linear combination of state variables and inputs, and also includes a term, $\alpha_i\, t$, which could be used to generate a linear ramp.

This boundary condition equation is versatile, allowing most of the switching mechanisms of switching power stages to be modelled.

Equation (3.5) is not the only way to describe a boundary condition equation, but is given as an example. A more general form was used in COSMIR[1], which allows for frequency modulation.

$$0 = e_i[c_i\, x(t_i) + d_i\, u(t_i)] + \alpha_i[t_i - t_0] + \beta_i \ , \tag{3.6}$$

or

$$0 = e_i\, y(t_i) + \alpha_i[t_i - t_0] + \beta_i \ , \tag{3.7}$$

3.2.1 Piecewise-Linear Simulation

If the ideal-switch approximation has been made and the system has been modeled by a sequence of piecewise-linear equations, then if a further assumption is made that the system has a *periodic operating trajectory*, then the system may be modeled by a periodic, cyclical series of piecewise-linear equations. A periodic operating trajectory is defined as a set of steady state waveforms that repeat with a fixed period. If a system's waveforms are periodic then the system is said to be in *periodic steady-state*(PSS).

Assume that a power electronics circuit has been formulated using the piecewise-linear representation of equation (3.3) and equation (3.4) with boundary equations as in equation (3.6). If an input, $u_0(t)$, is applied to the system of equations, along with the initial condition $x(t_0)$, then equation (3.3) may be solved for the state trajectory, $x(t)$. If the solution

of the system is allowed to go out far enough in time, it is assumed that the system response will converge to some sort of steady-state solution, either time-invariant or else periodic. If there is no steady-state solution, then it is not possible to go any further with small-signal analysis. If the steady-state solution is periodic, then we will denote this special response by:

$$\dot{x}_0(t) = f(x_0, u_0, t) \tag{3.8}$$

and

$$y_0(t) = g(x_0, u_0, t) \tag{3.9}$$

The fundamental period of the system will be defined as T_s, with the corresponding frequency, f_s, being defined as the inverse of T_s. Note that autonomous systems are allowed, since a constant u_0 also falls within the definition of periodicity. Also, the case of the input, $u_0(t)$, having a frequency that is an integer multiple of f_s is also allowed, since the system will settle out to a period T_t that is commensurate.

If there are Q-modes within a period, T_s, of the converter, then in steady-state operation the state-vector at the beginning of the first mode will be equal the state-vector at the end of the last mode, or:

$$x(t_0) = x(t_Q) \ . \tag{3.10}$$

If we define a unit step function to be:

$$v(t-\tau) = \left\{ \begin{matrix} 1, & t \geq \tau \\ 0, & t < \tau \end{matrix} \right\} \tag{3.11}$$

then we may represent the sequence of piecewise-linear segments of the system in one equation:

$$\begin{aligned} \dot{x}(t) &= f(x,u,t) \\ &= \sum_{i=1}^{Q} \{a_i x(t) + b_i u(t)\} \{v(t - t_{i-1}) - v(t - t_i)\} \end{aligned} \tag{3.12a}$$

and

$$\begin{aligned} y(t) &= g(x,u,t) \\ &= \sum_{i=1}^{Q} \{c_i x(t) + d_i u(t)\} \{v(t - t_{i-1}) - v(t - t_i)\} \end{aligned} \tag{3.12b}$$

along with the set of corresponding boundary condition equations:

$$0 = e_i c_i x(t_i) + e_i d_i u(t_i) + \alpha_i (t_i - t_0) + \beta_i \tag{3.12c}$$

for $1 \leq i \leq Q$.

3.3 THE SET-UP OF THE SMALL-SIGNAL PROBLEM

One method to solve for the small-signal response would be to simulate it using a large-signal method by placing a small-signal stimulus on top of an existing large-signal source. The system would be simulated in the time-domain for a period commensurate with the stimulus frequency and the switching frequency, and the resulting data would be transformed into the frequency domain, probably using a FFT. Then the harmonic coefficient of the response at the same frequency as the stimulus would be selected to compute the transfer function. This is such a brute-force method as to be impractical for most problems, since one complete simulation would need to be performed for each frequency of interest. The author has heard undocumented stories of this approach being used as a method of last resort, but can't recall this method ever being documented in the literature, probably since it is so impractical.

This method will work, although there are several drawbacks. In order to not excite unwanted nonlinear effects, the stimulus should be small. This means the response to this small stimulus will also be small. These small responses may have substantial error associated with them. The error may come from the convergence and error controls of the simulator as well as numerical roundoff problems. Error will also come out of the FFT process. All in all, this is a numerically intensive process.

The approach taken here will be similar to the brute-force method in that it will be posed as a time-domain problem over a period commensurate with the switching frequency and the small-signal stimulus frequency. The difference will be that the nonlinear large-signal component will be linearized out. So, the response of this linearized system will be evaluated over the period.

The period of the switching power system is defined to be T_s, with associated switching frequency f_s. The period of the small-signal stimulus is defined to be T_m, with associated stimulus frequency f_m. An overall period T_t will be defined, being commensurate with both T_m and T_s.

$$T_t = NT_s = MT_m \tag{3.13}$$

where N and M are integers. This means there are N complete cycles of the switching power converter operation and M complete periods of the stimulus in one overall period T_t.

The notation for the time variables needs to be expanded at this point. Up to now, the notation t_i was used to denote the value of time at the end of the i-th mode of the converter. Now, the notation of identifying cycles needs to be added. For example, $t_i^{(k)}$ will be used to denote the value of time at the end of the ith mode of the k-th cycle.

The representation of the system by piecewise-linear segments in equation (3.12a) and equation (3.12b) may now be expanded to cover the period between 0 and T_t by including the N cycles.

$$\begin{aligned} \dot{x}(t) &= f(x,u,t) \\ &= \sum_{p=1}^{N} \sum_{i=1}^{Q} \{a_i x(t) + b_i u(t)\} \left\{ v(t - t_{i-1}^{(p)}) - v(t - t_i^{(p)}) \right\} \end{aligned} \tag{3.14a}$$

and

$$y(t) = g(x,u,t)$$
$$= \sum_{p=1}^{N} \sum_{i=1}^{Q} \{c_i x(t) + d_i u(t)\} \left\{ v(t - t_{i-1}^{(p)}) - v(t - t_i^{(p)}) \right\} \tag{3.14b}$$

along with the set of corresponding boundary condition equations:

$$0 = e_i c_i x(t_i^{(p)}) + e_i d_i u(t_i^{(p)}) + \alpha_i (t_i^{(p)} - t_0^{(p)}) + \beta_i \tag{3.14c}$$

3.4 HARMONIC BALANCE METHOD FOR LARGE-SIGNAL ANALYSIS

In this section, we will show how a general system of nonlinear time-domain equations may be transformed into the form of harmonic-balance. The resulting equations will then be perturbed and linearized in a later section so that the small-signal responses may be calculated.

The derivation of this general case will closely follow the method described in [31]. In a later section we will substitute into this general form the special-case equations of a piecewise-linear system.

We will use this to transform the large-signal periodic-steady-state response of a power system out of COSMIR into a harmonic-balance representation. This representation will describe the steady-state harmonic structure of the power system.

For the general nonlinear case, we will assume that the system of equations may be posed in the form of

$$\dot{x}(t) = f(x(t), u(t)) \tag{3.15a}$$

and

$$y(t) = g(x(t), u(t)) \ . \tag{3.15b}$$

We will also assume that there exists a periodic-steady-state operating trajectory for this circuit, and therefore that all waveforms are periodic. We will call this set of steady-state responses $\dot{x}_0(t)$, $x_0(t)$, and $u_0(t)$.

The harmonic-balance method takes a system of equations of the form equation (3.15a) and equation (3.15b) and transforms the system into a set of frequency-domain equations:

$$j\omega_t X(i) = F(X, U, i) \tag{3.16a}$$

and

$$Y(i) = G(X, U, i) \tag{3.16b}$$

for all integer i, where $\omega_t = \frac{2\pi i}{T_t}$, and where the definition of X is the set of harmonic components:

$$X = \{ \ldots, \ X(-2), \ X(-1), \ X(0), \ X(1), \ X(2), \ \ldots \} \ . \tag{3.17a}$$

Likewise for U and Y:

$$U = \{ \ldots, \ U(-2), \ U(-1), \ U(0), \ U(1), \ U(2), \ \ldots \} \tag{3.17b}$$

$$Y = \{ \ldots, \ Y(-2), \ Y(-1), \ Y(0), \ Y(1), \ Y(2), \ \ldots \} \tag{3.17c}$$

To perform this transformation, we will use the assumption that the system is in periodic steady state. This means that all waveforms and quantities are periodic. With restrictions of a finite number of maxima and minima, as well as a finite number of finite discontinuities[32], we may replace all of the quantities of equation (3.15a) and equation (3.15b) with their Fourier series equivalents. These equivalents are:

$$x(t) = \sum_{k=-\infty}^{\infty} X(k) e^{j \frac{2\pi k}{T_t} t} \tag{3.18a}$$

$$u(t) = \sum_{i=-\infty}^{\infty} U(i) e^{j \frac{2\pi i}{T_t} t} \tag{3.18b}$$

$$y(t) = \sum_{k=-\infty}^{\infty} Y(k) e^{j \frac{2\pi k}{T_t} t} \tag{3.18c}$$

The equivalent for $\dot{x}(t)$ may be computed from equation (3.18a) by differentiating with respect to t :

$$\dot{x}(t) = \frac{\partial x(t)}{\partial t} = \frac{\partial}{\partial t} \sum_{k=-\infty}^{\infty} X(k) e^{j \frac{2\pi k}{T_t} t} = \sum_{k=-\infty}^{\infty} jX(k) \frac{2\pi k}{T_t} e^{j \frac{2\pi k}{T_t} t} \quad . \tag{3.18d}$$

In equation (3.15a), since we have computed a replacement for the left-hand side, $\dot{x}(t)$, and since we have restricted $x(t)$ and $u(t)$ to be periodic, we may also compute a replacement for the right-hand side of equation (3.15a).

$$f(x(t), u(t)) = \sum_{i=-\infty}^{\infty} F(X, U, i) e^{j \frac{2\pi i}{T_t} t} \quad . \tag{3.19a}$$

Similarly, we may compute the equivalent for the right-hand side of equation (3.15b):

$$g(x(t), u(t)) = \sum_{i=-\infty}^{\infty} G(X, U, i) e^{j \frac{2\pi i}{T_t} t} \quad . \tag{3.19b}$$

Equation (3.18a) through equation (3.19b) may be substituted into equation (3.15a) and equation (3.15b) to give:

$$\sum_{k=-\infty}^{\infty} jX(k)\frac{2\pi k}{T_t}e^{j\frac{2\pi k}{T_t}t} = \sum_{i=-\infty}^{\infty} F(X,U,i)e^{j\frac{2\pi i}{T_t}t} \tag{3.20a}$$

and

$$\sum_{k=-\infty}^{\infty} Y(k)e^{j\frac{2\pi k}{T_t}t} = \sum_{i=-\infty}^{\infty} G(X,U,i)e^{j\frac{2\pi i}{T_t}t} \; . \tag{3.20b}$$

We will multiply both sides of equation (3.20a) and equation (3.20b) by a suitable constant, $e^{-j\frac{2\pi h}{T_t}t}$. This constant exploits the fact the the integration of a complex exponential over a full period will be nonzero only for a special case.

$$\sum_{k=-\infty}^{\infty} jX(k)\frac{2\pi k}{T_t}e^{j\frac{2\pi(k-h)}{T_t}t} = \sum_{i=-\infty}^{\infty} F(X,U,i)e^{j\frac{2\pi(i-h)}{T_t}t} \tag{3.21a}$$

and

$$\sum_{k=-\infty}^{\infty} Y(k)e^{j\frac{2\pi(k-h)}{T_t}t} = \sum_{i=-\infty}^{\infty} G(X,U,i)e^{j\frac{2\pi(i-h)}{T_t}t} \; . \tag{3.21b}$$

Equation (3.21a) and equation (3.21b) will be integrated over one period, T_t. If a value for k is chosen, than the only case where the left-hand sides of equation (3.21a) and equation (3.21b) will be nonzero is for $h = k$. This same logic carries over to the right-hand side, which is nonzero only for $i = h = k$. This allows us to equate the harmonics on each side:

$$jX(k)\frac{2\pi k}{T_t} = F(X,U,k), \tag{3.22a}$$

and

$$Y(k) = G(X, U, k) \tag{3.22b}$$

for all integer k.

Equation (3.22a) and equation (3.22b) each describe one equation in a set of equations, where there is one each of equation (3.22a) and equation (3.22b) for each frequency harmonic k. At this stage, there are an infinite number of harmonics to be considered. To make the problem solvable, the infinite series of harmonics of X will be truncated to some number. This is a reasonable thing to do, since the systems being studied have finite energy, which means that the magnitude of the harmonic will go to zero in the limit as the frequency of the harmonic goes to infinity.

This approach for the large-signal model is commonly known as the *harmonic balance method* [31, 33, 34]. Harmonic balance is used primarily in the field of microwave circuit simulation[35]. This approach assumes firstly that a solution exists, and secondly that the solution is periodic and is composed of related harmonic components.

Harmonic Balance is a mixed frequency-time method. Conventional usage of it will split a circuit into two blocks: one containing linear elements, and the other containing nonlinear elements. This is described in Figure 3-1.

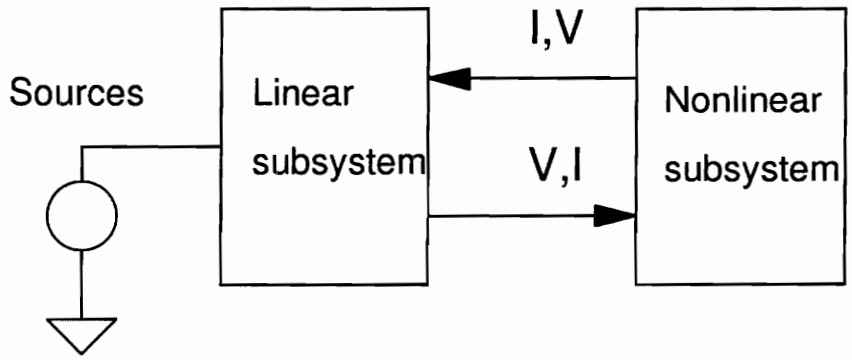

Figure 3-1. A representation of the harmonic balance method.

In this method, an initial guess would be made for the voltages and currents at the interface between subcircuits, going into the linear side. This initial set would be transformed to the frequency domain using perhaps a FFT. The linear subcircuit would be analyzed in the frequency domain, and the outputs out of the linear subcircuit would be converter back to the time domain, perhaps using an Inverse FFT. This set of voltages and currents would be used to compute the responses of the nonlinear subcircuit using time-domain methods. Finally, the output out of the nonlinear block would be compared against the initial guess, and the difference would be used to drive an iterative method.

3.5 LINEARIZATION FOR SMALL-SIGNAL ANALYSIS

Small-signal linearization will be accomplished by performing a Taylor's Series expansion of equation (3.22a) and equation (3.22b), dropping the higher order terms, subtracting out the known information, and solving for only the small-signal portion. This results in:

$$j\hat{X}(k)\frac{2\pi k}{T_t} = \frac{\partial F(X,U,k)}{\partial X}\hat{X} + \frac{\partial F(X,U,k)}{\partial U}\hat{U} \tag{3.23a}$$

and

$$\hat{Y}(k) = \frac{\partial G(X,U,k)}{\partial X}\hat{X} + \frac{\partial G(X,U,k)}{\partial U}\hat{U} \ . \tag{3.23b}$$

Now, since X and Y represent sets, or vectors, of harmonic coefficients, the above equations really represent an infinite sum of small perturbations. One of the terms from above will be expanded to demonstrate:

$$\begin{aligned}\frac{\partial F(X,U,k)}{\partial X}\hat{X} &= \cdots + \frac{\partial F(X,U,k)}{\partial X(-1)}\hat{X}(-1) + \frac{\partial F(X,U,k)}{\partial X(0)}\hat{X}(0) + \frac{\partial F(X,U,k)}{\partial X(1)}\hat{X}(1) + \cdots \\ &= \sum_{i=-\infty}^{\infty}\frac{\partial F(X,U,k)}{\partial X(i)}\hat{X}(i)\end{aligned} \tag{3.24}$$

Equation (3.23a) and equation (3.23b) may now be written in terms of infinite sums instead of the compact notation:

$$j\hat{X}(k)\frac{2\pi k}{T_t} = \sum_{i=-\infty}^{\infty}\frac{\partial F(X, U, k)}{\partial X(i)}\hat{X}(i) + \sum_{i=-\infty}^{\infty}\frac{\partial F(X, U, k)}{\partial U(i)}\hat{U}(i) \tag{3.25a}$$

and

$$\hat{Y}(k) = \sum_{i=-\infty}^{\infty}\frac{\partial G(X, U, k)}{\partial X(i)}\hat{X}(i) + \sum_{i=-\infty}^{\infty}\frac{\partial G(X, U, k)}{\partial U(i)}\hat{U}(i) \tag{3.25b}$$

Since we are interested in the small-signal response, and would like to be able to compare the responses of this small-signal model against laboratory measurements, we will restrict the input vector, $\hat{u}(t)$, to be a simple sinusoidal signal. Since the system is small-signal and linear, the amplitude of the stimulus is not critical. This allows us to pick a special value which will simplify the equations at a later point. We will choose the stimulus to be:

$$\hat{u}(t) = 2\cos(\frac{2\pi}{T_m}t) \ . \tag{3.26}$$

The period of the stimulus was defined earlier in equation (3.13) to be T_m. We will integrate equation (3.26) over the overall period, T_n, to find the Fourier series frequency components. When this is done, we find that the only nonzero components exist at plus and minus the stimulus frequency:

$$\hat{U}(l) = \left\{ \begin{array}{ll} 1, & l=M \\ 1, & l=-M \\ 0, & otherwise \end{array} \right\} \quad . \tag{3.27}$$

This result is for a $\hat{u}(t)$ that has a fundamental period of T_m, but where the Fourier series has been computed over a commensurate period M-times longer. This result may be used to somewhat simplify equation (3.25a) and equation (3.25b).

We may rearrange equation (3.25a) and equation (3.25b), also substutuing in this restriction in the input stimulus:

$$j\omega_k \hat{X}(k) - \sum_{i=-\infty}^{\infty} \frac{\partial F(X, U, k)}{\partial X(i)} \hat{X}(i) = \frac{\partial F(X, U, k)}{\partial U(M)} \hat{U}(M) + \frac{\partial F(X, U, k)}{\partial U(-M)} \hat{U}(-M) \tag{3.28a}$$

and

$$\hat{Y}(k) = \sum_{i=-\infty}^{\infty} \frac{\partial G(X, U, k)}{\partial X(i)} \hat{X}(i) + \frac{\partial G(X, U, k)}{\partial U(M)} \hat{U}(M) + \frac{\partial G(X, U, k)}{\partial U(-M)} \hat{U}(-M) \qquad (3.28b)$$

3.5.1 System Fourier-Series

To solve equation (3.28a) and equation (3.28b), we must first describe the system equation as a Fourier series, and then compute the appropriate partial derivatives.

In equation (3.14a) and equation (3.14b), the functionals $f(x(t), u(t))$ and $g(x(t), u(t))$ were defined. These definitions will be used to compute the Fourier series representation $F(X, U, k)$ and $G(X, U, k)$.

The Fourier series components of the functional, f, may be computed as:

$$\begin{aligned} F(X, U, k) &= \frac{1}{T_t} \int_0^{T_t} f(x, u, \tau) e^{-j \frac{2\pi k}{T_t} \tau} d\tau \\ &= \frac{1}{T_t} \int_0^{T} \sum_{p=1}^{N} \sum_{i=1}^{Q} \{a_i x(\tau) + b_i u(\tau)\} \left\{ v(\tau - t_{i-1}^{(p)}) - v(\tau - t_i^{(p)}) \right\} e^{-j \frac{2\pi k}{T_t} \tau} d\tau \qquad (3.29a) \\ &= \frac{1}{T_t} \sum_{p=1}^{N} \sum_{i=1}^{Q} \int_{t_{i-1}^{(p)}}^{t_i^{(p)}} [a_i x(\tau) + b_i u(\tau)] e^{-j \frac{2\pi k}{T_t} \tau} d\tau \ . \end{aligned}$$

Likewise, the Fourier series of g may be computed as:

$$G(X, U, k) = \frac{1}{T_t}\int_0^{T_t} g(x(\tau), u(\tau))e^{-j\frac{2\pi k}{T_t}\tau}d\tau$$
$$= \frac{1}{T_t}\sum_{p=1}^{N}\sum_{i=1}^{Q}\int_{t_{i-1}^{(p)}}^{t_i^{(p)}}[c_i x(\tau) + d_i u(\tau)]e^{-j\frac{2\pi k}{T_t}\tau}d\tau \ . \tag{3.29b}$$

Equation (3.29a) and equation (3.29b) are subject to the boundary condition equations from equation (3.14c).

3.5.2 Linearization of System Fourier series

To evaluate equation (3.28a) and equation (3.28b) we must evaluate the partial derivatives of equation (3.29a) and equation (3.29b) to find $\frac{\partial F(X, U, k)}{\partial X(i)}$, $\frac{\partial F(X, U, k)}{\partial U(M)}$, $\frac{\partial F(X, U, k)}{\partial U(-M)}$, $\frac{\partial G(X, U, k)}{\partial X(i)}$, $\frac{\partial G(X, U, k)}{\partial U(M)}$, and $\frac{\partial G(X, U, k)}{\partial U(-M)}$. We will do a slight change of variable to prevent the misuse of i, and solve for $\frac{\partial F(X, U, k)}{\partial X(v)}$, $\frac{\partial F(X, U, k)}{\partial U(v)}$, $\frac{\partial G(X, U, k)}{\partial X(v)}$, and $\frac{\partial G(X, U, k)}{\partial U(v)}$. We will do this by using Leibnitz's Rule [36] to take the partial derivatives of the integrals of the piecewise-linear segments. We must remember that the switching instant, $t_i^{(p)}$, is an implicit function of $x(t)$ and $u(t)$ due to the boundary condition equation (3.14c). We first start with taking the partial derivatives of equation (3.29a):

$$\frac{\partial F(X, U, k)}{\partial X(v)} = \frac{1}{T_t} \sum_{p=1}^{N} \sum_{i=1}^{Q} \left[a_i x(t_i^{(p)}) + b_i u(t_i^{(p)}) \right] e^{-j \frac{2\pi k}{T_t} t_i^{(p)}} \frac{\partial t_i^{(p)}}{\partial X(v)}$$

$$- \frac{1}{T_t} \sum_{p=1}^{N} \sum_{i=1}^{Q} \left[a_i x(t_{i-1}^{(p)}) + b_i u(t_{i-1}^{(p)}) \right] e^{-j \frac{2\pi k}{T_t} t_{i-1}^{(p)}} \frac{\partial t_{i-1}^{(p)}}{\partial X(v)} \qquad (3.30)$$

$$+ \frac{1}{T_t} \sum_{p=1}^{N} \sum_{i=1}^{Q} \int_{t_{i-1}^{(p)}}^{t_i^{(p)}} a_i \frac{\partial x(\tau)}{\partial X(v)} e^{-j \frac{2\pi k}{T_t} \tau} d\tau$$

If we do a slight change of index on the middle portion of equation (3.30), we will be able to line up the summations of the first two portions with the exception of the first and last points. We will change the summation of $1 \le i \le Q$ in the second portion to become $0 \le i \le (Q - 1)$:

$$\frac{\partial F(X, U, k)}{\partial X(v)} = \frac{1}{T_t} \sum_{p=1}^{N} \sum_{i=1}^{Q} \left[a_i x(t_i^{(p)}) + b_i u(t_i^{(p)}) \right] e^{-j \frac{2\pi k}{T_t} t_i^{(p)}} \frac{\partial t_i^{(p)}}{\partial X(v)}$$

$$- \frac{1}{T_t} \sum_{p=1}^{N} \sum_{i=0}^{Q-1} \left[a_{i+1} x(t_i^{(p)}) + b_{i+1} u(t_i^{(p)}) \right] e^{-j \frac{2\pi k}{T_t} t_i^{(p)}} \frac{\partial t_i^{(p)}}{\partial X(v)} \qquad (3.31)$$

$$+ \frac{1}{T_t} \sum_{p=1}^{N} \sum_{i=1}^{Q} \int_{t_{i-1}^{(p)}}^{t_i^{(p)}} a_i \frac{\partial x(\tau)}{\partial X(v)} e^{-j \frac{2\pi k}{T_t} \tau} d\tau$$

The only thing preventing the merging of the first two portions of equation (3.31) are the two points $\{p = 1, i = 0\}$ and $\{p = N, i = Q\}$. This translates into the two times: $t_0^{(1)}$ and $t_N^{(Q)}$. Because we have defined a system with overall periodicity T_t, we know that

$$x(t_0^{(1)}) = x(t_N^{(Q)}) \tag{3.32}$$

and

$$u(t_0^{(1)}) = u(t_N^{(Q)}) \tag{3.33}$$

since they are the very first and last points in a periodic waveform. Since the waveform is periodic, the derivatives will also be periodic at these endpoints.

We may use the equivalence of the first and last points in the cyclical operation to merge the first two portions of equation (3.31):

$$\frac{\partial F(X, U, k)}{\partial X(v)} = \sum_{p=1}^{N} \sum_{i=1}^{Q} \frac{1}{T_t} \left[a_i x(t_i^{(p)}) + b_i u(t_i^{(p)}) - a_{i+1} x(t_i^{(p)}) - b_{i+1} u(t_i^{(p)}) \right] e^{-j \frac{2\pi k}{T_t} t_i^{(p)}} \frac{\partial t_i^{(p)}}{\partial X(v)}$$
$$+ \sum_{p=1}^{N} \sum_{i=1}^{Q} a_i \frac{1}{T_t} \int_{t_{i-1}^{(p)}}^{t_i^{(p)}} \frac{\partial x(\tau)}{\partial X(v)} e^{-j \frac{2\pi k}{T_t} \tau} d\tau \tag{3.34}$$

By making the following substitution,

$$\Xi_i = \left[a_i x(t_i^{(p)}) + b_i u(t_i^{(p)}) - a_{i+1} x(t_i^{(p)}) - b_{i+1} u(t_i^{(p)}) \right] \tag{3.35}$$

we may rewrite this as

$$\begin{aligned} \frac{\partial F(X, U, k)}{\partial X(v)} = & \sum_{p=1}^{N} \sum_{i=1}^{Q} \frac{1}{T_t} \Xi_i e^{-j\frac{2\pi k}{T_t} t_i^{(p)}} \frac{\partial t_i^{(p)}}{\partial X(v)} \\ & + \sum_{p=1}^{N} \sum_{i=1}^{Q} a_i \frac{1}{T_t} \int_{t_{i-1}^{(p)}}^{t_i^{(p)}} \frac{\partial x(\tau)}{\partial X(v)} e^{-j\frac{2\pi k}{T_t}\tau} d\tau \end{aligned} \tag{3.36}$$

We may now take the partial derivative of equation (3.18a):

$$\frac{\partial x(\tau)}{\partial X(v)} = e^{j\frac{2\pi v}{T_t}\tau} \tag{3.37a}$$

and insert it into equation (3.36) to give:

$$\frac{\partial F(X, U, k)}{\partial X(v)} = \sum_{p=1}^{N} \sum_{i=1}^{Q} \frac{1}{T_t} \Xi_i e^{-j\frac{2\pi k}{T_t} t_i^{(p)}} \frac{\partial t_i^{(p)}}{\partial X(v)}$$
$$+ \sum_{p=1}^{N} \sum_{i=1}^{Q} a_i \frac{1}{T_t} \int_{t_{i-1}^{(p)}}^{t_i^{(p)}} e^{-j\frac{2\pi(k-v)}{T_t}\tau} d\tau \tag{3.38}$$

Similar operations may be performed to find $\frac{\partial F(X, U, k)}{\partial U(v)}$.

$$\frac{\partial F(X, U, k)}{\partial U(v)} = \sum_{p=1}^{N} \sum_{i=1}^{Q} \frac{1}{T_t} \Xi_i e^{-j\frac{2\pi k}{T_t} t_i^{(p)}} \frac{\partial t_i^{(p)}}{\partial U(v)}$$
$$+ \sum_{p=1}^{N} \sum_{i=1}^{Q} b_i \frac{1}{T_t} \int_{t_{i-1}^{(p)}}^{t_i^{(p)}} e^{-j\frac{2\pi(k-v)}{T_t}\tau} d\tau \tag{3.38b}$$

The Fourier series components of the functional $g(x(t), u(t))$ may be computed as:

$$G(X, U, k) = \frac{1}{T_t}\int_0^{T_t} g(x(\tau), u(\tau))e^{-j\frac{2\pi k}{T_t}\tau}d\tau$$
$$= \frac{1}{T_t}\sum_{p=1}^{N}\sum_{i=1}^{Q}\int_{t_{i-1}^{(p)}}^{t_i^{(p)}} [c_i x(\tau) + d_i u(\tau)]e^{-j\frac{2\pi k}{T_t}\tau}d\tau \tag{3.39}$$

In the same manner as for $f(x, u, t)$, the partial derivatives may be found to be:

$$\frac{\partial G(X, U, k)}{\partial X(v)} = \sum_{p=1}^{N}\sum_{i=1}^{Q}\frac{1}{T_t}Z_i e^{-j\frac{2\pi k}{T_t}t_i^{(p)}}\frac{\partial t_i^{(p)}}{\partial X(v)}$$
$$+ \sum_{p=1}^{N}\sum_{i=1}^{Q} c_i\frac{1}{T_t}\int_{t_{i-1}^{(p)}}^{t_i^{(p)}} e^{-j\frac{2\pi(k-v)}{T_t}\tau}d\tau \tag{3.40}$$

and

$$\frac{\partial G(X, U, k)}{\partial U(v)} = \sum_{p=1}^{N} \sum_{i=1}^{Q} \frac{1}{T_t} Z_i e^{-j\frac{2\pi k}{T_t} t_i^{(p)}} \frac{\partial t_i^{(p)}}{\partial U(v)}$$
$$+ \sum_{p=1}^{N} \sum_{i=1}^{Q} d_i \frac{1}{T_t} \int_{t_{i-1}^{(p)}}^{t_i^{(p)}} e^{-j\frac{2\pi(k-v)}{T_t}\tau} d\tau \tag{3.41}$$

where

$$Z_i = \left[a_i x(t_i^{(p)}) + b_i u(t_i^{(p)}) - a_{i+1} x(t_i^{(p)}) - b_{i+1} u(t_i^{(p)}) \right] . \tag{3.42}$$

3.5.3 Perturbation of Switching Boundaries

The partials of the switching instants with respect to the state vector is detailed next. Recalling the equation for the boundary between segments i and $i + 1$ from equation (3.14c):

$$0 = e_i \left[c_i x(t_i^{(p)}) + d_i u(t_i^{(p)}) \right] + \alpha_i \left[t_i^{(p)} - t_0^{(p)} \right] + \beta_i . \tag{3.43}$$

A good example of a boundary condition equation is from the current-mode converter of 4.4, "Boost - PWM - Continuous Mode - Current Mode Control." In this converter, the peak inductor current is controlled by a control input. When the scaled inductor current ramps up

to equal the control signal, the FET turns off causing the inductor current to decrease. In this example a resistor, RX, bridges the control signal and a resistor in the Source of the FET. When the voltage across the Source resistor exceeds the control signal, the voltage across RX will be negative. So, the boundary condition will be to detect when V(RX) is less than or equal to zero and turn the FET off. A plot of this waveform is in Figure 3-2.

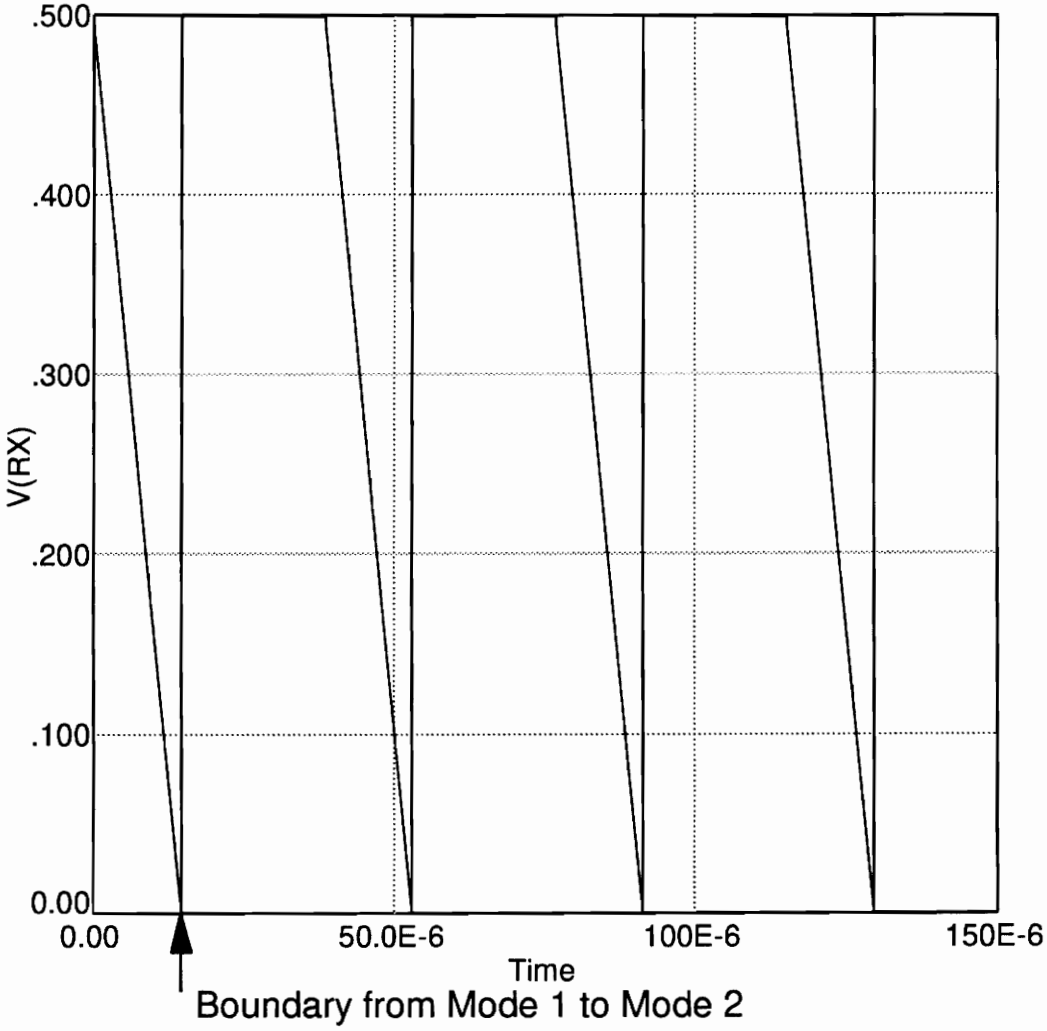

Figure 3-2. An Example of a Boundary Condition from a Current-Mode Converter

In Figure 3-2, the voltage V(RX) is composed of a linear combination of the state and input vectors. In the notation used here, this particular voltage would be described by $e_i[c_i\, x(t) + d_i\, u(t)]$.

The term e_i is a selection vector that selects one of the output variables. Each output is itself a linear combination of states and input quantities, which is governed by the c_i and the d_i matrices. The term α_i is used to generate a linear ramp signal which is reset at the beginning of a cycle. The term β_i describes a constant that may be used possibly as an offset in conjunction with α_i for the generation of fixed time delays.

We will differentiate equation (3.43) using implicit differentiation:

$$0 = e_i c_i\, \delta x(t_i^{(p)}) + e_i c_i \dot{x}(t_i^{(p)})\, \delta t_i^{(p)} + e_i d_i\, \delta u(t_i^{(p)}) + e_i d_i \dot{u}(t_i^{(p)})\, \delta t_i^{(p)} + \alpha_i\, \delta t_i^{(p)} - \alpha_i\, \delta t_0^{(p)} \qquad (3.44)$$

We will now collect terms to give

$$\left(e_i c_i \dot{x}(t_i^{(p)}) + e_i d_i \dot{u}(t_i^{(p)}) + \alpha_i\right)\delta t_i^{(p)} = -\, e_i c_i\, \delta x(t_i^{(p)}) - e_i d_i\, \delta u(t_i^{(p)}) + \alpha_i\, \delta t_0^{(p)} \quad . \qquad (3.45)$$

In equation (3.38), equation (3.38b), equation (3.40), and equation (3.41), partial derivatives that represent the change in the time of the switching instants as a function of the harmonics of the state vector and the input need to be computed. We will find these partial derivatives by taking the partial

$$\frac{\partial t_i^{(p)}}{\partial X(v)} = \frac{-e_i c_i}{e_i c_i \dot{x}(t_i^{(p)}) + e_i d_i \dot{u}(t_i^{(p)}) + \alpha_i} \frac{\partial x(t_i^{(p)})}{\partial X(v)} + \frac{\alpha_i}{e_i c_i \dot{x}(t_i^{(p)}) + e_i d_i \dot{u}(t_i^{(p)}) + \alpha_i} \frac{\partial t_0^{(p)}}{\partial X(v)} \tag{3.46a}$$

and

$$\frac{\partial t_i^{(p)}}{\partial U(v)} = \frac{-e_i d_i}{e_i c_i \dot{x}(t_i^{(p)}) + e_i d_i \dot{u}(t_i^{(p)}) + \alpha_i} \frac{\partial u(t_i^{(p)})}{\partial U(v)} + \frac{-e_i c_i}{e_i c_i \dot{x}(t_i^{(p)}) + e_i d_i \dot{u}(t_i^{(p)}) + \alpha_i} \frac{\partial x(t_i^{(p)})}{\partial U(v)} + \frac{\alpha_i}{e_i c_i \dot{x}(t_i^{(p)}) + e_i d_i \dot{u}(t_i^{(p)}) + \alpha_i} \frac{\partial t_0^{(p)}}{\partial U(v)} \tag{3.46b}$$

The term $\frac{\partial x(t_i^{(p)})}{\partial X(v)}$ is of interest. Since the system is being represented by a series of piecewise-linear segments, the state variables will be continuous but the first derivative of the state variables will have jump discontinuities. If a boundary equation is a function of one of the state variables that is changing its derivative right at the boundary point, many harmonic terms will be necessary to adequately predict the value of the state variable at the boundary point. Instead, we will back up in time away from the boundary point, and shoot down to the boundary point by solving the state equations of that segment.

If the system is in the i-th segment of the k-th cycle, then the boundary condition equation will be satisfied at time $t_i^{(p)}$. We will back up to some time $t_i^{(p)}$ that is between $t_{i-1}^{(p)}$ and $t_i^{(p)}$.

$$t_{i-1}^{(p)} \le t_{i'}^{(p)} \le t_i^{(p)} \tag{3.47}$$

The solution of the state equations is well known:

$$\begin{aligned} x(t_i^{(p)}) &= e^{a_i(t_i^{(p)} - t_{i'}^{(p)})} x(t_{i'}^{(p)}) + a_i^{-1} \left\{ e^{a_i(t_i^{(p)} - t_{i'}^{(p)})} - I \right\} b_i u(t_{i'}^{(p)}) \\ &= \Phi_i(t_i^{(p)}, t_{i'}^{(p)})\, x(t_{i'}^{(p)}) + \Psi_i(t_i^{(p)}, t_{i'}^{(p)})\, u(t_{i'}^{(p)}) \end{aligned} \tag{3.48}$$

The partial derivatives of this equation may be computed as:

$$\begin{aligned} \frac{\partial x(t_i^{(p)})}{\partial X(v)} &= \frac{\partial}{\partial X(v)} \left\{ \Phi_i(t_i^{(p)}, t_{i'}^{(p)})\, x(t_{i'}^{(p)}) \right\} + \frac{\partial}{\partial X(v)} \left\{ \Psi_i(t_i^{(p)}, t_{i'}^{(p)})\, u(t_{i'}^{(p)}) \right\} \\ &= \Phi_i(t_i^{(p)}, t_{i'}^{(p)}) \frac{\partial x(t_{i'}^{(p)})}{\partial X(v)} \end{aligned} \tag{3.49a}$$

and

$$\begin{aligned} \frac{\partial x(t_i^{(p)})}{\partial U(v)} &= \frac{\partial}{\partial U(v)} \left\{ \Phi_i(t_i^{(p)}, t_{i'}^{(p)})\, x(t_{i'}^{(p)}) \right\} + \frac{\partial}{\partial U(v)} \left\{ \Psi_i(t_i^{(p)}, t_{i'}^{(p)})\, u(t_{i'}^{(p)}) \right\} \\ &= \Psi_i(t_i^{(p)}, t_{i'}^{(p)}) \frac{\partial u(t_{i'}^{(p)})}{\partial U(v)} \end{aligned} \tag{3.49b}$$

We may now take the partial derivative of equation (3.18a):

$$\frac{\partial x(t_i^{(p)})}{\partial X(v)} = e^{j\frac{2\pi v}{T_i}t_i^{(p)}} \quad . \tag{3.50a}$$

Similarly, take the partial derivative of equation (3.18b):

$$\frac{\partial u(t_i^{(p)})}{\partial U(v)} = e^{j\frac{2\pi v}{T_i}t_i^{(p)}} \tag{3.50b}$$

If we define:

$$\Lambda_i = \frac{\alpha_i}{e_i c_i \dot{x}(t_i^{(p)}) + e_i d_i \dot{u}(t_i^{(p)}) + \alpha_i} \quad , \tag{3.51a}$$

$$\Gamma_i = -\frac{e_i c_i}{e_i c_i \dot{x}(t_i^{(p)}) + e_i d_i \dot{u}(t_i^{(p)}) + \alpha_i} \quad , \tag{3.51b}$$

and

$$\mathrm{H}_i = -\frac{e_i d_i}{e_i c_i \dot{x}(t_i^{(p)}) + e_i d_i \dot{u}(t_i^{(p)}) + \alpha_i} \quad , \tag{3.51c}$$

then we have:

$$\frac{\partial t_i^{(p)}}{\partial X(v)} = \Gamma_i \Phi_i(t_i^{(p)}, t_i^{(p)}) e^{j\frac{2\pi v}{T_i} t_i^{(p)}} + \Lambda_i \frac{\partial t_0^{(p)}}{\partial X(v)} \tag{3.52a}$$

and

$$\frac{\partial t_i^{(p)}}{\partial U(v)} = \mathrm{H}_i e^{j\frac{2\pi v}{T_i} t_i^{(p)}} + \Gamma_i \Psi_i(t_i^{(p)}, t_i^{(p)}) e^{j\frac{2\pi v}{T_i} t_i^{(p)}} + \Lambda_i \frac{\partial t_0^{(p)}}{\partial U(v)} \quad . \tag{3.52b}$$

3.6 SOLUTION OF SMALL-SIGNAL MODEL

At this point, everything has been defined that is necessary to solve this system for a small-signal perturbation. The main equation to solve is equation (3.28a). In this equation, the integer k is free to take on any value, and thus may be used to solve for any harmonic coefficient of $\hat{X}(K)$. However, the scope of the problem has been limited due to the restriction to a sinusoidal stimulus. The overall system under this small-signal stimulus will generate frequency components at predictable harmonic coefficients.

To understand this process, first look at one of the right-hand side terms of equation equation (3.28a), for instance $\frac{\partial F(X, U, k)}{\partial U(M)}$. By inspecting equation (3.38b), it is apparent that the integration of the complex exponential over multiple periods of T_s will have a non-zero component only for:

$$\frac{(k - M)}{N} = i \tag{3.53}$$

where i is an integer. This means that k will take on the following values:

$$k = iN + M \tag{3.54}$$

In order to make this problem solvable, the number of harmonic coefficients will be truncated to some value P. This will make the maximum value of k equal to $PN + M$ and the minimum will be $-PN + M$.

These harmonic coefficients may be translated back to discrete frequencies through the use of the following equation:

$$\begin{aligned} f &= \frac{k}{T_t} = \frac{iN + M}{T_t} \\ &= \frac{iN}{T_t} + \frac{M}{T_t} \\ &= \frac{iN}{NT_s} + \frac{M}{MT_m} \\ &= if_s + f_m \end{aligned} \tag{3.55}$$

This will make the maximum frequency of the computed harmonics to be $Pf_s + f_m$ and the minimum to be $-Pf_s + f_m$.

Since equation (3.28a) represents many equations due to the freedom of k, the approach used will be to substitute in many values for k and generate many equations. Because of the restriction for $k = iN + M$, the terms $\hat{X}(k)$ will be common to all equations, and the many equations may be gathered together into a matrix solution to solve for $\hat{X}(k)$ since there will be as many equations as there are unknowns.

For example, pick $k = N + M$ and $P = 1$:

$$j\omega_{N+M}\hat{X}(N+M) - \frac{\partial F(X, U, N+M)}{\partial X(N+M)}\hat{X}(N+M) - \frac{\partial F(X, U, N+M)}{\partial X(M)}\hat{X}(M) - \frac{\partial F(X, U, N+M)}{\partial X(-N+M)}\hat{X}(-N+M) = \frac{\partial F(X, U, N+M)}{\partial U(M)}\hat{U}(M) \tag{3.56}$$

We can make the following substitutions to simplify the notation:

$$A(k,v) = \frac{\partial F(X, U, k)}{\partial X(v)} \tag{3.57a}$$

$$B(k,v) = \frac{\partial F(X, U, k)}{\partial U(v)} \tag{3.57b}$$

This will simplify the above equation slightly:

$$j\omega_{N+M}\ \hat{X}(N+M) - A(N+M, N+M)\ \hat{X}(N+M) - A(N+M, M)\ \hat{X}(M) - A(N+M, -N+M)\ \hat{X}(-N+M) = B(N+M, M)\ \hat{U}(M) \tag{3.58}$$

Similarly, choose $k = M$ and $P = 1$:

$$j\omega_{M}\ \hat{X}(N+M) - A(M, N+M)\ \hat{X}(N+M) - A(M, M)\ \hat{X}(M) - A(M, -N+M)\ \hat{X}(-N+M) = B(M, M)\ \hat{U}(M) \tag{3.59}$$

and $k = -N + M$ and $P = 1$:

$$j\omega_{-N+M}\,\hat{X}(N+M) - A(-N+M, N+M)\,\hat{X}(N+M) - A(-N+M, M)\,\hat{X}(M) - A(-N+M, -N+M)\,\hat{X}(-N+M) = B(-N+M, M)\,\hat{U}(M) \tag{3.60}$$

These three equations may be gathered together to form:

$$\overline{A}\hat{X} = \overline{B}\hat{U}(M) \tag{3.61}$$

where

$$\overline{A} = j\begin{bmatrix} \omega_{N+M}I & 0 & 0 \\ 0 & \omega_M I & 0 \\ 0 & 0 & \omega_{-N+M}I \end{bmatrix} - \begin{bmatrix} A(N+M, N+M) & A(N+M, M) & A(N+M, -N+M) \\ A(M, N+M) & A(M, M) & A(M, -N+M) \\ A(-N+M, N+M) & A(-N+M, M) & A(-N+M, -N+M) \end{bmatrix} \tag{3.62}$$

$$\hat{X} = \begin{bmatrix} \hat{X}(N+M) \\ \hat{X}(M) \\ \hat{X}(-N+M) \end{bmatrix} \tag{3.63}$$

and

$$\overline{B} = \begin{bmatrix} B(N+M, M) \\ B(M, M) \\ B(-N+M, M) \end{bmatrix} \tag{3.64}$$

Equation (3.61) may be solved for $\hat{X}$ by performing a linear system solve:

$$\hat{X} = \overline{A}^{-1}\overline{B}\hat{U}(M) \tag{3.65}$$

Similar operations may be performed to find the output equation:

$$\hat{Y} = \overline{C}\hat{X} + \overline{D}\hat{U}(M) \tag{3.66}$$

The actual dimensions of $\overline{A}$ and $\overline{B}$ will vary as a function of the number of harmonics, P, but the basic form of equation (3.61) will remain the same. This will be shown in the next section as we look at the special case of $P = 0$.

3.7 A COMPARISON WITH AVERAGING

To show that this new method is equivalent to the averaging method in the simplest case, we will set $P = 0$, which prevents any harmonics other than the modulation fundamental from being included in the solution. We will also set the number of modes to be equal to two, which will allow us to compare against equation (2.6a), the well-known continuous-mode PWM average equation. In this case, equation (3.61)with substitutions for $\overline{A}$ and $\overline{B}$ will simplify to:

$$\left[j\omega_M I - \frac{\partial F(X, U, M)}{\partial X(M)} \right] \left[\hat{X}(M) \right] = \left[\frac{\partial F(X, U, M)}{\partial U(-M)} \right] \left[\hat{U}(M) \right] \tag{3.67}$$

Since we have restricted the case to that of continuous-mode operation, there will be only two modes, so in equation (3.38), $Q = 2$. In the average equations, the control input was $\hat{d}$, the duty cycle modulation. The duty cycle modulation was then handled by auxiliary equations. We will handle this simplification by pretending the duty cycle modulation, $\hat{d}$, is an element of the input vector.

The next step is to find the left and right sides of the above equation. The left first:

$$\begin{aligned}
\frac{\partial F(X, U, M)}{\partial X(M)} &= \sum_{p=1}^{N} \sum_{i=1}^{2} \frac{1}{T_t} \Xi_i e^{-j \frac{2\pi M}{T_t} t_i^{(p)}} \frac{\partial t_i^{(p)}}{\partial X(M)} \\
&+ \sum_{p=1}^{N} \sum_{i=1}^{2} a_i \frac{1}{T_t} \int_{t_{i-1}^{(p)}}^{t_i^{(p)}} e^{-j \frac{2\pi(M-M)}{T_t} \tau} d\tau \\
&= \frac{N}{T_t} \Xi_1 e^{-j \frac{2\pi M}{T_t} t_1} \frac{\partial t_1}{\partial X(M)} + \frac{N}{T_t} \Xi_2 e^{-j \frac{2\pi M}{T_t} t_2} \frac{\partial t_2}{\partial X(M)} \\
&+ a_1 \frac{N}{T_t} \int_{t_0}^{t_1} d\tau + a_2 \frac{N}{T_t} \int_{t_1}^{t_2} d\tau
\end{aligned} \tag{3.68}$$

In this case of a fixed frequency PWM converter, the modulation of t_2 will be zero, since that is the end of the period, and is controlled by a fixed clock. Going ahead and performing the integration, as well as realizing that $T_t = NT_s$, leads to:

$$\frac{\partial F(X, U, M)}{\partial X(M)} = \frac{N}{T_t} \Xi_1 e^{-j\frac{2\pi M}{T_t}t_1} \frac{\partial t_1}{\partial X(M)} + a_1 \frac{t_1 - t_0}{T_s} + a_2 \frac{t_2 - t_1}{T_s} \tag{3.69}$$

In this special case, t_0 will be the beginning of the cycle, and so will be zero. The final time, t_2, will be equal to T_s.

$$\frac{\partial F(X, U, M)}{\partial X(M)} = \frac{N}{T_t} \Xi_1 e^{-j\frac{2\pi M}{T_t}t_1} \frac{\partial t_1}{\partial X(M)} + a_1 \frac{t_1 - 0}{T_s} + a_2 \frac{T_s - t_1}{T_s} \tag{3.70}$$

If we define a duty cycle variable, d, so as to match the notation of Averaging, this will give us:

$$\frac{\partial F(X, U, M)}{\partial X(M)} = \frac{N}{T_t} \Xi_1 e^{-j\frac{2\pi M}{T_t}t_1} \frac{\partial t_1}{\partial X(M)} + a_1 d + a_2(1 - d) \tag{3.71}$$

Next, remember that the duty cycle modulation is set up here to be part of the input vector. This means that the state vector will not contribute to the modulation of the switching instants. This means that $\Xi_1 = 0$, and the equation simplifies to:

$$\frac{\partial F(X, U, M)}{\partial X(M)} = a_1 d + a_2(1 - d) \tag{3.72}$$

We will now consider the right-hand side of equation (3.67). If we proceed the same way as above, we will get to:

$$\frac{\partial F(X, U, M)}{\partial U(M)} = \frac{N}{T_t} \Xi_1 e^{-j\frac{2\pi M}{T_t} t_1} \frac{\partial t_1}{\partial U(M)} + b_1 d + b_2(1 - d) \tag{3.73}$$

We can substitute in and fill out the definition of Ξ:

$$\Xi_1 = (a_1 - a_2)x(t_1) + (b_1 - b_2)u(t_1) \tag{3.74}$$

Next, remember that the duty cycle modulation is set up here to be part of the input vector. This means that the state vector will not contribute to the modulation of the switching instants. This means that $\Xi_1 = 0$, and the equation that describes the modulation of the switching instant simplifies to:

$$\frac{\partial t_1}{\partial U(M)} = \mathrm{H}_1 e^{j\frac{2\pi M}{T_t} t_1} \tag{3.75}$$

This substitutes in to give:

$$\frac{\partial F(X, U, M)}{\partial U(M)} = \frac{N}{T_t} \Xi_1 H_1 + b_1 d + b_2(1 - d) \tag{3.76}$$

Now, we need to examine H_1 in closer detail.

$$H_1 = - \frac{e_1 d_1}{e_1 c_1 \dot{x}(t_1) + e_1 d_1 \dot{u}(t_1) + \alpha_1} \tag{3.77}$$

We said that in order to manipulate this formulation into a similar form as the average equations, we were going to consider the duty cycle modulation input as part of the input vector. Since the duty cycle modulation is not really a physical variable, like a voltage or a current, we will have to resort to some contortions to map this out. It is easier in this formulation to use the H_1 equation to model a PWM modulator of gain equal to one. This means that the voltage ramp of the simple PWM modulator changes one volt in T_s seconds.

With this background, the numerator of equation (3.77) is basically a selection vector to select the input to the simple PWM modulator. The denominator is the one volt per T_s seconds, which will be cancelled by the $\frac{N}{T_t}$ term. This then allows us to substitute in:

$$\frac{\partial F(X, U, M)}{\partial U(M)} = \Xi_1 = [a_1 - a_2] x(t_1) + [b_1 - b_2] u(t_1) \tag{3.78}$$

The above equation is valid for the case where the input is modulating the converter through a simple PWM converter with a period of T_s and a magnitude of one volt.

Putting all of this together gives us:

$$[jI\omega_M - A]\left[\hat{X}(M)\right] = [(a_1 - a_2)x(t_1) + (b_1 - b_2)u(t_1)]\left[\hat{U}\right] \tag{3.79}$$

This compares directly with the averaged equations of equation (2.7a) when the time averaging of the state and input vectors is taken into account. This means that $x(t_1) = \bar{x}$ and $u(t_1) = \bar{u}$.

In conclusion, this new method is much more encompassing of effects it takes into account, but if the same restrictions and simplifications are placed on it as are placed on averaging, the results are the same.

3.8 IMPLEMENTATION

We now know everything we need to fill in equation (3.61) and solve for $\hat{X}(M)$, which will be the frequency component of the perturbed state-vector at the same frequency as the small-signal stimulus. A fully worked-out solution at a single frequency is included in Appendix B, "An Example Solution of the Discontinuous-Mode Boost Converter."

The approximate algorithm will be:

1. Decide on the number of harmonics, P, to include in the solution.

2. Build a system equation using equation (3.61). The contents and size of the $\overline{A}$ and $\overline{B}$ matrices will be a function of P.

3. Fill in the left hand side of equation (3.61) by evaluating equation (3.38), equation (3.35), and equation (3.52a).

4. Fill in the right hand side of equation (3.61) by evaluating equation (3.38b), equation (3 .35), and equation (3.52b).

5. Solve equation (3.61) using complex linear system solve method.

6. This will give $\hat{X}(M)$, which is the state vector at the same frequency as the stimulus.

A similar method is used to solve for the Y vector, given $\hat{X}(M)$.

3.9 CONCLUSIONS

In this chapter, a new method for small-signal analysis has been derived, and algorithms for a computer implementation given. The method presumes a piecewise-linear circuit formulation, and the existance of a periodic-steady-state operating point.

The problem that this method actually solves is the periodic steady-state solution of the original switching power system with the addition of a sinusoidal small-signal stimulus. The frequency component of the output variable that is at the same frequency as the stimulus will be used to measure the small-signal transfer function.

The new method has also been compared with averaging, and is found to be equivalent when the same simplifications and restrictions are in place. In this approach, taking no additional harmonics into account, $P = 0$, will give the average response.

4.0 Examples

4.1 INTRODUCTION

Four examples will be given in this chapter. The first example is a simple open-loop boost converter running at a fixed-frequency with pulse-width modulation, and continuous inductor current. This converter was designed so that the requirement of state-space averaging for the power stage time constants to be significantly longer than the period of the converter was not well met. It is shown in this example that this new method compares very well against the measured control-to-output transfer function, but that averaging diverges from the measured response significantly below half the switching frequency. Averaging is also compared against this new method for Audiosusceptibility and output impedance.

The second example is the same power stage as before, except running in the discontinuous mode of operation. Again, this new method compares well against the measured response.

The third example is the same power stage, except that the control method has been changed to current-mode control. This example is used to show how this new method predicts the peaking at half the switching frequency as the duty cycle approaches 0.5. The predicted response compares well against the measured.

The fourth example is a complete converter in closed-loop operation. This is a low performance converter that is used to provide bias to circuitry inside a power supply. It runs from an input voltage of 100 to 400V, and provides a 13V output at a maximum of 1A,

typically less than 0.5A. Predictions are made for loop gain, output impedance, and Audiosusceptibility.

4.2 BOOST - PWM - CONTINUOUS MODE - OPEN LOOP

The power converter circuit used in this example is a simple pulse-width modulated (PWM) boost converter running in the continuous inductor current mode. In this particular mode of operation the inductor current never remains at zero for any appreciable length of time. The schematic for the experimental lab hardware is detailed in Figure 4-1

As can be seen from this schematic, the converter was not running in a closed-loop fashion, but was instead running in an open-loop mode. This was done to verify the correct functioning of the PWM and the power stage in the simulation. The potentiometer R1 is used to divide down the reference voltage to provide a signal which will be used to determine the duty cycle of the PWM. The error amplifier in the control module U1 is connected as a unity-gain, non-inverting amplifier. The potentiometer R1 is connected to the input of this amplifier. The output of the error amplifier is connected internally within the control module to a comparator. The other input of the comparator is connected internally to a ramp generator.

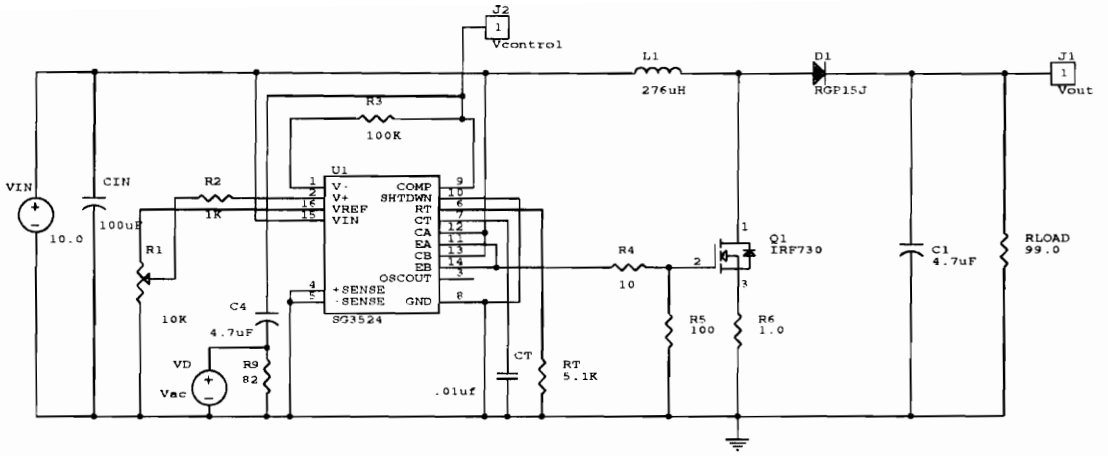

Figure 4-1. Boost Converter Schematic

The output stages of the control module are connected in parallel to drive to power FET, Q1, through the gate resistor R4. The resistor R5 is used to guarantee an "off"-drive for Q1 even when the control module is not powered. Resistor R5 is not strictly necessary. The FET Q1 has a current sense resistor, R6, in the source lead. This resistor is also not strictly necessary for the functioning of this circuit, but was put into the circuit to make measuring the current through Q1 simpler.

The timing components RT and CT are chosen to give a switching frequency of about 22KHz.. The inductor L1 and the capacitor C1 form the actual LC components of the power stage, and were chosen to give a resonant frequency much closer to the switching frequency than would normally be chosen. This was done on order to stress the requirements for state-space averaging, which needs a fairly low power stage resonant frequency to satisfy the

requirements of linear ripple. This gives an output capacitance, C1, which is much lower in value than would normally be chosen.

The schematic that describes what was actually simulated is in Figure 4-2. This is a much simpler schematic for several reasons. First, the power FET, Q1, and the output diode, D1, are modelled as resistors of values PSW1 and PSW2, respectively. The values of PSW1 and PSW2 are specified by Table 4-1.

Table 4-1. Values of Parameters PSW1 and PSW2 as a function of Switching Mode. Parameters PSW1 and PSW2 take on different values depending on the conditions of the ideal switches Q1 and D1. If a switch is "on" then the parameter will have a resistance very close to an ideal short circuit, otherwise the parameter will have a resistance approximating an open circuit.

Parameter, Ohms	**Mode 1 (Q1 on, D1 off)**	**Mode 2 (Q1 off, D1 on)**
PSW1	1e-6	1e6
PSW2	1e6	1e-6

The second reason the schematic is simpler is that the PWM control module and its surrounding circuitry has been abstracted and simplified down to the barest minimum linear elements along with algebraic equations describing the boundary conditions governing the switching from one switch mode to another.

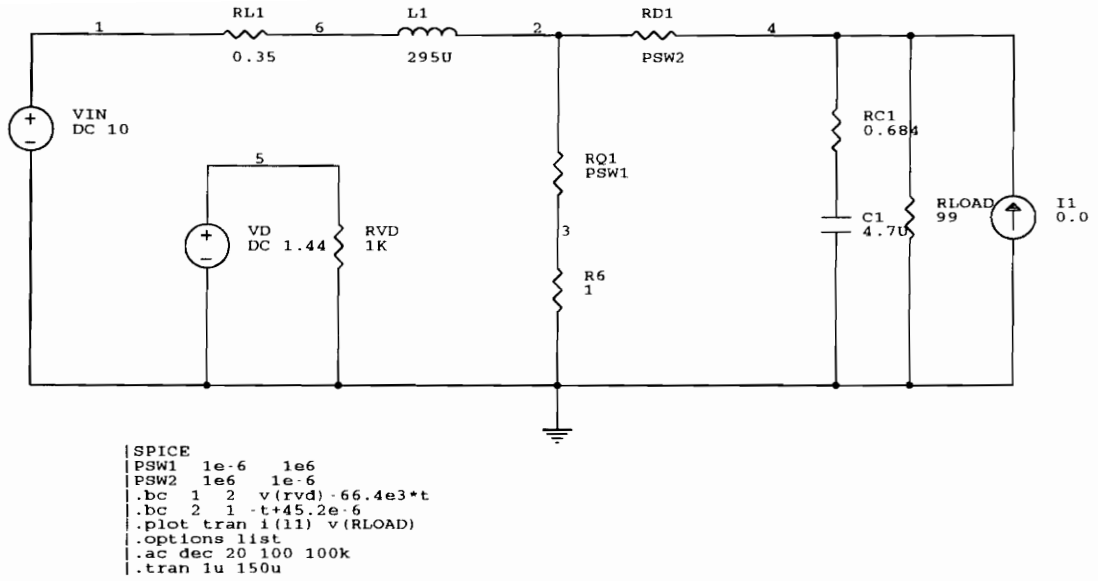

Figure 4-2. Boost Converter Simulation Schematic

In a continuous inductor current mode of operation, the switches will cycle back and forth between Modes 1 and 2. To describe the boundary condition equation governing the transition between Mode 1 and 2, it is first necessary to determine an equation describing the ramp generated inside the control module. From the specifications of the module, this will be

$$Vramp(t) = 66.4 \times 10^3 \times t \tag{4.1}$$

Referring back to Figure 4-1, the modulation signal that is measured is forced in and directly compared against the internal ramp, *Vramp* . When these two voltages equal in value, the output stage of the control module turns Q1 "off," and the resulting circuit

equations will require that D1 turns "on" in order to satisfy the requirement that the current in L1 cannot change instantaneously. The equation describing this boundary condition will then be:

$$Vcontrol - Vramp(t) = 0 = V(Rvd) - 66.4e3 \times T \tag{4.2}$$

The change from Mode 2 back to Mode 1 is governed simply by the timing out of the switching period. This boundary condition equation is described by

$$-T + 44.5E - 6 = 0 \tag{4.3}$$

The netlist for the schematic of Figure 4-2 was automatically generated, and is listed in Figure 4-3.

The netlist from Figure 4-3 was used as the input to the new program STAEQ2. This program solves for the systems of state-space equations for all of the required combinations of switches. The output of STAEQ2 is then used as the input for the modified COSMIR program SIMU. SIMU is used to compute the steady-state operating trajectory of the circuit. SIMU has been modified to additionally feed out the necessary information for input to the ACF program, which calculates the small-signal AC transfer functions.

The plot in Figure 4-4 shows the transfer function from the control to the output voltage with several harmonics being taken into account. For reference, the actual hardware measurement is also displayed.

```
PSW1  1E-6   1E6
PSW2  1E6   1E-6
.BC  1  2  V(RVD)-66.4E3*T
.BC  2  1 -T+45.2E-6
.PLOT TRAN I(L1) V(RLOAD)
.OPTIONS LIST
.AC DEC 20 100 100K
.TRAN 1U 150U
I1 0 4 0.0
RL1 1 6 0.35
RC1 10006 4 0.684
R6 3 0 1
RVD 5 0 1K
L1 6 2 295U
C1 10006 0 4.7U
RLOAD 4 0 99
VD 5 0 DC 1.44
VIN 1 0 DC 10
RQ1 2 3 PSW1
RD1 2 4 PSW2
.END
```

Figure 4-3. Simulation Netlist

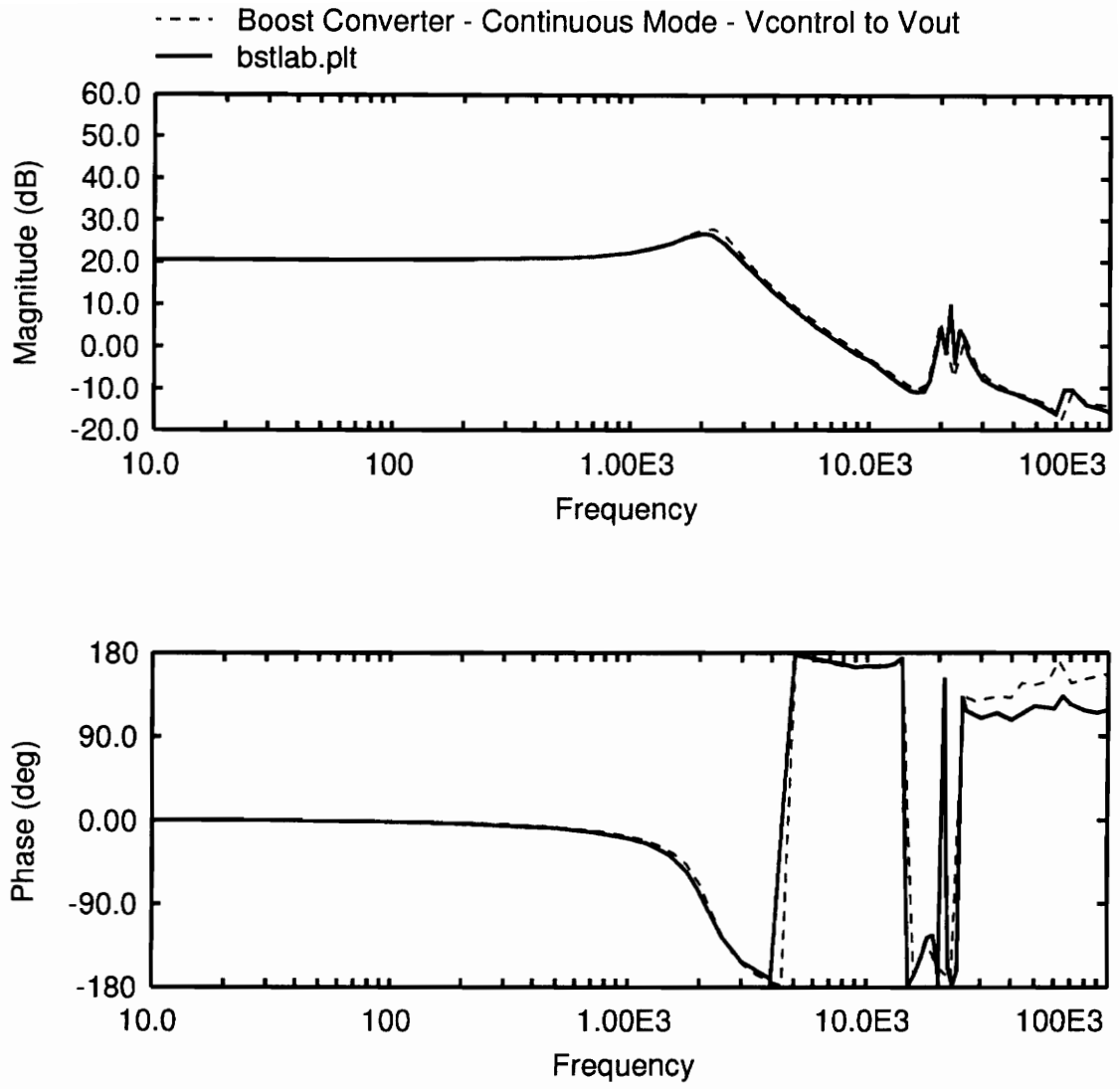

Figure 4-4. Vcontrol to Vout Transfer Function - 3 Harmonics

As a point of reference, the same control to output transfer function was computed using state-space averaging, and is compared against the actual hardware measurement in

Figure 4-5. Notice the large discrepancy between the prediction and measurement at frequencies well before the one-half switching frequency point.

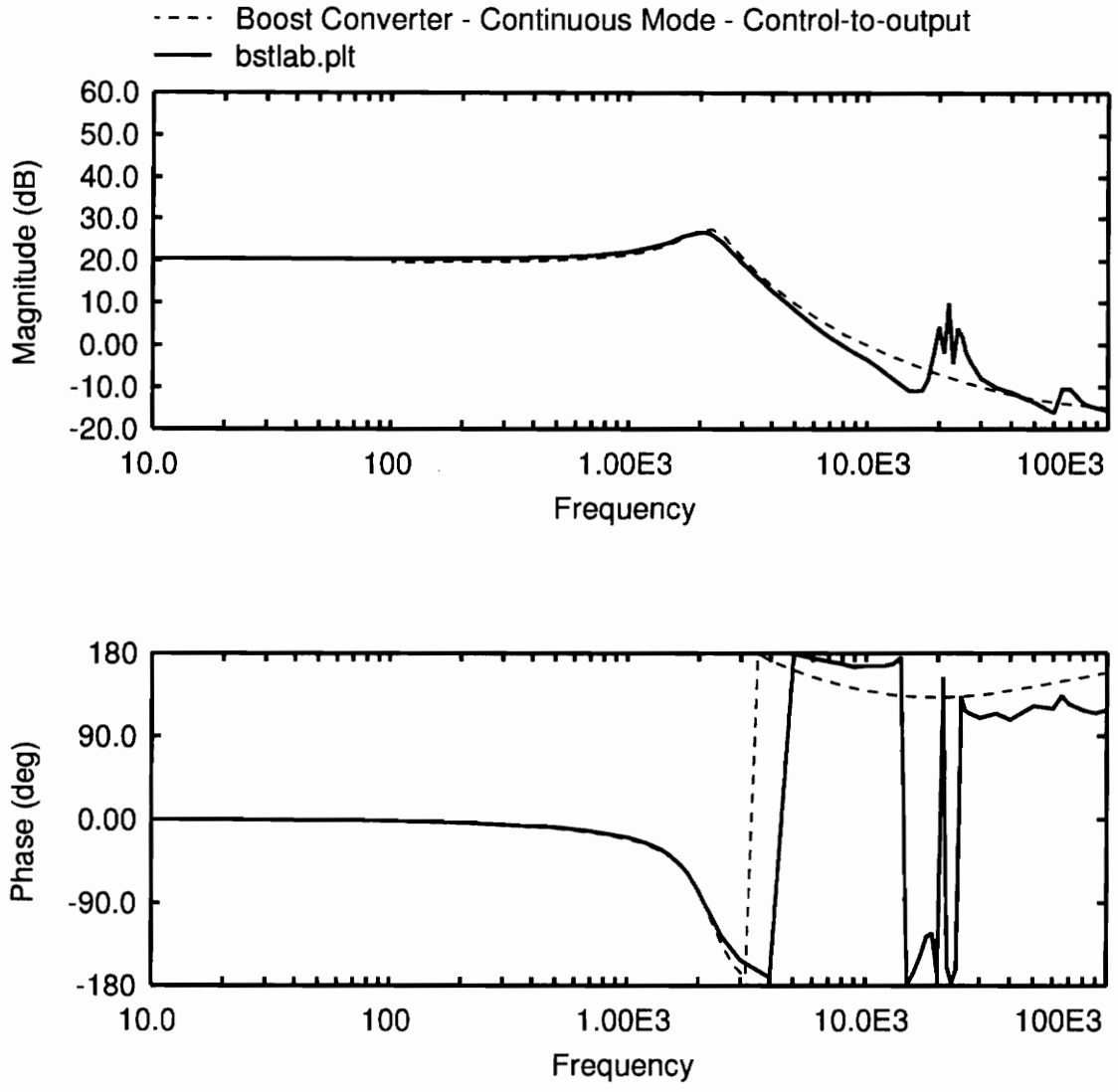

Figure 4-5. Vcontrol to Vout Transfer Function - Average Model

The small-signal output impedance was calculated by running the ACF program again, this time stimulating the current source I1, and measuring the ratio of V(RLOAD) and I1. The resulting output impedance plot is in Figure 4-6

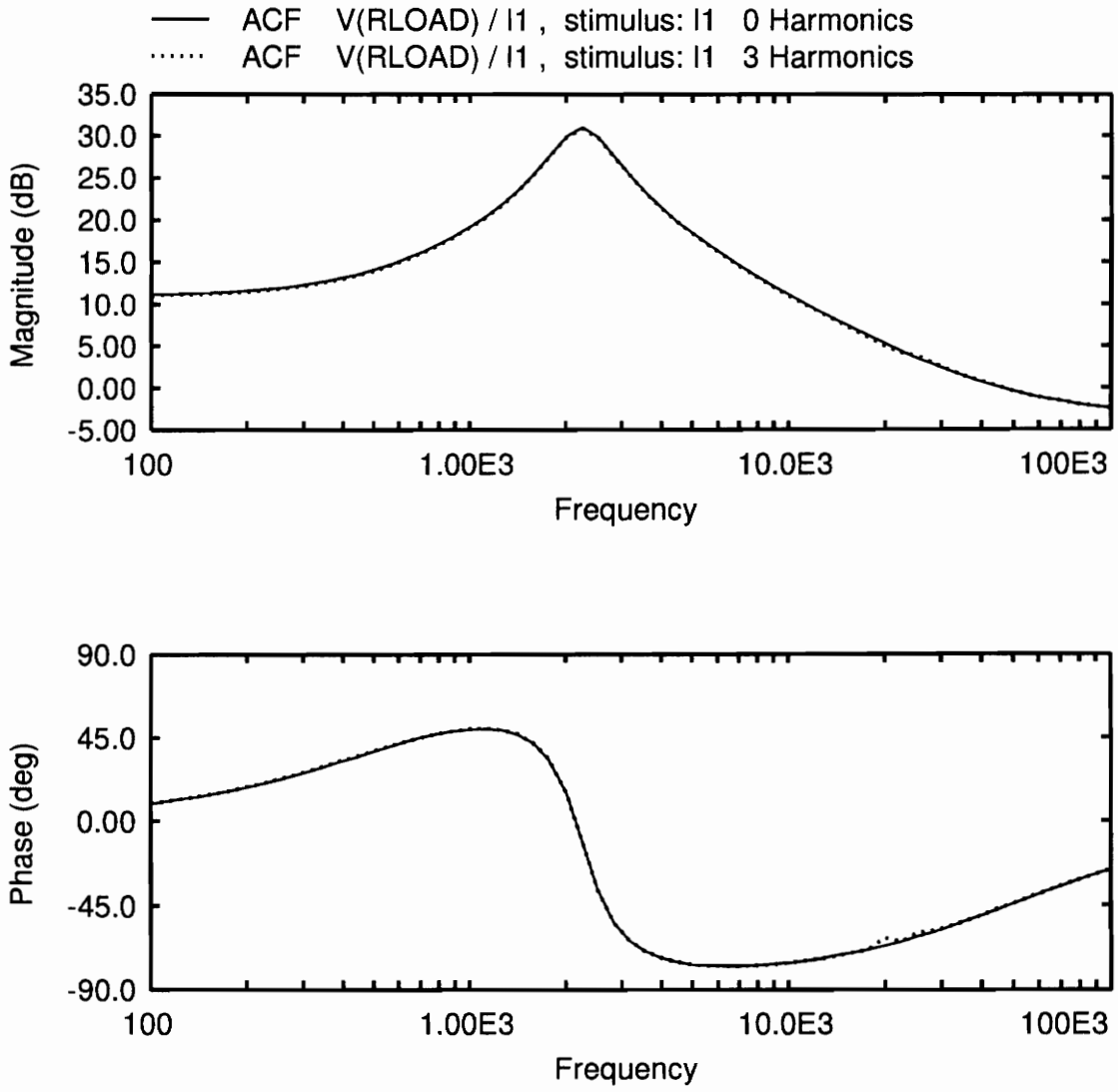

Figure 4-6. Small-Signal Output Impedance

The Audiosusceptibility was computed by running ACF again, this time stimulating the input voltage source VIN and measuring the ratio of V(RLOAD) and VIN. A plot of this response is in Figure 4-7.

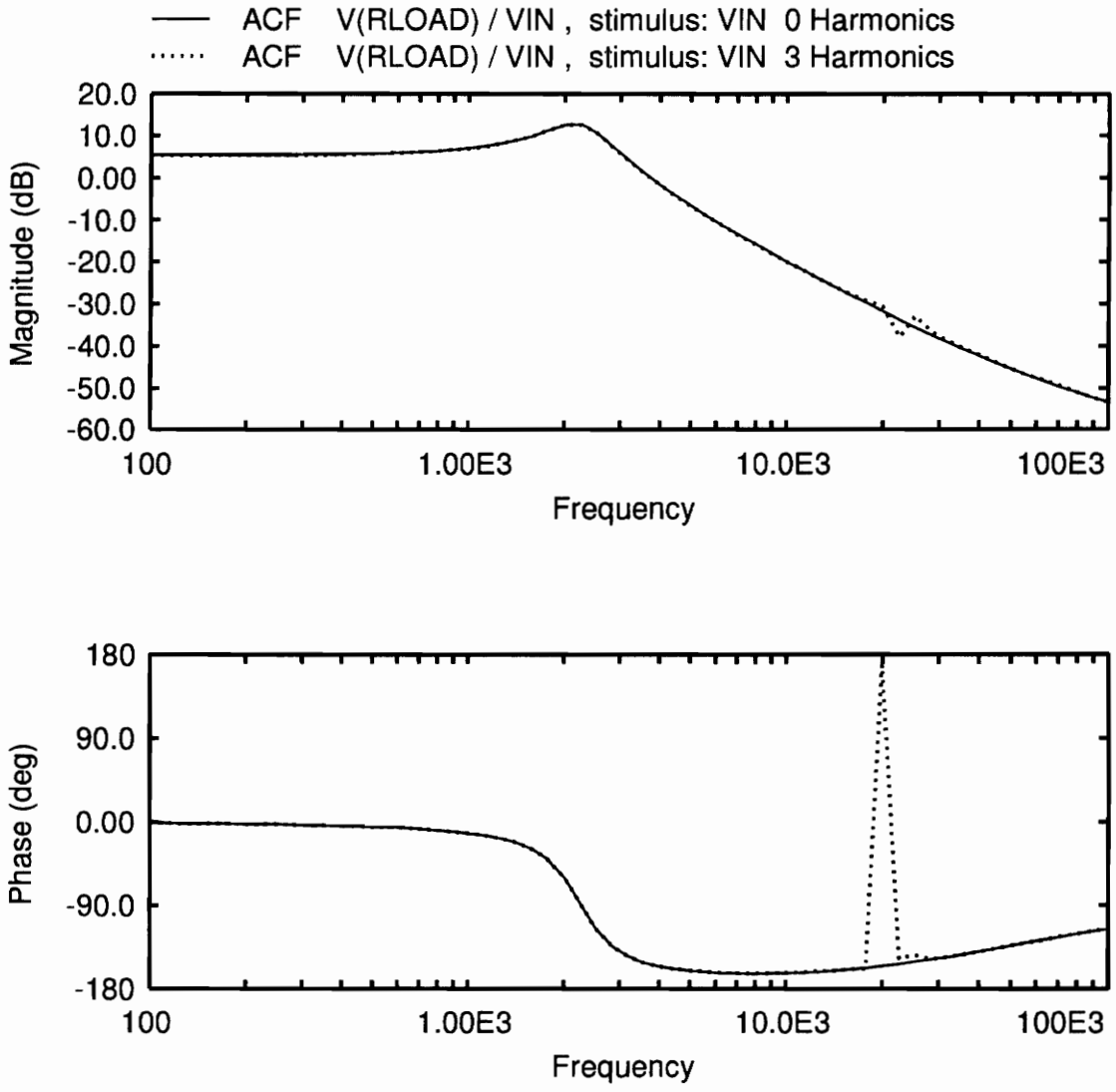

Figure 4-7. Audiosusceptibility

4.3 BOOST - PWM - DISCONTINUOUS MODE - OPEN LOOP

This is essentially the same converter as the previous example except for the load resistor being increased in value. This places the power stage into the discontinuous inductor current mode of operation. In this mode, the inductor current remains at zero for a significant portion of a switching period. A characteristic of this type of operation is the reduction of the number of poles in the transfer function from a complex pair to a pair of widely split real poles. The pair of real poles is so widely split that it appears to be a single pole system[13]. The schematic for the actual lab hardware is detailed in Figure 4-8.

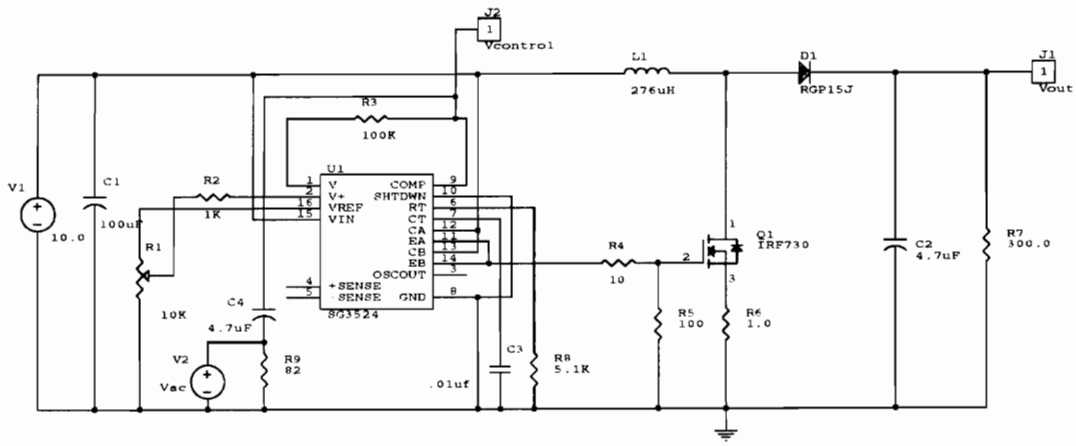

Figure 4-8. Discontinuous Boost Converter Schematic

In this converter there are three switching modes. Mode 1 and 2 are the same as the previous example. An additional mode, Mode 3 corresponds to both Q1 and D1 being "off." This is described by the following table:

Table 4-2. Values of Parameters PSW1 and PSW2 as a function of Switching Mode. Parameters PSW1 and PSW2 take on different values depending on the conditions of the ideal switches Q1 and D1. If a switch is "on" then the parameter will have a resistance very close to an ideal short circuit, otherwise the parameter will have a resistance approximating an open circuit.

Parameter, Ohms	**Mode 1 (Q1 on, D1 off)**	**Mode 2 (Q1 off, D1 on)**	**Mode 3 (Q1 off, D1 off)**
PSW1	1e-6	1e6	1e6
PSW2	1e6	1e-6	1e6

The schematic used for simulation is in Figure 4-9.

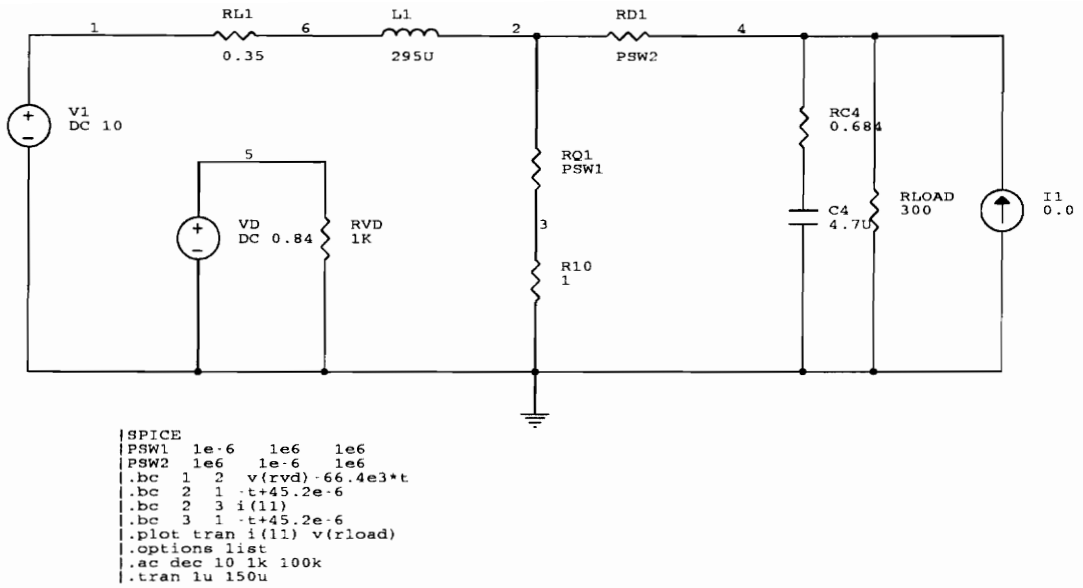

Figure 4-9. Discontinuous Boost Converter Simulation Schematic

In discontinuous mode, there are additional boundary condition equations to be considered. Besides the two boundary conditions from the previous example, there are an additional two equations. In the case of this particular circuit, it is possible to also go from Mode 2 to Mode 3, and from Mode 3 to Mode 1. To go from Mode 2 to Mode 3 requires that both Q1 and D1 are "off." Since in Mode 2 Q1 is "off" and D1 is "on," the inductor current going to zero also signifies the diode current going to zero. This will signal the time for D1 to turn "off." The equation describing this is

$$I(L1) = 0 \tag{4.4}$$

The boundary equation signifying the transition from Mode 3 to Mode 1 is simply the end of the switching period:

$$-T + 44.5E - 6 = 0 \tag{4.5}$$

The netlist for the schematic of Figure 4-9 was automatically generated, and is listed in Figure 4-10.

The programs STAEQ2 and SIMU were run to find the state-space equations and to solve for periodic steady state. The ACF program was run to solve for the control to output transfer function, which is plotted in Figure 4-11 along with actual hardware measurements.

```
PSW1  1E-6   1E6   1E6
PSW2  1E6   1E-6   1E6
.BC  1  2  V(RVD)-66.4E3*T
.BC  2  1 -T+45.2E-6
.BC  2  3 I(L1)
.BC  3  1 -T+45.2E-6
.PLOT TRAN I(L1) V(RLOAD)
.OPTIONS LIST
.AC DEC 10 1K 100K
.TRAN 1U 150U
I1 0 4 0.0
RL1 1 6 0.35
RC4 10006 4 0.684
R10 3 0 1
RVD 5 0 1K
L1 6 2 295U
RLOAD 4 0 300
C4 10006 0 4.7U
VD 5 0 DC 0.84
V1 1 0 DC 10
RQ1 2 3 PSW1
RD1 2 4 PSW2
.END
```

Figure 4-10. Simulation Netlist

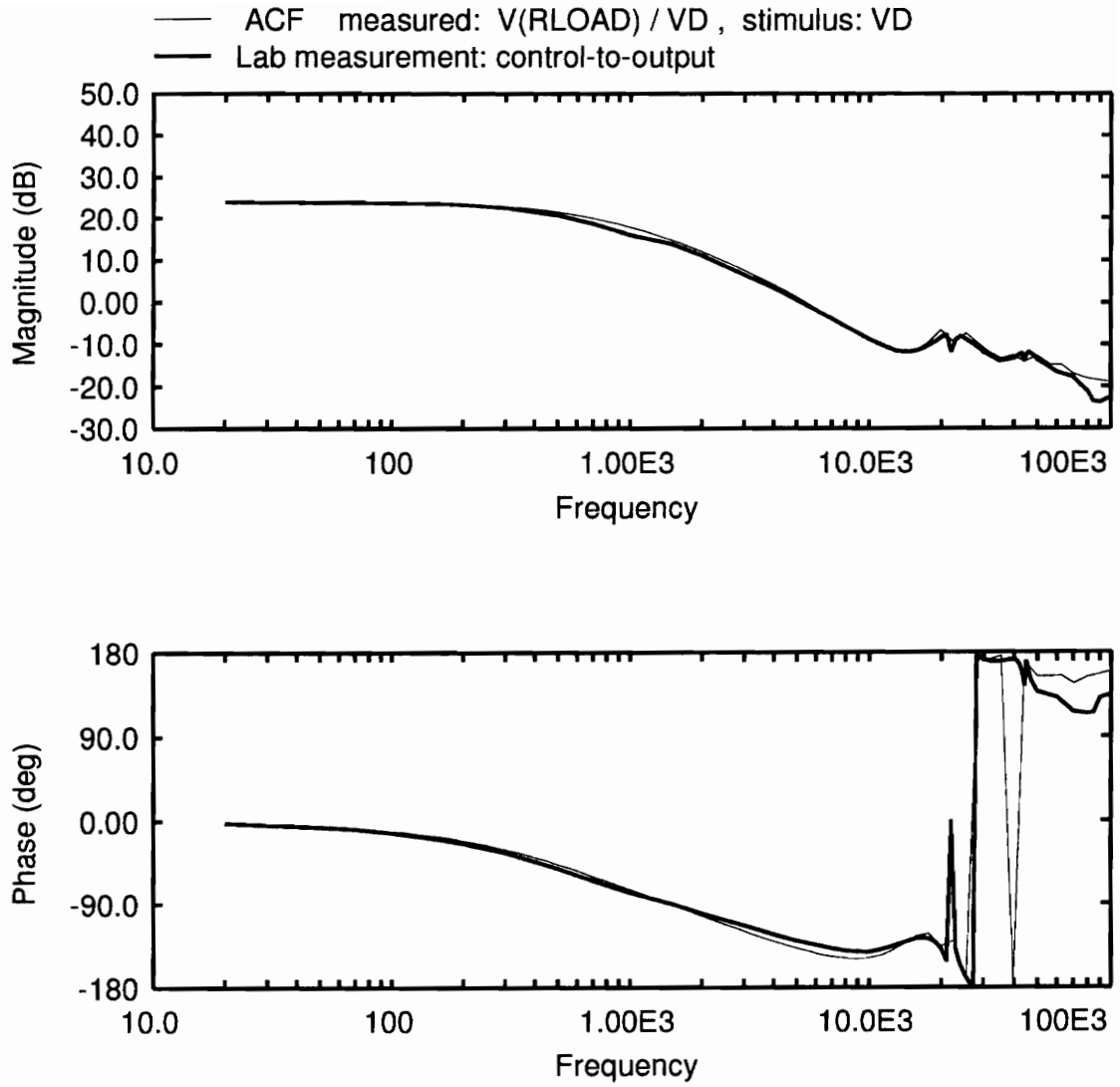

Figure 4-11. Vcontrol to Vout Transfer Function

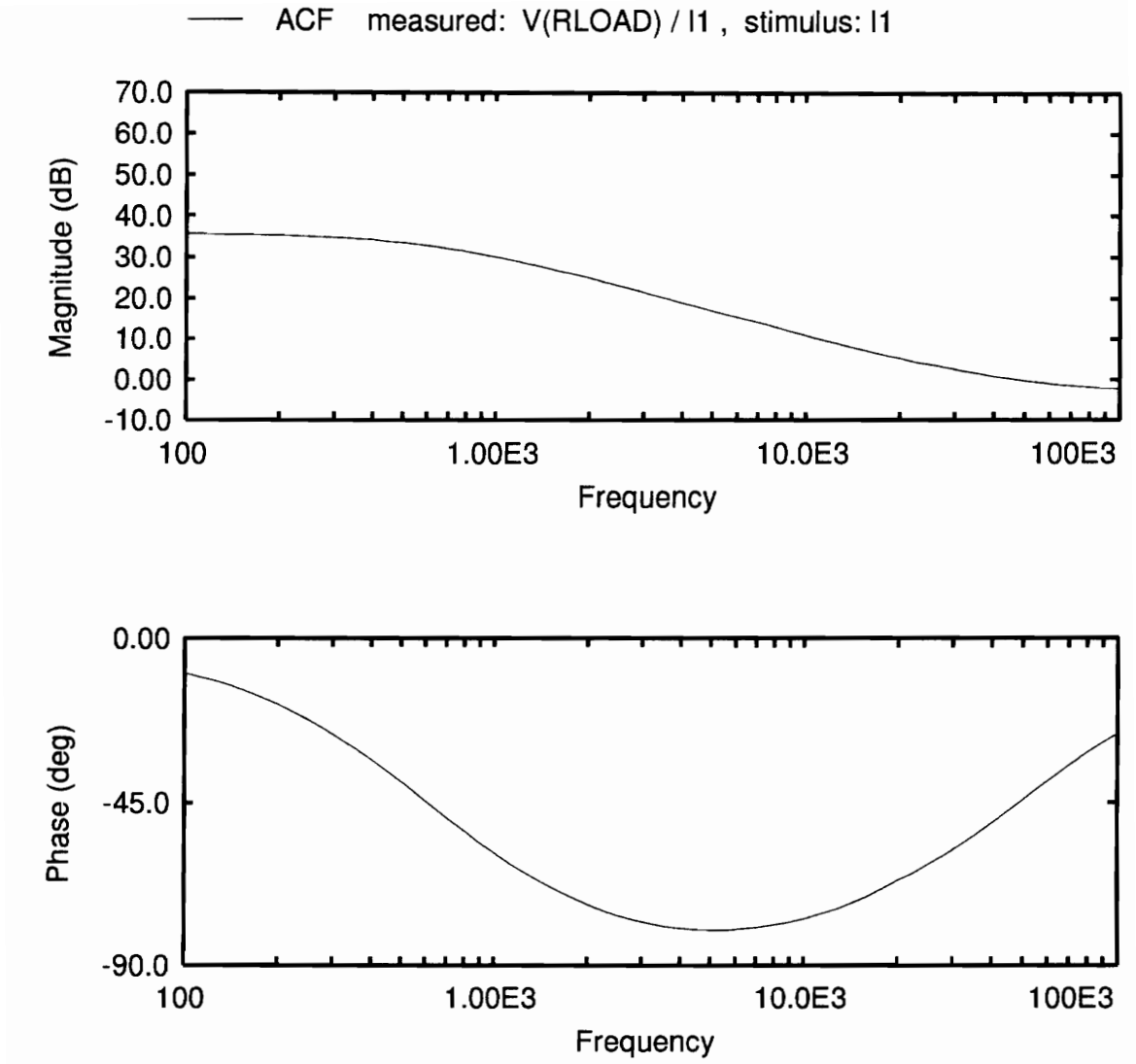

Figure 4-12. Small-Signal Output Impedance

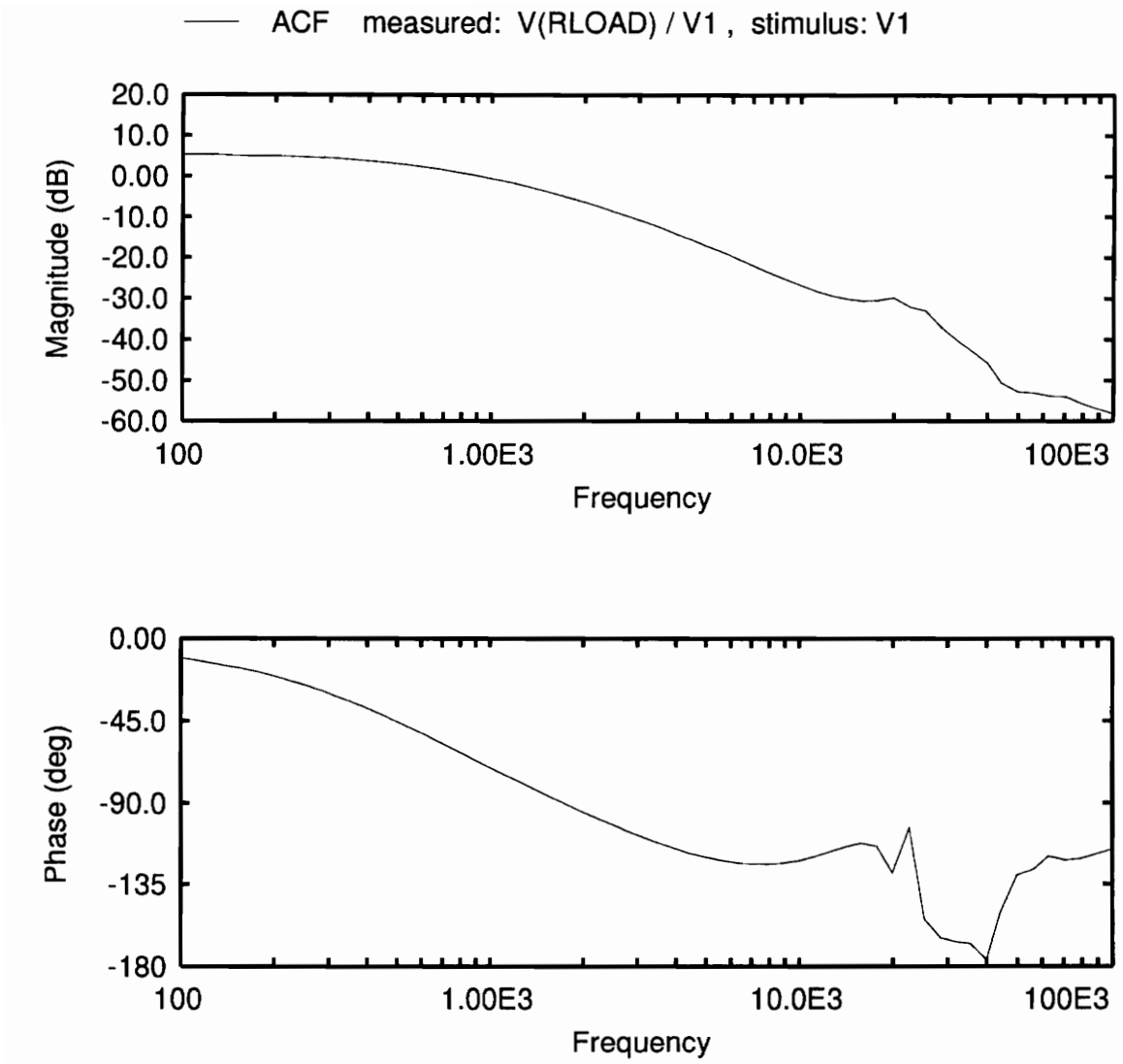

Figure 4-13. Audiosusceptibility

4.4 BOOST - PWM - CONTINUOUS MODE - CURRENT MODE CONTROL

This example uses the same power stage from the previous examples, this time with a different control system. Current-mode control is implemented with a UC3842 control module. In this form of control the error voltage is compared against the natural ramp of the inductor current to control the "on" time of the power FET.

In Figure 4-14, it can be seen that the power stage is running off of a different voltage supply than the control module. Source V3 supplies the control module U1, which requires a startup voltage of 17V just to activate the module. Once the module was started, V3 was backed down to 12V to minimize stress on the module and the gate of the power FET.

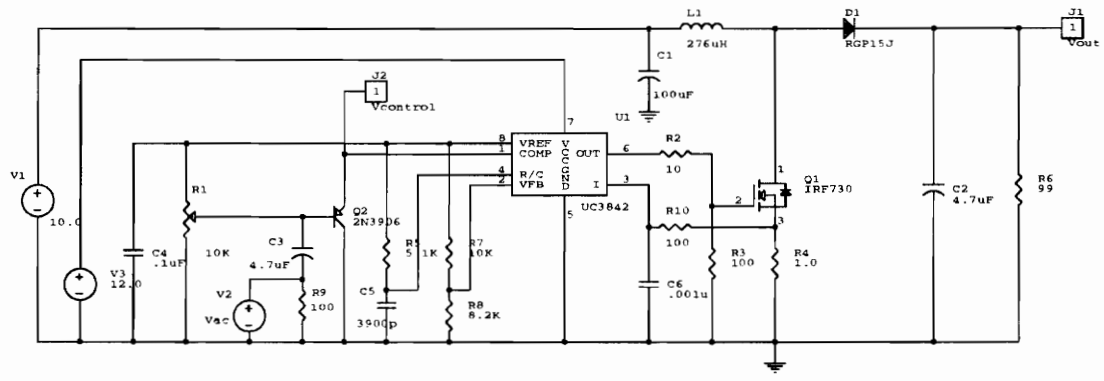

Figure 4-14. Current-Mode Control Boost Converter Schematic

The output of the error amplifier of the control module is configured by resistors R7 and R8 to be biased high all the time. PNP transistor Q2 is biased by variable resistor R1 so that Q2 will pull down the output of the error amplifier. This allows the voltage on the COMP pin to be controlled by adjusting R1. Internal to U1, the voltage on the COMP pin is divided down and compared against the voltage on pin 3, the current sense pin, thus adjusting the "on" time of the power FET.

The stimulus source from the network analyzer is capacitively coupled to the base of Q2 by capacitor C3. This places modulation onto the COMP pin, which will cause the peak of the current sense pin to be modulated. The voltage on the COMP pin, Vcontrol, is measured to determine the amount of reference signal stimulating the circuit.

The current through Q1 is measured by the current sense resistor R4, and filtered by R3 and C6. This filter is necessary to eliminate false triggering due to the leading edge current spike caused by turning on Q1 and turning off D1.

The circuit that was actually simulated is in Figure 4-15.

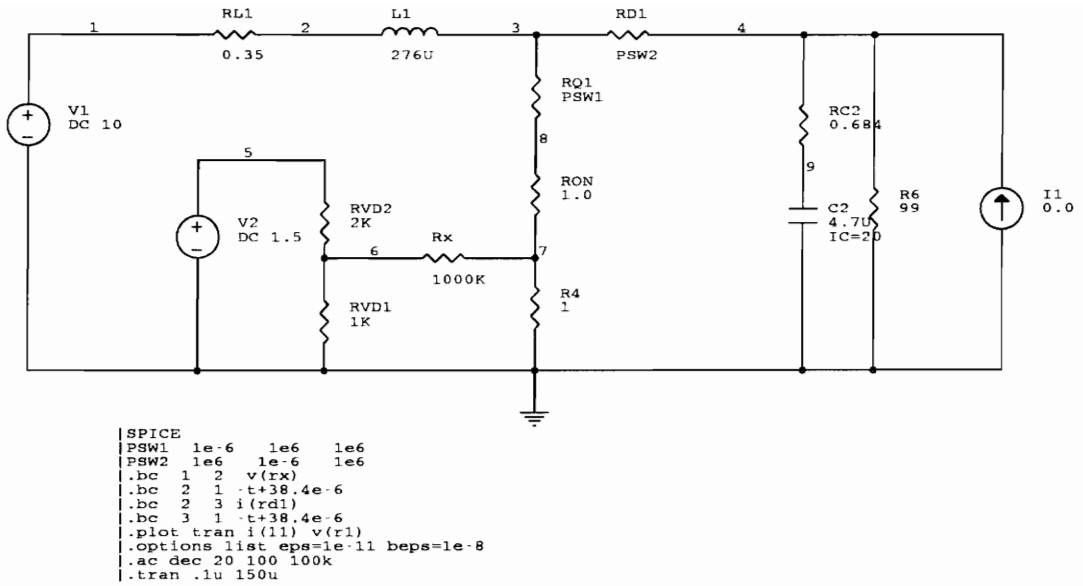

Figure 4-15. Current-Mode Control Boost Converter Simulation Schematic

```
*
*
PSW1  1E-6   1E6   1E6
PSW2  1E6   1E-6   1E6
.BC  1  2  V(RX)
.BC  2  1 -T+38.4E-6
.BC  2  3 I(RD1)
.BC  3  1 -T+38.4E-6
.PLOT TRAN I(L1) V(R1)
.OPTIONS LIST EPS=1E-11 BEPS=1E-8
.AC DEC 20 100 100K
.TRAN .1U 150U
I1 0 4 0.0
RL1 1 2 0.35
RC2 9 4 0.684
R4 7 0 1
RON 8 7 1.0
RX 6 7 1000K
RVD1 6 0 1K
L1 2 3 276U
RVD2 5 6 2K
C2 9 0 4.7U IC=20
R6 4 0 99
V2 5 0 DC 1.5
V1 1 0 DC 10
RQ1 3 8 PSW1
RD1 3 4 PSW2
.END
```

Figure 4-16. Simulation Netlist

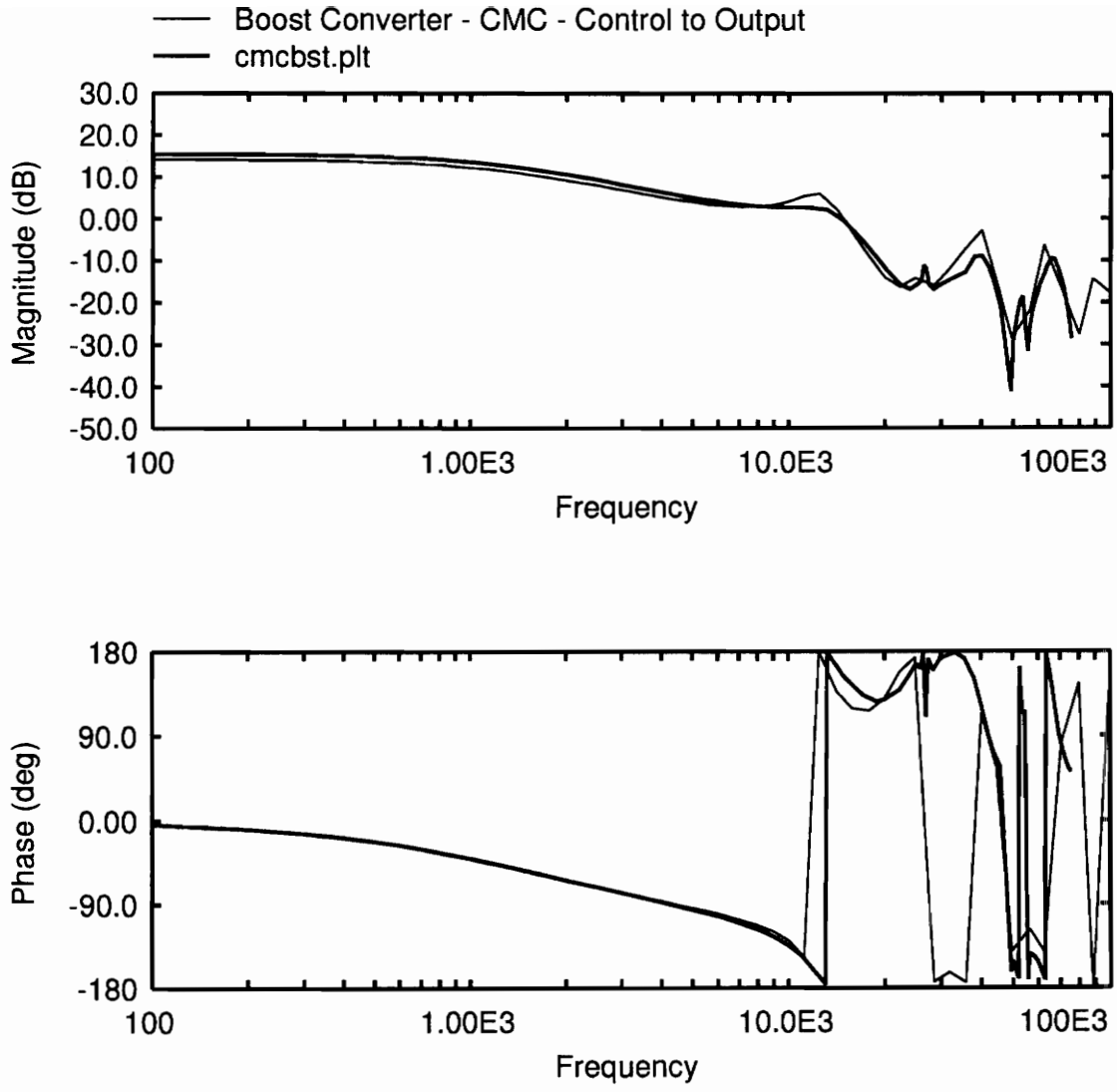

Figure 4-17. Vcontrol to Vout Transfer Function

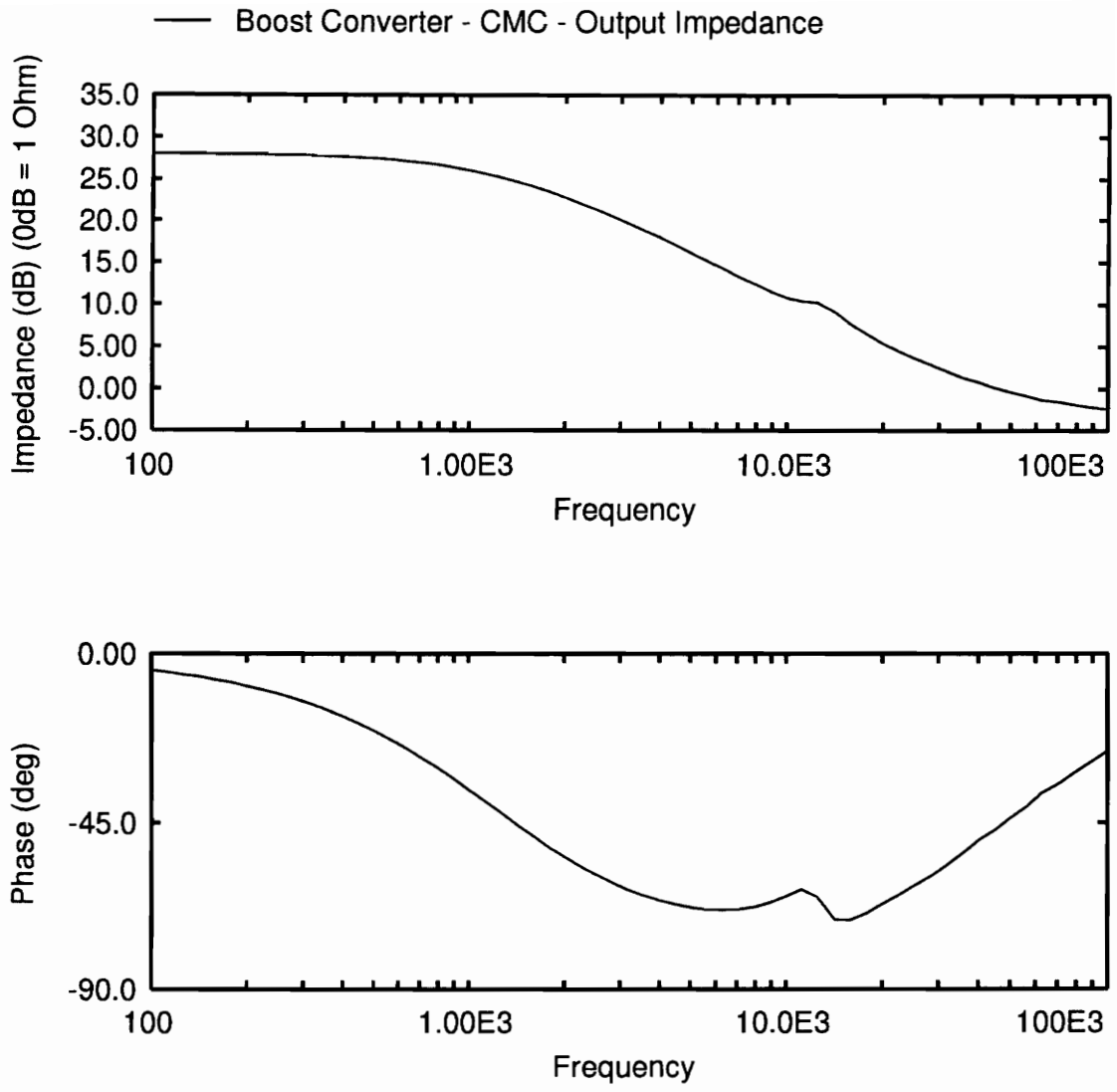

Figure 4-18. Small-Signal Output Impedance

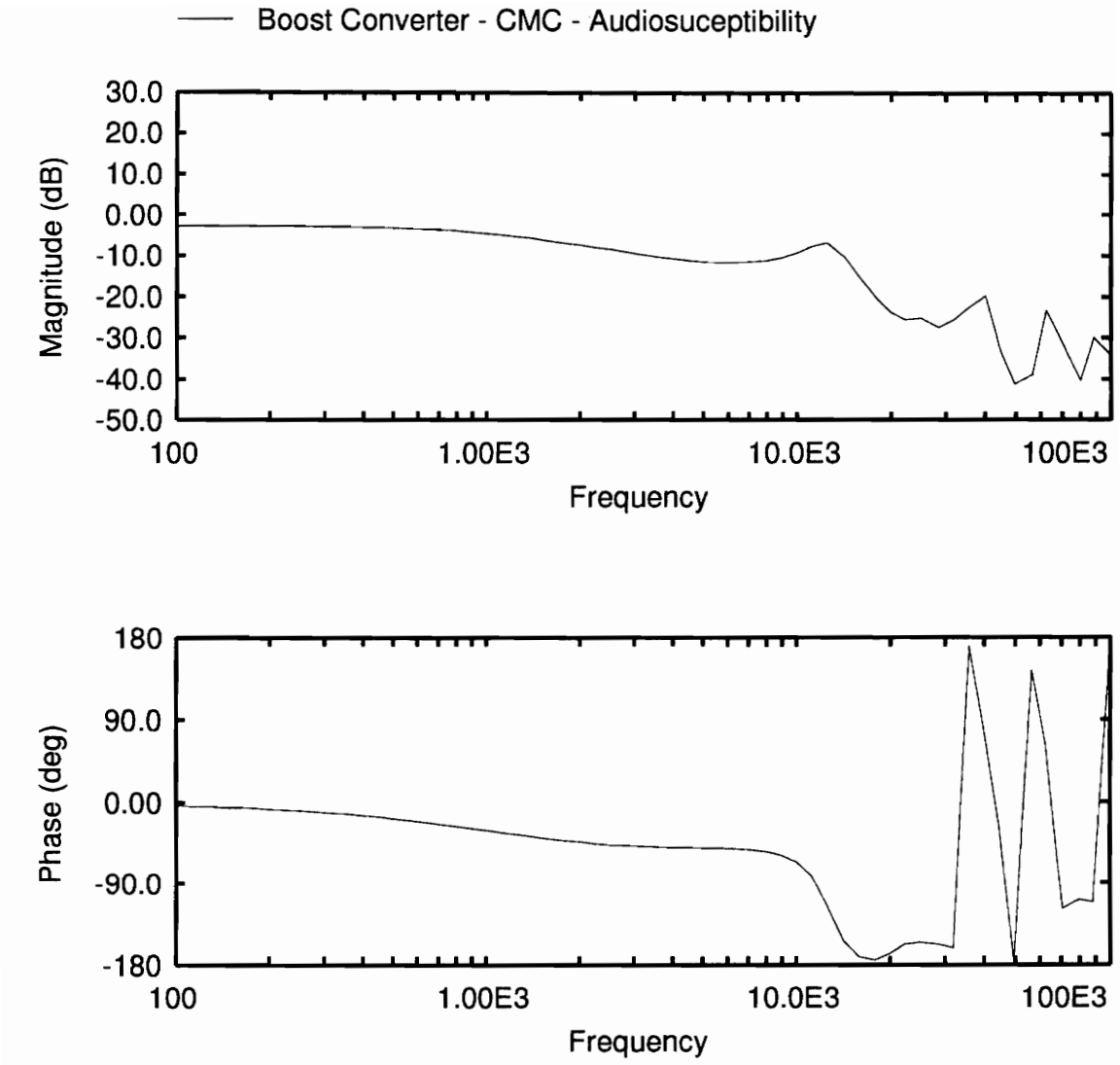

Figure 4-19. Audiosusceptibility

4.5 CURRENT-MODE CONTROL FLYBACK BIAS REGULATOR

The last example is a complete regulator system. This utilizes a discontinuous-mode flyback converter, with a current-mode control PWM control module. To keep the losses low, this converter was designed to operate at a relatively low switching frequency of about 30KHz.. The complete schematic is in Figure 4-20.

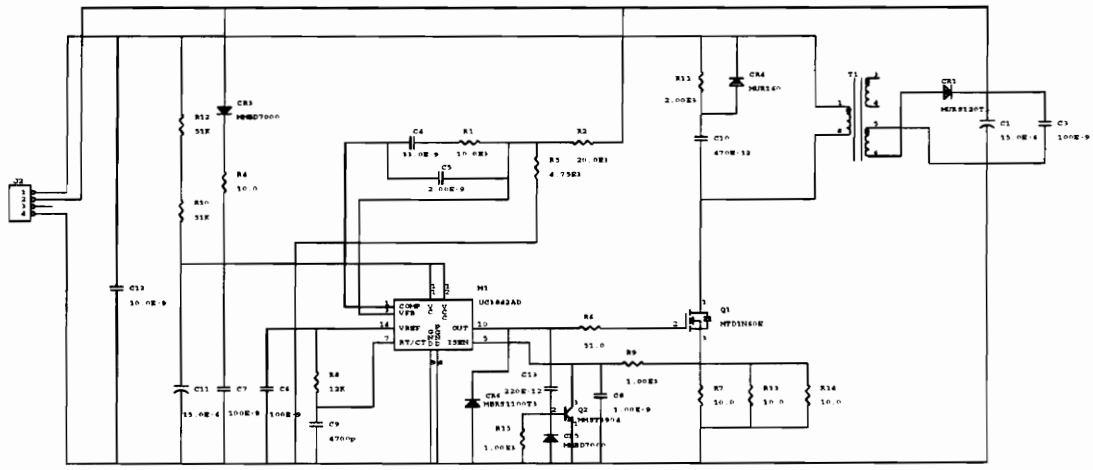

Figure 4-20. Flyback Bias Converter Schematic

The control module, a UC3842, is initially biased from a total of 102KΩ from the input bus, which varies between 100V and 400V. The resistor values of R10 and R12 are chosen to guarantee that the module will be able to start up at 100V input voltage, and also to limit the dissipation at the high input of 400V. Once the converter gets up and running, the

module will be bootstrapped off of the output winding through CR3 and current-limiting resistor, R4.

The current through the switching Fet, Q1, is monitored by the parallel combination of R7, R13, and R14. These resistors were paralleled only to get the necessary value of resistance, 3.3Ω, which was not in our parts library. The voltage across these resistors will have a large leading edge spike when the fet turns on, due to device capacitances. The parts C13, R15, CR5, Q2, C8, and R9 form a filter that blanks out the leading edge spike. The small transistor, Q2, briefly turns on during the leading edge of the current sensed across R7, and so shorts out the leading edge spike. It quickly releases, and the voltage across R7 ramps up as expected.

The diode from ground to the gate drive, CR6, is used to clamp any possible negative spikes on the gate drive pin that would upset the internal chip device isolation beds.

There is some slight snubbing used, which are components R11, CR4, and C10. Since the power output of this converter is only about 15 Watts, and since it operates in discontinuous mode, it doesn't really need a lot of snubbing. If it operated in continuous mode, the output diode, CR1, would need some snubbing.

The divider composed of R2 and R5 divide the 13V output down to the 2.5V that the control module expects. The feedback components, C4, R1, and C5, work in conjunction with R2 and R5 to set the frequency response of the error amplifier.

The circuit that was simulated in COSMIR is in Figure 4-21. This is a much simpler circuit than the complete schematic of Figure 4-20, although it does need explanation.

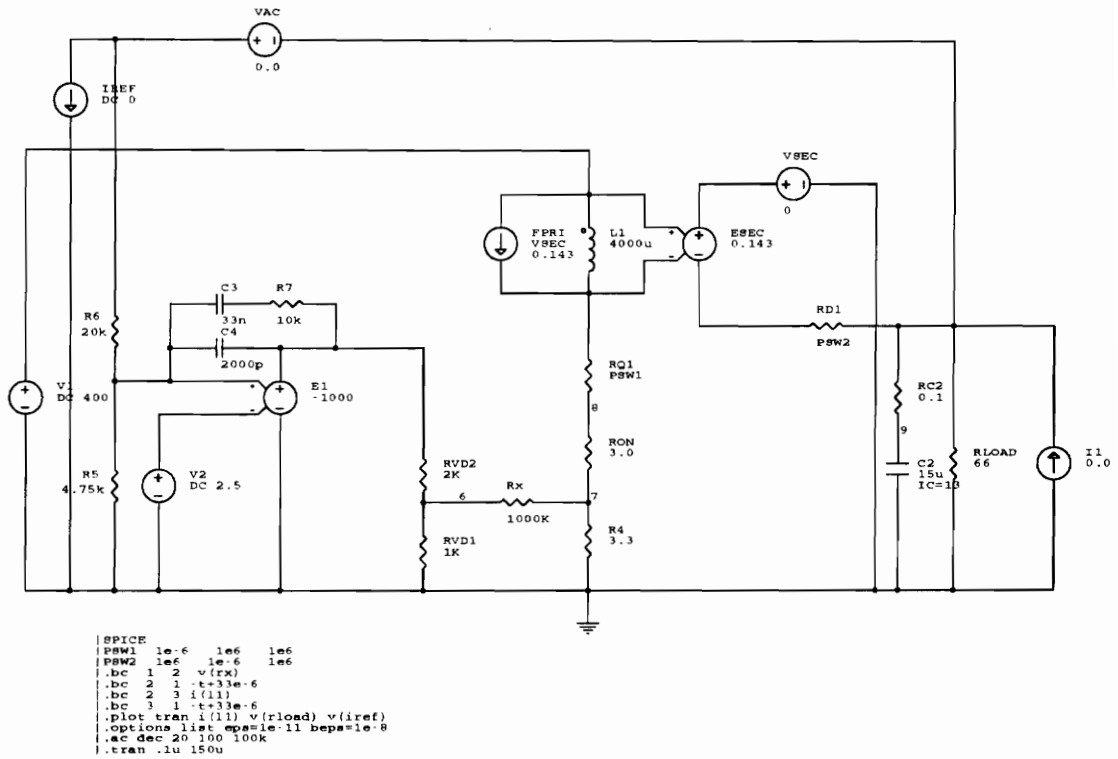

Figure 4-21. Flyback Bias Converter Simulation Schematic

The transformer is modelled using L1, which represents the primary magnetizing inductance of the transformer, and using mutually dependent sources, ESEC and FPRI. The output diode is modelled as an ideal resistor whose value is a parameter which takes on three values. The switching Fet is also modelled as an ideal resistor and parameter. The error amplifier of the control module is modelled as a voltage-controlled voltage source, E1. The UC3842 as an internal divider which divides the signal at the output of the error amplifier by three before it is compared against the current sense voltage. This divider is modelled by

resistors RVD2 and RVD1. The voltage across resistor RX is used to compare the divided error amplifier voltage against the current sense voltage.

This is modelled so that the circuit will come up and regulate in a closed-loop fashion, but the loop injection components are included so that the AC small-signal loop-gain transfer function may be easily measured. The loop injection components are modelled by the zero-valued voltage source, VAC, and the zero-valued current source, IREF. An injection point into the output for output impedance measurements is modelled by the zero-valued current source, I1.

The netlist that was generated by the schematic of Figure 4-21 is detailed below.

When steady-state was found, then the ACF program was used to simulate various transfer functions. The first was the loop-gain transfer function which was simulated by connecting the stimulus to VAC. Then the ratio of V(RLOAD) to V(IREF) was computed to get the loop gain. This is shown in Figure 4-23. It is not a high performance regulator.

```
*  Flyback Bias Converter
PSW1  1E-6   1E6   1E6
PSW2  1E6   1E-6   1E6
.BC  1  2  V(RX)
.BC  2  1 -T+33E-6
.BC  2  3 I(L1)
.BC  3  1 -T+33E-6
.PLOT TRAN I(L1) V(RLOAD) V(IREF)
.OPTIONS LIST EPS=1E-11 BEPS=1E-8
.AC DEC 20 100 100K
.TRAN .1U 150U
E1 10009 0 10007 10011 -1000
VSEC 10003 0 0
I1 0 10002 0.0
RC2 9 10002 0.1
ESEC 10003 10006 10004 10005 0.143
RX 6 7 1000K
R7 10008 10009 10K
C2 9 0 15U IC=13
RVD1 6 0 1K
C4 10007 10009 2000P
R6 10001 10007 20K
RVD2 10009 6 2K
RON 8 7 3.0
R4 7 0 3.3
C3 10007 10008 33N
R5 10007 0 4.75K
L1 10004 10005 4000U
RLOAD 10002 0 66
IREF 10001 0 DC 0
VAC 10001 10002 DC 0
V2 10011 0 DC 2.5
V1 10004 0 DC 400
RQ1 10005 8 PSW1
RD1 10006 10002 PSW2
FPRI 10004 10005 VSEC 0.143
.END
```

Figure 4-22. Simulation Netlist

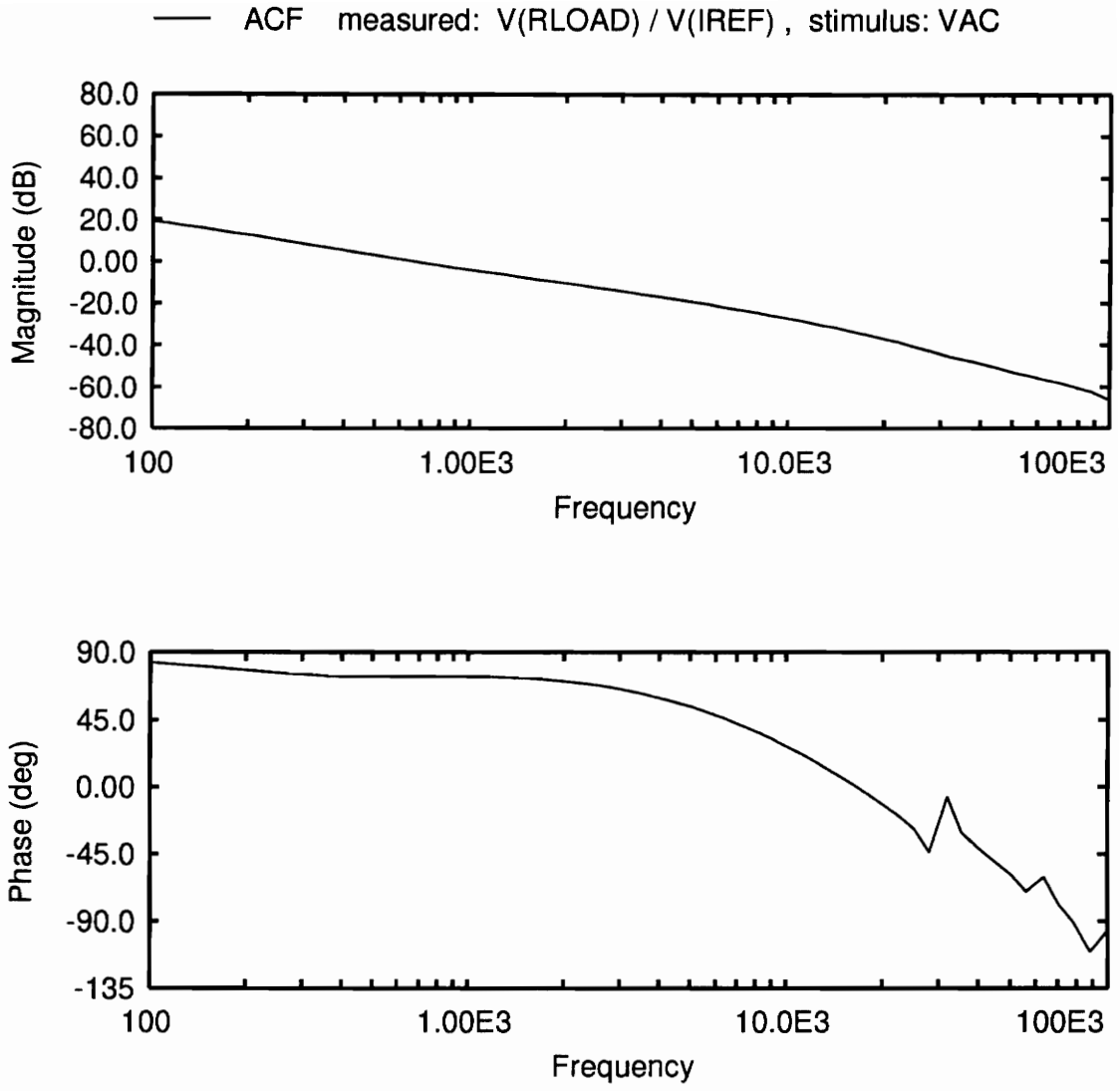

Figure 4-23. Loop-Gain Transfer Function

The output impedance was computed by stimulating I1 and measuring the ratio of V(RLOAD) to I1. This response is shown in Figure 4-24. The impedance is increasing as the

loop gain rolls off, up to a maximum of about 20dB, which corresponds to about 10Ω, at a frequency of about 600 Hz.. This is not very good, but the typical load is only about 0.2A, with no dynamics. The output impedance could be greatly improved by increasing the band-width of the converter, and by increasing the amount of output capacitance.

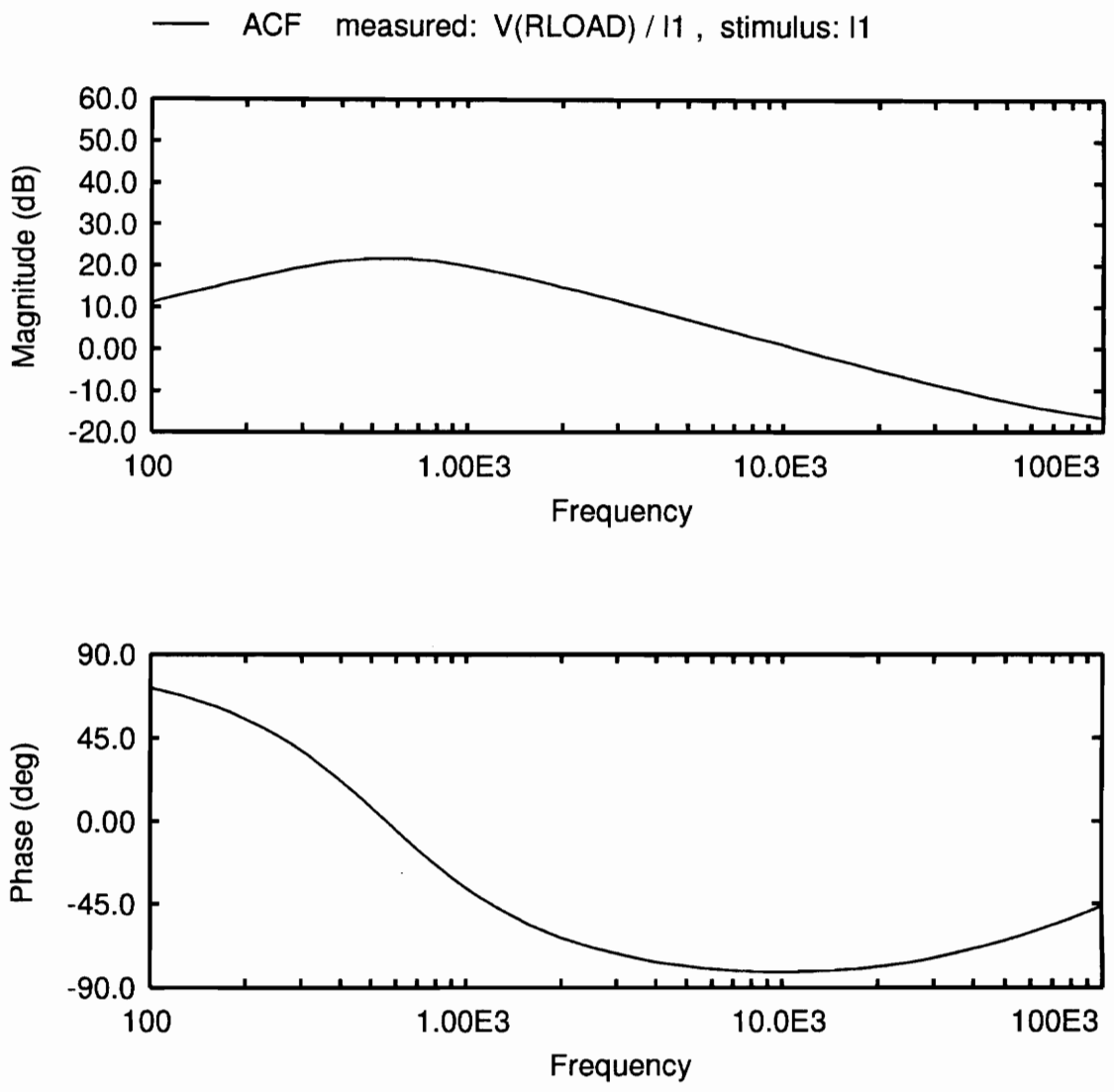

Figure 4-24. Small-Signal Output Impedance

The Audiosusceptibility was simulated by stimulating the input voltage source, V1, and measuring the amount of signal that shows up on the load resistor, V(RLOAD). This is

shown in Figure 4-25. This shows that a negligible amount of signal will get through to the output.

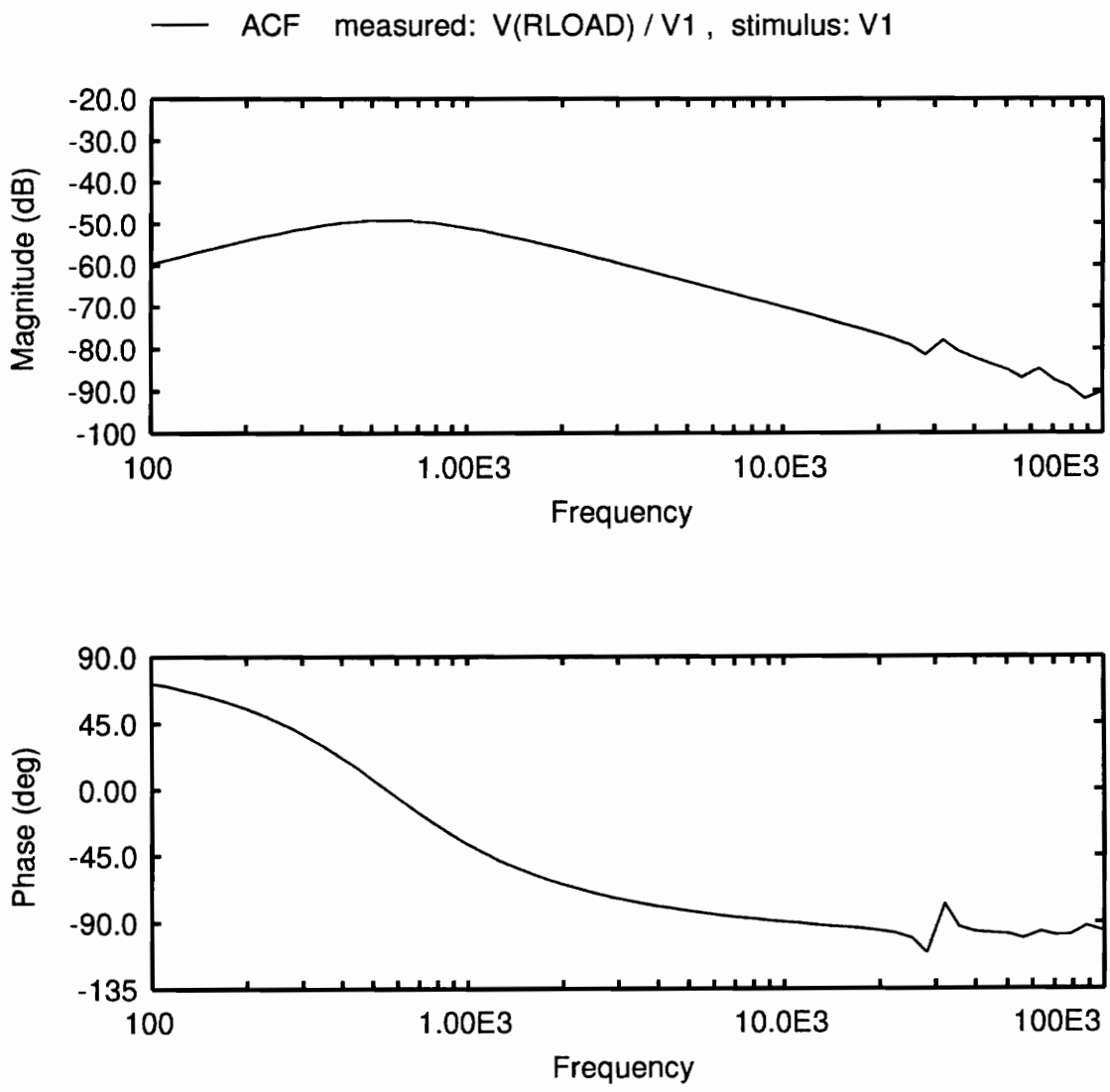

Figure 4-25. Audiosusceptibility

4.6 CONCLUSIONS

The examples given here show many attributes of the new small-signal simulation method, as well as the design environment of OrCAD, STAEQ, SIMU, and ACF. In general, the new method performs very well in predicting low frequency and high frequency responses of switching regulator circuits.

5.0 Conclusions

A new method for the computation of the small-signal analysis for power electronics circuits has been developed. The method is completely derived, algorithms written, and implemented in a computer program. The new program works in conjunction with the COSMIR program to give a comprehensive set of tools for switching power supply analysis, both transient and small-signal.

The need for small-signal analysis was reviewed. A simple converter was simulated in the time-domain, both unmodulated and with small-signal modulation, to understand the frequency harmonics present in the output waveforms. The measurement process of switching power converters using a network analyzer was covered, showing how the input tracking bandpass filters select only signals at the same frequency as the stimulus.

The new method uses the idea of solving for the new steady-state response of a periodic converter that is being stimulated with a small-signal stimulus of commensurate frequency to the switching frequency. Since the original steady-state is known, only the sidebands around the harmonics of the switching frequency need to be computed. This will compute the complete small-signal response of the converter to the stimulus, including harmonics generated by the modulation process and other nonlinearities.

Several examples have been given that show the capabilities of the new method. The predictions of this new method compare very closely with measured responses. It simulates

accurately the response of continuous-mode and discontinuous-mode operation, as well as predicting the subharmonic oscillation possible in fixed-frequency current-mode control.

This approach was first published in 1988 as [29] and [30]. Since then, there has been at least one work published having similar goals and performing similarly[37]. Also, there has been a derivative work based off of this method[38].

Overall, this method shows promise to be a good general purpose small-signal simulation algorithm. This approach could be used by designer to model the small-signal response of switching power supplies, and to help determine the control system elements for the converter. Properly implemented, the user would have no need to understand the underlying principles of the analysis.

Appendix A. Definition of Symbols

In general, the following notation will be used throughout this paper: lower-case letters will represent time-domain variables and functions, and upper-case letters will represent frequency-domain variables and functions. There will be exceptions to this, some of which are detailed below. An integer in parenthesis following an upper-case letter will be used to represent harmonic coefficients in a Fourier-Series representation. Subscripts on a lower-case variable represent a particular piecewise-linear segment. Superscripts in parenthesis indicate a particular period of a signal that repeats periodically several times.

Term	Definition
n_x	the number of state variables
n_u	the number of inputs
n_y	the number of output variables
T_s	the unperturbed steady-state basic period of the switching power system.
f_s	the basic switching frequency of the switching power system, the inverse of T_s
T_m	the period of the small-signal modulation stimulus
f_m	the frequency of the small-signal modulation stimulus, the inverse of T_m

T_t the period of the resulting system under small-signal perturbation

f_t the frequency of the resulting system, the inverse of T_t

j $\sqrt{-1}$

$\boldsymbol{x(t)}$ the values of the state variables of the system. In electrical network analysis, this consists of a subset of capacitor voltages and inductor currents. A real vector of length n_x.

$\boldsymbol{y(t)}$ the values of the outputs of the system. A real vector of length n_y.

$\boldsymbol{u(t)}$ the values of the inputs to the system. In electrical network analysis, this consists of all independent voltage and current sources. A real vector of length n_u.

$\boldsymbol{f(x(t),u(t))}$ A function that maps the state variables and the inputs into a real vector of length n_x.

$\boldsymbol{g(x(t),u(t))}$ A function that maps the state variables and the inputs into a real vector of length n_y.

$\boldsymbol{X(k)}$ The harmonic coefficients of the Fourier series representation of $x(t)$, where k is the index of the harmonic. Each value of $X(k)$ is a complex vector of length n_x.

$\boldsymbol{Y(k)}$ The harmonic coefficients of the Fourier series representation of $y(t)$, where k is the index of the harmonic. Each value of $Y(k)$ is a complex vector of length n_y.

U(k) The harmonic coefficients of the Fourier series representation of $y(t)$, where k is the index of the harmonic. Each value of $U(k)$ is a complex vector of length n_u.

F(X,U,k) The Fourier series representation of $f(x(t), u(t))$, where k is the index of the harmonic coefficitne. Each value of $F(X,U,k)$ is a complex vector of length n_x.

G(X,U,k) The Fourier series representation of $g(x(t), u(t))$, where k is the index of the harmonic coefficient. Each value of $G(X,U,k)$ is a complex vector of length n_y.

ω_i $\omega_i = \frac{2\pi i}{T_t}$

i,h,k,p,q integers used in computations

M The integer number of cycles of the stimulus in the overall period, T_t.

N The integer number of cycles of the power converter in the overall period, T_t.

Q The integer number of modes in one cycle of the power converter

P The integer number of harmonics that will be included in the computations. The system will be truncated to include only $\pm P$ harmonics in the solution.

I The identity matrix, whose dimensions will be specified when used.

a_i, b_i, c_i, d_i the set of state space matrices valid in the i-th period

e_i A selector matrix of dimension $1 \times n_y$ valid in the i-th mode of operation. It is used in the boundary condition equation to select one of the output variables to measure in order to determine the time of boundary condition crossing.

Nothing will be done to notationally differentiate between scalar variables and matrices. Almost all variables used will be matrices, and they will be defined when used as to dimension and type.

When complex numbers are discussed, they will be represented by a comma-delimited number-pair inside parenthesis.

$$\text{re} + j\,\text{im} = (\text{re}, \text{im}) \tag{A.1}$$

Appendix B. An Example Solution of the Discontinuous-Mode Boost Converter

In this chapter we will go through the solution of the discontinuous boost converter from the examples chapter. We will only analyze the control - to - output function at a single frequency. Since the stimulus frequency and the switching frequency must be commensurate, we will choose the stimulus frequency to be exactly one third the switching frequency. This will give us $N = 3$ and $M = 1$. We will also choose to include one harmonic in the solution, or $P = 1$. We will also see that this converter has three modes of operation contained within one cycle of operation, or $Q = 3$.

To start off, we will repeat the schematic of the boost converter, along with the netlist:

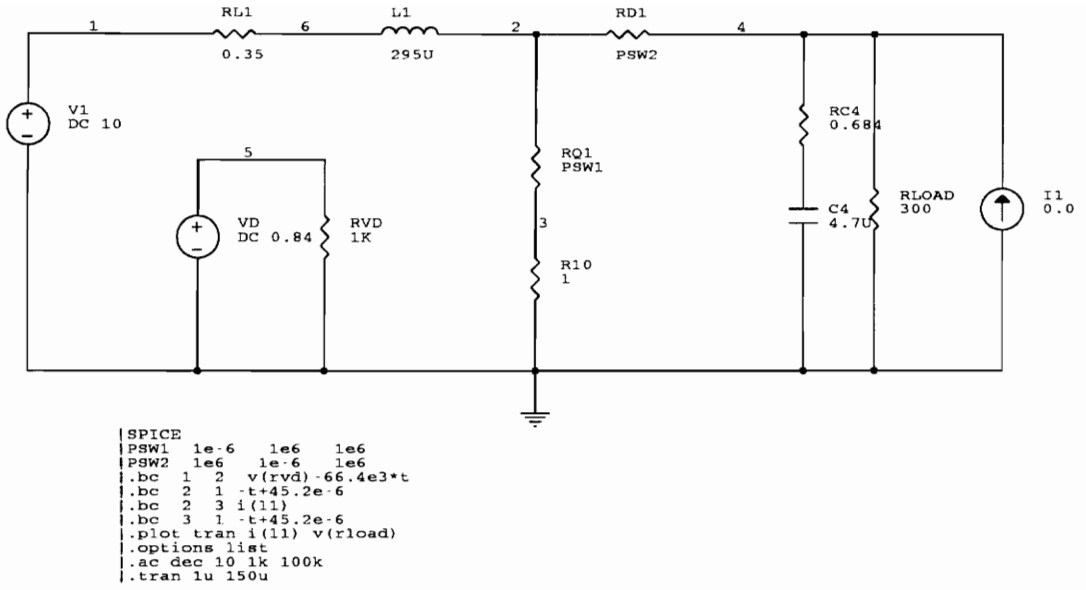

Figure B-1. Discontinuous Boost Converter Simulation Schematic

The STAEQ program is run on the netlist from Figure B-2, and the following system equations are computed:

$$a_1 = \begin{bmatrix} -7.078E+02 & 2.123E-01 \\ -3.382E-03 & -4.576E+03 \end{bmatrix} \tag{B.1}$$

$$a_2 = \begin{bmatrix} -7.078E+02 & 2.123E+05 \\ -3.382E+03 & -3.500E+03 \end{bmatrix} \tag{B.2}$$

```
PSW1  1E-6   1E6   1E6
PSW2  1E6   1E-6   1E6
.BC  1  2  V(RVD)-66.4E3*T
.BC  2  1 -T+45.2E-6
.BC  2  3 I(L1)
.BC  3  1 -T+45.2E-6
.PLOT TRAN I(L1) V(RLOAD)
.OPTIONS LIST
.AC DEC 10 1K 100K
.TRAN 1U 150U
I1 0 4 0.0
RL1 1 6 0.35
RC4 10006 4 0.684
R10 3 0 1
RVD 5 0 1K
L1 6 2 295U
RLOAD 4 0 300
C4 10006 0 4.7U
VD 5 0 DC 0.84
V1 1 0 DC 10
RQ1 2 3 PSW1
RD1 2 4 PSW2
.END
```

Figure B-2. Simulation Netlist

$$a_3 = \begin{bmatrix} -7.077E+02 & 0.000E+00 \\ 0.000E+00 & 0.000E+00 \end{bmatrix} \tag{B.3}$$

$$b_1 = \begin{bmatrix} 0.000E+00 & 0.000E+00 & 2.123E+05 \\ 3.390E+03 & 0.000E+00 & -2.313E-03 \end{bmatrix} \tag{B.4}$$

$$b_2 = \begin{bmatrix} 0.000E+00 & 0.000E+00 & 2.123E+05 \\ 3.390E+03 & 0.000E+00 & -2.313E+03 \end{bmatrix} \tag{B.5}$$

$$b_3 = \begin{bmatrix} 0.000E+00 & 0.000E+00 & 2.123E+05 \\ 0.000E+00 & 0.000E+00 & 0.000E+00 \end{bmatrix} \tag{B.6}$$

$$c_1 = \begin{bmatrix} 0.000E+00 & 0.000E+00 \\ 0.000E+00 & 1.000E+00 \\ 9.977E-01 & 6.824E-07 \end{bmatrix} \tag{B.7}$$

$$c_2 = \begin{bmatrix} 0.000E+00 & 0.000E+00 \\ 0.000E+00 & 1.000E+00 \\ 9.977E-01 & 6.824E-01 \end{bmatrix} \tag{B.8}$$

$$c_3 = \begin{bmatrix} 0.000E+00 & 0.000E+00 \\ 0.000E+00 & 1.000E+00 \\ 9.977E-01 & 3.412E-01 \end{bmatrix} \tag{B.9}$$

$$d_1 = \begin{bmatrix} 0.000E+00 & 1.000E+00 & 0.000E+00 \\ 0.000E+00 & 0.000E+00 & 0.000E+00 \\ 0.000E+00 & 0.000E+00 & 6.824E-01 \end{bmatrix} \tag{B.10}$$

$$d_2 = \begin{bmatrix} 0.000E+00 & 1.000E+00 & 0.000E+00 \\ 0.000E+00 & 0.000E+00 & 0.000E+00 \\ 0.000E+00 & 0.000E+00 & 6.824E-01 \end{bmatrix} \tag{B.11}$$

$$d_3 = \begin{bmatrix} 0.000E+00 & 1.000E+00 & 0.000E+00 \\ 0.000E+00 & 0.000E+00 & 0.000E+00 \\ 0.000E+00 & 0.000E+00 & 6.824E-01 \end{bmatrix} \tag{B.12}$$

$$u = \begin{bmatrix} 1.000E+01 \\ 8.400E-01 \\ 0.000E+00 \end{bmatrix} = \begin{bmatrix} \text{V1} \\ \text{VD} \\ \text{I1} \end{bmatrix} \tag{B.13}$$

The names of the output variables contained in Y are:

$$y = \begin{bmatrix} \text{V(RVD)} \\ \text{I(L1)} \\ \text{V(RLOAD)} \end{bmatrix} \tag{B.14}$$

The STAEQ program also details the boundary condition equations in the form of equation (3.7), which is copied here for convenience:

$$0 = e_i\, y(t_i) + \alpha_i[t_i - t_0] + \beta_i \ , \tag{B.15}$$

$$\alpha_1 = -6.640E+04 \tag{B.16}$$

$$\alpha_2 = 0.000E+00 \tag{B.17}$$

$$\alpha_3 = -1.000E+00 \tag{B.18}$$

$$\beta_1 = 0.000E+00 \tag{B.19}$$

$$\beta_2 = 0.000E+00 \tag{B.20}$$

$$\beta_3 = 4.520E-05 \tag{B.21}$$

$$e_1 = [1.000E+00 \quad 0.000E+00 \quad 0.000E+00] \tag{B.22}$$

$$e_2 = [0.000E+00 \quad 1.000E+00 \quad 0.000E+00] \tag{B.23}$$

$$e_3 = [0.000E+00 \quad 0.000E+00 \quad 0.000E+00] \tag{B.24}$$

From the above coefficients, we can see that the three boundary condition equations that govern the transition from the first to second mode is:

$$[1.00 \quad 0.00 \quad 0.00]\begin{bmatrix} \text{V(RVD)} \\ \text{I(L1)} \\ \text{V(RLOAD)} \end{bmatrix} - 6.640E+04 \times (t_1 - t_0) + 0.00 \tag{B.25}$$

The boundary condition equation that governs the transition from the second to third mode is:

$$[0.00 \quad 1.00 \quad 0.00]\begin{bmatrix} \text{V(RVD)} \\ \text{I(L1)} \\ \text{V(RLOAD)} \end{bmatrix} + 0.00 \times (t_2 - t_0) + 0.00 \tag{B.26}$$

And finally, the boundary condition equation that governs the transition from the third back to first mode is:

$$[0.00 \quad 0.00 \quad 0.00]\begin{bmatrix} \text{V(RVD)} \\ \text{I(L1)} \\ \text{V(RLOAD)} \end{bmatrix} - 1.00 \times (t_3 - t_0) + 4.520E - 05 \tag{B.27}$$

When the SIMU program is run, it computes the steady-state values of the X-vector and also finds the times spent in each mode of operation. This data is contained in the working file "output.dat" which is generated by SIMU.

In this particular case, the time spent in mode 1 is 1.265060E-05, the time spent in mode 2 is 1.359934E-05, and the time spent in the third mode is 1.895005E-05. One switching cycle of the converter bas a basic period of $T_s = 45.2E - 6$.

Given that $N = 3$, this makes a complete period of the sustem under perturbation to be $T_t = 135.60E - 6$. We may yse this information to define the nine switching instants of the perturbed system:

$$t_1^{(1)} = 12.65E - 6 \tag{B.28}$$

$$t_2^{(1)} = 26.25E - 6 \tag{B.29}$$

$$t_3^{(1)} = 45.20E - 6 \tag{B.30}$$

$$t_1^{(2)} = 57.85E - 6 \tag{B.31}$$

$$t_2^{(2)} = 71.45E - 6 \tag{B.32}$$

$$t_3^{(2)} = 90.40E - 6 \tag{B.33}$$

$$t_1^{(3)} = 103.05E - 6 \tag{B.34}$$

$$t_2^{(3)} = 116.65E - 6 \tag{B.35}$$

$$t_3^{(3)} = 135.60E - 6 \tag{B.36}$$

The values of the X-vector at the switching instants is:

$$x(t_1) = \begin{bmatrix} 1.856E + 01 \\ 4.167E - 01 \end{bmatrix} \tag{B.37}$$

$$x(t_2) = \begin{bmatrix} 1.898E + 01 \\ 1.324E - 11 \end{bmatrix} \tag{B.38}$$

$$x(t_3) = \begin{bmatrix} 1.872E+01 \\ 1.324E-11 \end{bmatrix} \tag{B.39}$$

Once steady-state is computed, the ACF program may be run. The first thing ACF does in precompute several matrix values which are used repeatedly.

The first batch of matrices are the elements of equation (3.52a) and equation (3.52b):

$$\Phi_1 = \begin{bmatrix} 1.000E+00 & 0.000E+00 \\ -3.086E-23 & 1.000E+00 \end{bmatrix} \tag{B.40}$$

$$\Phi_2 = \begin{bmatrix} 1.000E+00 & 7.969E-18 \\ -3.374E-36 & 1.000E+00 \end{bmatrix} \tag{B.41}$$

$$\Phi_3 = \begin{bmatrix} 1.000E+00 & 0.000E+00 \\ 0.000E+00 & 1.000E+00 \end{bmatrix} \tag{B.42}$$

$$\Psi_1 = \begin{bmatrix} 0.000E+00 & 0.000E+00 & 0.000E+00 \\ 0.000E+00 & 0.000E+00 & 0.000E+00 \end{bmatrix} \tag{B.43}$$

$$\Psi_2 = \begin{bmatrix} 0.000E+00 & 0.000E+00 & 0.000E+00 \\ 0.000E+00 & 0.000E+00 & 0.000E+00 \end{bmatrix} \tag{B.44}$$

$$\Psi_3 = \begin{bmatrix} 0.000E+00 & 0.000E+00 & 0.000E+00 \\ 0.000E+00 & 0.000E+00 & 0.000E+00 \end{bmatrix} \quad \text{(B.45)}$$

$$\Gamma_1 = [0.000E+00 \quad 0.000E+00] \quad \text{(B.46)}$$

$$\Gamma_2 = [0.000E+00 \quad 3.303E-05] \quad \text{(B.47)}$$

$$\Gamma_3 = [0.000E+00 \quad 0.000E+00] \quad \text{(B.48)}$$

$$H_1 = [0.000E+00 \quad 1.506E-05 \quad 0.000E+00] \quad \text{(B.49)}$$

$$H_2 = [0.000E+00 \quad 0.000E+00 \quad 0.000E+00] \quad \text{(B.50)}$$

$$H_3 = [0.000E+00 \quad 0.000E+00 \quad 0.000E+00] \quad \text{(B.51)}$$

$$\Lambda_1 = [1.000E + 00] \tag{B.52}$$

$$\Lambda_2 = [0.000E + 00] \tag{B.53}$$

$$\Lambda_3 = [1.000E + 00] \tag{B.54}$$

The next batch of precomputed matrices is for equation (3.35) and equation (3.42).

$$\Xi_1 = \begin{bmatrix} -8.846E + 04 \\ 6.232E + 04 \end{bmatrix} \tag{B.55}$$

$$\Xi_2 = \begin{bmatrix} -2.010E + 00 \\ -3.029E + 04 \end{bmatrix} \tag{B.56}$$

$$\Xi_3 = \begin{bmatrix} 1.982E + 00 \\ -3.390E + 04 \end{bmatrix} \tag{B.57}$$

$$Z_1 = \begin{bmatrix} 0.000E+00 \\ 0.000E+00 \\ -2.844E-01 \end{bmatrix} \tag{B.58}$$

$$Z_2 = \begin{bmatrix} 0.000E+00 \\ 0.000E+00 \\ -6.462E-06 \end{bmatrix} \tag{B.59}$$

$$Z_3 = \begin{bmatrix} 0.000E+00 \\ 0.000E+00 \\ 6.373E-06 \end{bmatrix} \tag{B.60}$$

At this point, the ACF program enters a loop. Each pass through the loop represents one frequency point. For this example, we are only going to consider one frequency point, where the stimulus is exactly one-third the switching frequency. For this example, $N = 3$ and $M = 1$, so there is exactly three switching periods contained in one period of the stimulus.

We are also going to choose $P = 1$, which will include one harmonic into the solution.When we do this, the $\overline{A}$ matrix will have the following form:

$$\overline{A} = j\begin{bmatrix} \omega_4 I & 0 & 0 \\ 0 & \omega_1 I & 0 \\ 0 & 0 & \omega_{-2} I \end{bmatrix} - \begin{bmatrix} A(4,4) & A(4,1) & A(4,-2) \\ A(1,4) & A(1,1) & A(1,-2) \\ A(-2,4) & A(-2,1) & A(-2,-2) \end{bmatrix} \tag{B.61}$$

and the $\hat{X}$ and $\overline{B}$ matrices will look like:

$$\hat{X} = \begin{bmatrix} \hat{X}(4) \\ \hat{X}(1) \\ \hat{X}(-2) \end{bmatrix} \tag{B.62}$$

and

$$\overline{B} = \begin{bmatrix} B(4,1) \\ B(1,1) \\ B(-2,1) \end{bmatrix} \tag{B.63}$$

After looking at $\overline{A}$, we will need to compute nine of the $A(k,v)$ matrices, detailed below:

- A(4,4)
- A(4,1)
- A(4,-2)
- A(1,4)
- A(1,1)
- A(1,-2)
- A(-2,4)

- A(-2,1)
- A(-2,-2)

Likewise, we will need three of the $B(k,v)$ matrices:

- B(4,1)
- B(1,1)
- B(-2,1)

Since the computation of each of the nine $A(k,v)$ matrices is so similar, we will only document the computation of one of them. We will pick $A(4,1)$. We will use equation (3.38) to compute $A(4,1)$:

$$\frac{\partial F(X,U,k)}{\partial X(v)} = \sum_{p=1}^{N}\sum_{i=1}^{Q} \frac{1}{T_t}\Xi_i e^{-j\frac{2\pi k}{T_t}t_i^{(p)}} \frac{\partial t_i^{(p)}}{\partial X(v)} + \sum_{p=1}^{N}\sum_{i=1}^{Q} a_i \frac{1}{T_t}\int_{t_{i-1}^{(p)}}^{t_i^{(p)}} e^{-j\frac{2\pi(k-v)}{T_t}\tau} d\tau \quad \text{(B.64)}$$

Plugging in N, Q, k, v gives:

$$\frac{\partial F(X, U, 4)}{\partial X(1)} = \sum_{p=1}^{3} \sum_{i=1}^{3} \frac{1}{T_t} \Xi_t e^{-j\frac{2\pi k}{T_t} t_i^{(p)}} \frac{\partial t_i^{(p)}}{\partial X(v)}$$
$$+ \sum_{p=1}^{3} \sum_{i=1}^{3} a_i \frac{1}{T_t} \int_{t_{i-1}^{(p)}}^{t_i^{(p)}} e^{-j\frac{2\pi(k-v)}{T_t}\tau} d\tau \qquad \text{(B.65)}$$

Expanding this gives:

$$\frac{\partial F(X,U,4)}{\partial X(1)} = \frac{1}{T_t}\Xi_1 e^{-j\frac{2\pi 4}{T_t}t_1^{(1)}}\frac{\partial t_1^{(1)}}{\partial X(1)} + \frac{1}{T_t}\Xi_2 e^{-j\frac{2\pi 4}{T_t}t_2^{(1)}}\frac{\partial t_2^{(1)}}{\partial X(1)} + \frac{1}{T_t}\Xi_3 e^{-j\frac{2\pi 4}{T_t}t_3^{(1)}}\frac{\partial t_3^{(1)}}{\partial X(1)}$$
$$+ \frac{1}{T_t}\Xi_1 e^{-j\frac{2\pi 4}{T_t}t_1^{(2)}}\frac{\partial t_1^{(2)}}{\partial X(1)} + \frac{1}{T_t}\Xi_2 e^{-j\frac{2\pi 4}{T_t}t_2^{(2)}}\frac{\partial t_2^{(2)}}{\partial X(1)} + \frac{1}{T_t}\Xi_3 e^{-j\frac{2\pi 4}{T_t}t_3^{(2)}}\frac{\partial t_3^{(2)}}{\partial X(1)}$$
$$+ \frac{1}{T_t}\Xi_1 e^{-j\frac{2\pi 4}{T_t}t_1^{(3)}}\frac{\partial t_1^{(3)}}{\partial X(1)} + \frac{1}{T_t}\Xi_2 e^{-j\frac{2\pi 4}{T_t}t_2^{(3)}}\frac{\partial t_2^{(3)}}{\partial X(1)} + \frac{1}{T_t}\Xi_3 e^{-j\frac{2\pi 4}{T_t}t_3^{(3)}}\frac{\partial t_3^{(3)}}{\partial X(1)}$$
$$+ a_1\frac{1}{T_t}\int_{t_0^{(1)}}^{t_1^{(1)}} e^{-j\frac{2\pi(3)}{T_t}\tau}d\tau + a_2\frac{1}{T_t}\int_{t_1^{(1)}}^{t_2^{(1)}} e^{-j\frac{2\pi(3)}{T_t}\tau}d\tau + a_3\frac{1}{T_t}\int_{t_2^{(1)}}^{t_3^{(1)}} e^{-j\frac{2\pi(3)}{T_t}\tau}d\tau \quad \text{(B.66)}$$
$$+ a_1\frac{1}{T_t}\int_{t_0^{(2)}}^{t_1^{(2)}} e^{-j\frac{2\pi(3)}{T_t}\tau}d\tau + a_2\frac{1}{T_t}\int_{t_1^{(2)}}^{t_2^{(2)}} e^{-j\frac{2\pi(3)}{T_t}\tau}d\tau + a_3\frac{1}{T_t}\int_{t_2^{(2)}}^{t_3^{(2)}} e^{-j\frac{2\pi(3)}{T_t}\tau}d\tau$$
$$+ a_1\frac{1}{T_t}\int_{t_0^{(3)}}^{t_1^{(3)}} e^{-j\frac{2\pi(3)}{T_t}\tau}d\tau + a_2\frac{1}{T_t}\int_{t_1^{(3)}}^{t_2^{(3)}} e^{-j\frac{2\pi(3)}{T_t}\tau}d\tau + a_3\frac{1}{T_t}\int_{t_2^{(3)}}^{t_3^{(3)}} e^{-j\frac{2\pi(3)}{T_t}\tau}d\tau$$

The only things we don't know in the above equation are the perturbation in switching instant as a function of the state vector. We may use equation (3.52a) to solve for these quantities, which is copied below.

$$\frac{\partial t_i^{(p)}}{\partial X(v)} = \Gamma_i \Phi_i(t_i^{(p)}, t_{i'}^{(p)}) e^{j\frac{2\pi v}{T_t}t_i^{(p)}} + \Lambda_i \frac{\partial t_0^{(p)}}{\partial X(v)} \quad \text{(B.67)}$$

At this point, the variables become complex. I will use comma-separated number pairs inside parenthesis to represent a complex number:

$$\text{re} + j\,\text{im} = (\text{re}, \text{im}) \tag{B.68}$$

Now, we can solve for the nine switching instants:

$$\begin{aligned}\frac{\partial t_1^{(1)}}{\partial X(1)} &= \Gamma_1 \Phi_1(t_1^{(1)}, t_1^{(1)}) e^{j\frac{2\pi 1}{T_t} t_1^{(1)}} + \Lambda_1 \frac{\partial t_0^{(1)}}{\partial X(1)} \\ &= [(0.000D + 00,\ 0.000D + 00) \quad (0.000D + 00,\ 0.000D + 00)]\end{aligned} \tag{B.69}$$

$$\begin{aligned}\frac{\partial t_2^{(1)}}{\partial X(1)} &= \Gamma_2 \Phi_2(t_2^{(1)}, t_2^{(1)}) e^{j\frac{2\pi 1}{T_t} t_2^{(1)}} + \Lambda_2 \frac{\partial t_0^{(1)}}{\partial X(1)} \\ &= [(0.000D + 00,\ 0.000D + 00) \quad (1.146D - 05,\ 3.097D - 05)]\end{aligned} \tag{B.70}$$

$$\begin{aligned}\frac{\partial t_3^{(1)}}{\partial X(1)} &= \Gamma_3 \Phi_3(t_3^{(1)}, t_3^{(1)}) e^{j\frac{2\pi 1}{T_t} t_3^{(1)}} + \Lambda_3 \frac{\partial t_0^{(1)}}{\partial X(1)} \\ &= [(0.000D + 00,\ 0.000D + 00) \quad (0.000D + 00,\ 0.000D + 00)]\end{aligned} \tag{B.71}$$

$$\begin{aligned}\frac{\partial t_1^{(2)}}{\partial X(1)} &= \Gamma_1 \Phi_1(t_1^{(2)}, t_1^{(2)}) e^{j\frac{2\pi 1}{T_t} t_1^{(2)}} + \Lambda_1 \frac{\partial t_0^{(2)}}{\partial X(1)} \\ &= [(0.000D + 00,\ 0.000D + 00) \quad (0.000D + 00,\ 0.000D + 00)]\end{aligned} \tag{B.72}$$

$$\begin{aligned}\frac{\partial t_2^{(2)}}{\partial X(1)} &= \Gamma_2 \Phi_2(t_2^{(2)}, t_2^{(2)}) e^{j\frac{2\pi 1}{T_t} t_2^{(2)}} + \Lambda_2 \frac{\partial t_0^{(2)}}{\partial X(1)} \\ &= [(0.000D + 00,\ 0.000D + 00) \quad (1.146D - 05,\ 3.097D - 05)]\end{aligned} \tag{B.73}$$

$$\frac{\partial t_3^{(2)}}{\partial X(1)} = \Gamma_3 \Phi_3(t_3^{(2)}, t_3^{(2)}) e^{j\frac{2\pi 1}{T_t} t_3^{(2)}} + \Lambda_3 \frac{\partial t_0^{(2)}}{\partial X(1)} \tag{B.74}$$
$$= [(0.000D + 00,\ 0.000D + 00)\quad (0.000D + 00,\ 0.000D + 00)]$$

$$\frac{\partial t_1^{(3)}}{\partial X(1)} = \Gamma_1 \Phi_1(t_1^{(3)}, t_1^{(3)}) e^{j\frac{2\pi 1}{T_t} t_1^{(3)}} + \Lambda_1 \frac{\partial t_0^{(3)}}{\partial X(1)} \tag{B.75}$$
$$= [(0.000D + 00,\ 0.000D + 00)\quad (0.000D + 00,\ 0.000D + 00)]$$

$$\frac{\partial t_2^{(3)}}{\partial X(1)} = \Gamma_2 \Phi_2(t_2^{(3)}, t_2^{(3)}) e^{j\frac{2\pi 1}{T_t} t_2^{(3)}} + \Lambda_2 \frac{\partial t_0^{(3)}}{\partial X(1)} \tag{B.76}$$
$$= [(0.000D + 00,\ 0.000D + 00)\quad (1.146D - 05,\ 3.097D - 05)]$$

$$\frac{\partial t_3^{(3)}}{\partial X(1)} = \Gamma_3 \Phi_3(t_3^{(3)}, t_3^{(3)}) e^{j\frac{2\pi 1}{T_t} t_3^{(3)}} + \Lambda_3 \frac{\partial t_0^{(3)}}{\partial X(1)} \tag{B.77}$$
$$= [(0.000D + 00,\ 0.000D + 00)\quad (0.000D + 00,\ 0.000D + 00)]$$

These values for the perturbation in switching instant as a function of state vector make sense. The transition from the second to the third mode is due to the diode turning off because the current through it and the inductor goes to zero. None of the other switching instants are a function of the state vector.

We can now start computing the individual components of equation (B.66). We will start with the integral computations:

$$\frac{1}{T_t}\int_{t_0^{(1)}}^{t_1^{(1)}} e^{-j\frac{2\pi(3)}{T_t}\tau}d\tau = \frac{1}{T_t}\int_{t_0^{(2)}}^{t_1^{(2)}} e^{-j\frac{2\pi(3)}{T_t}\tau}d\tau = \frac{1}{T_t}\int_{t_0^{(3)}}^{t_1^{(3)}} e^{-j\frac{2\pi(3)}{T_t}\tau}d\tau \tag{B.78}$$
$$= (5.212D - 02, -6.296D - 02)$$

$$\frac{1}{T_t}\int_{t_1^{(1)}}^{t_2^{(1)}} e^{-j\frac{2\pi(3)}{T_t}\tau}d\tau = \frac{1}{T_t}\int_{t_1^{(2)}}^{t_2^{(2)}} e^{-j\frac{2\pi(3)}{T_t}\tau}d\tau = \frac{1}{T_t}\int_{t_1^{(3)}}^{t_2^{(3)}} e^{-j\frac{2\pi(3)}{T_t}\tau}d\tau \tag{B.79}$$
$$= (-7.790D - 02, -3.646D - 02)$$

$$\frac{1}{T_t}\int_{t_2^{(1)}}^{t_3^{(1)}} e^{-j\frac{2\pi(3)}{T_t}\tau}d\tau = \frac{1}{T_t}\int_{t_2^{(2)}}^{t_3^{(2)}} e^{-j\frac{2\pi(3)}{T_t}\tau}d\tau = \frac{1}{T_t}\int_{t_2^{(3)}}^{t_3^{(3)}} e^{-j\frac{2\pi(3)}{T_t}\tau}d\tau \tag{B.80}$$
$$= (2.578D - 02, 9.942D - 02)$$

With these integral computations made, we can now compute the last nine portions of equation (B.66):

$$a_1 \frac{1}{T_t} \int_{t_0^{(1)}}^{t_1^{(1)}} e^{-j\frac{2\pi(3)}{T_t}\tau} d\tau = a_1 \frac{1}{T_t} \int_{t_0^{(2)}}^{t_1^{(2)}} e^{-j\frac{2\pi(3)}{T_t}\tau} d\tau = a_1 \frac{1}{T_t} \int_{t_0^{(3)}}^{t_1^{(3)}} e^{-j\frac{2\pi(3)}{T_t}\tau} d\tau = \tag{B.80c}$$

$$= \begin{bmatrix} (-3.689D+01, 4.456D+01) & (1.106D-02, -1.336D-02) \\ (-1.763D-04, 2.129D-04) & (-2.385D+02, 2.881D+02) \end{bmatrix}$$

$$a_2 \frac{1}{T_t} \int_{t_1^{(1)}}^{t_2^{(1)}} e^{-j\frac{2\pi(3)}{T_t}\tau} d\tau = a_2 \frac{1}{T_t} \int_{t_1^{(2)}}^{t_2^{(2)}} e^{-j\frac{2\pi(3)}{T_t}\tau} d\tau = a_2 \frac{1}{T_t} \int_{t_1^{(3)}}^{t_2^{(3)}} e^{-j\frac{2\pi(3)}{T_t}\tau} d\tau = \tag{B.80d}$$

$$= \begin{bmatrix} (5.514D+01, 2.581D+01) & (-1.654D+04, -7.741D+03) \\ (2.635D+02, 1.233D+02) & (2.726D+02, 1.276D+02) \end{bmatrix}$$

$$a_3 \frac{1}{T_t} \int_{t_2^{(1)}}^{t_3^{(1)}} e^{-j\frac{2\pi(3)}{T_t}\tau} d\tau = a_3 \frac{1}{T_t} \int_{t_2^{(2)}}^{t_3^{(2)}} e^{-j\frac{2\pi(3)}{T_t}\tau} d\tau = a_3 \frac{1}{T_t} \int_{t_2^{(3)}}^{t_3^{(3)}} e^{-j\frac{2\pi(3)}{T_t}\tau} d\tau = \tag{B.80e}$$

$$= \begin{bmatrix} (-1.824D+01, -7.036D+01) & (0.000D+00, 0.000D+00) \\ (0.000D+00, 0.000D+00) & (0.000D+00, 0.000D+00) \end{bmatrix}$$

The first nine components of equation (B.66) are also easily computed:

$$\frac{1}{T_t}\Xi_1 e^{-j\frac{2\pi 4}{T_t}t_1^{(1)}}\frac{\partial t_1^{(1)}}{\partial X(1)} = \\ = \begin{bmatrix} (0.000D+00,\ 0.000D+00) & (0.000D+00,\ 0.000D+00) \\ (0.000D+00,\ 0.000D+00) & (0.000D+00,\ 0.000D+00) \end{bmatrix} \tag{B.81a}$$

$$\frac{1}{T_t}\Xi_2 e^{-j\frac{2\pi 4}{T_t}t_2^{(1)}}\frac{\partial t_2^{(1)}}{\partial X(1)} = \\ = \begin{bmatrix} (0.000D+00,\ 0.000D+00) & (4.279D-01,\ -2.379D-01) \\ (0.000D+00,\ 0.000D+00) & (6.449D+03,\ -3.585D+03) \end{bmatrix} \tag{B.81b}$$

$$\frac{1}{T_t}\Xi_3 e^{-j\frac{2\pi 4}{T_t}t_3^{(1)}}\frac{\partial t_3^{(1)}}{\partial X(1)} = \\ = \begin{bmatrix} (0.000D+00,\ 0.000D+00) & (0.000D+00,\ 0.000D+00) \\ (0.000D+00,\ 0.000D+00) & (0.000D+00,\ 0.000D+00) \end{bmatrix} \tag{B.81c}$$

$$\frac{1}{T_t}\Xi_1 e^{-j\frac{2\pi 4}{T_t}t_1^{(2)}}\frac{\partial t_1^{(2)}}{\partial X(1)} = \\ = \begin{bmatrix} (0.000D+00,\ 0.000D+00) & (0.000D+00,\ 0.000D+00) \\ (0.000D+00,\ 0.000D+00) & (0.000D+00,\ 0.000D+00) \end{bmatrix} \tag{B.81d}$$

$$\frac{1}{T_t}\,\Xi_2 e^{-j\frac{2\pi 4}{T_t}t_2^{(2)}}\,\frac{\partial t_2^{(2)}}{\partial X(1)} = \tag{B.81e}$$
$$= \begin{bmatrix} (0.000D+00,\ 0.000D+00) & (4.279D-01,\ -2.379D-01) \\ (0.000D+00,\ 0.000D+00) & (6.449D+03,\ -3.585D+03) \end{bmatrix}$$

$$\frac{1}{T_t}\,\Xi_3 e^{-j\frac{2\pi 4}{T_t}t_3^{(2)}}\,\frac{\partial t_3^{(2)}}{\partial X(1)} = \tag{B.81f}$$
$$= \begin{bmatrix} (0.000D+00,\ 0.000D+00) & (0.000D+00,\ 0.000D+00) \\ (0.000D+00,\ 0.000D+00) & (0.000D+00,\ 0.000D+00) \end{bmatrix}$$

$$\frac{1}{T_t}\,\Xi_1 e^{-j\frac{2\pi 4}{T_t}t_1^{(3)}}\,\frac{\partial t_1^{(3)}}{\partial X(1)} = \tag{B.81g}$$
$$= \begin{bmatrix} (0.000D+00,\ 0.000D+00) & (0.000D+00,\ 0.000D+00) \\ (0.000D+00,\ 0.000D+00) & (0.000D+00,\ 0.000D+00) \end{bmatrix}$$

$$\frac{1}{T_t}\,\Xi_2 e^{-j\frac{2\pi 4}{T_t}t_2^{(3)}}\,\frac{\partial t_2^{(3)}}{\partial X(1)} = \tag{B.81h}$$
$$= \begin{bmatrix} (0.000D+00,\ 0.000D+00) & (4.279D-01,\ -2.379D-01) \\ (0.000D+00,\ 0.000D+00) & (6.449D+03,\ -3.585D+03) \end{bmatrix}$$

$$\frac{1}{T_t}\,\Xi_3 e^{-j\frac{2\pi 4}{T_t}t_3^{(3)}}\,\frac{\partial t_3^{(3)}}{\partial X(1)} = \tag{B.81i}$$
$$= \begin{bmatrix} (0.000D+00,\ 0.000D+00) & (0.000D+00,\ 0.000D+00) \\ (0.000D+00,\ 0.000D+00) & (0.000D+00,\ 0.000D+00) \end{bmatrix}$$

All of these 18 components of equation (B.66) may be added together to give:

$$A(4,1) = \begin{bmatrix} (8.189D-03,\ 3.159D-02) & (-4.961D+04,\ -2.322D+04) \\ (7.904D+02,\ 3.700D+02) & (1.945D+04,\ -9.508D+03) \end{bmatrix} \tag{B.82}$$

This process is repeated eight more times in order to build the entries for $\overline{A}$. A similar process is used to build the entries for $\overline{B}$.

When all of the sub-matrices for $\overline{A}$ are computed, $\overline{A}$ will be:

```
( 7.078D+02, 1.853D+05) (-6.387D+04, 2.448D-17) | (-8.189D-03,-3.159D-02) ( 4.961D+04, 2.322D+04) | ( 7.158D-03,-3.979D-03) (-2.054D+04,-2.463D+04)
                                                |                                                 |
( 1.818D+03, 0.000D+00) ( 2.447D+04, 1.853D+05) | (-7.904D+02,-3.700D+02) (-1.945D+04, 9.508D+03) | ( 3.273D+02, 3.924D+02) ( 1.189D+04,-1.910D+04)
------------------------------------------------------------------------------------------------------------------------------------------------------------
(-8.189D-03, 3.159D-02) ( 4.961D+04,-2.322D+04) | ( 7.078D+02, 4.634D+04) (-6.387D+04,-5.102D-17) | (-8.189D-03,-3.159D-02) ( 4.961D+04, 2.322D+04)
                                                |                                                 |
(-7.904D+02, 3.700D+02) (-1.945D+04,-9.508D+03) | ( 1.018D+03, 0.000D+00) ( 2.447D+04, 4.634D+04) | (-7.904D+02,-3.700D+02) (-1.945D+04, 9.508D+03)
------------------------------------------------------------------------------------------------------------------------------------------------------------
( 7.158D-03, 3.979D-03) (-2.054D+04, 2.463D+04) | (-8.189D-03, 3.159D-02) ( 4.961D+04,-2.322D+04) | ( 7.078D+02,-9.267D+04) (-6.387D+04,-4.414D-17)
                                                |                                                 |
( 3.273D+02,-3.924D+02) ( 1.189D+04, 1.910D+04) | (-7.904D+02, 3.700D+02) (-1.945D+04,-9.508D+03) | ( 1.018D+03, 0.000D+00) ( 2.447D+04,-9.267D+04)
```

Appendix C. Creation of the State Space Matrices

The computer generation of a system of state-space equations from a circuit description given by the user is one of the key prerequisites for analysis of the system. The goal for this section is to put forth the algorithms necessary for this task in a clear, simple manner. The algorithms of this section were implemented on a personal computer using the Pascal computing language for execution on a personal computer.

C.1 DEFINITIONS

Term	*Definition*
branch	An electrical element having two terminals.
node	The point at which the terminals of two or more branches connect.
hanging node	A point that has only one terminal of one branch connecting to it.
Kirchoff's Current Law	The algebraic sum of the currents entering any node of a lumped network is zero. Kirchoff's Current Law is usually abbreviated as KCL.

Kirchoff's Voltage Law

The sum of the voltages around any loop of a network is zero. Kirchoff's Voltage Law is usually abbreviated as KVL.

tree The minimum set of branches that will connect all of the nodes without loops.

cotree The set of branches that are not contained in the tree.

link A name for a branch that is contained in the tree.

chord A name for a branch that is contained in the cotree.

tree branch A name for a branch that is contained in the tree.

twig A name for a branch that is contained in the tree.

ground A node that is used as a reference potential, and is usually considered to be a zero Volts.

connected network

An electrical network where all nodes are connected together by branches. It is possible to follow a path of branches to any node contained in the network. No nodes are isolated off by themselves.

component equation

The algebraic or differential equation that describes the relationship between the terminal quantities of a branch element

netlist a description of a circuit, written in the input language of a simulator element.

C.2 BACKGROUND

Several formulations exist for the computer-aided solution of electrical networks, such as the nodal formulation[39], the modified-nodal method[2, 40], the tableau formulation[41], and the state-space formulation[42]. All of these methods are based upon a combination of Kirchoff's Voltage Law (KVL), Kirchoff's Current Law (KCL), and the component equations (CE), although they differ in the manner in which these equations are used.

The nodal method and the state-space formulation were the first computer-aided network analysis methods to be used. The strength of the nodal method is that building the solution matrices are trivial tasks. It is possible to scan each line of input netlist and directly enter values into the solution matrix and the stimulus vector. The nodal method has a serious restriction in that each branch of the circuit had to fit into the template of a "standard branch," which made writing the circuit netlist a difficult task. Also, dependent current sources were not allowed.

The state-space method was initially a very popular method[42], but had it's own limitations. The use of the state-space method in general computer-aided electrical network analysis programs faded as the modified-nodal and the tableau method came into being. The state-space method becomes complicated in the presence of nonlinear elements. The rank of the state-space matrices may dynamically change as nonlinear elements change. An example of this is a capacitor connected to the rest of a circuit through a forward-biased diode. In this example, we will assume that the capacitor voltage has been selected as a state-variable. If,

for some reason, the diode becomes reverse-biased, the capacitor will be isolated from the circuit and will cease to be a state variable.

C.3 FORMULATION

C.3.1 Network Topololgy

To formulate the state-space matrices, it is first necessary to review some portions of circuit topology theory. This will be rather brief.

An electrical circuit is composed of many connected *branches*, each branch having two terminal connections, called *nodes*. A branch has a sense of direction, determined by the direction of the current flowing in the branch. If the current is flowing from the *from* node to the *to* node, the branch is considered to be pointing towards the *to* node. The *from* node is also assumed to be more positive in voltage relative to the *to* node.

For an example of topology, a schematic of a sample electrical network is drawn in Figure C-1.

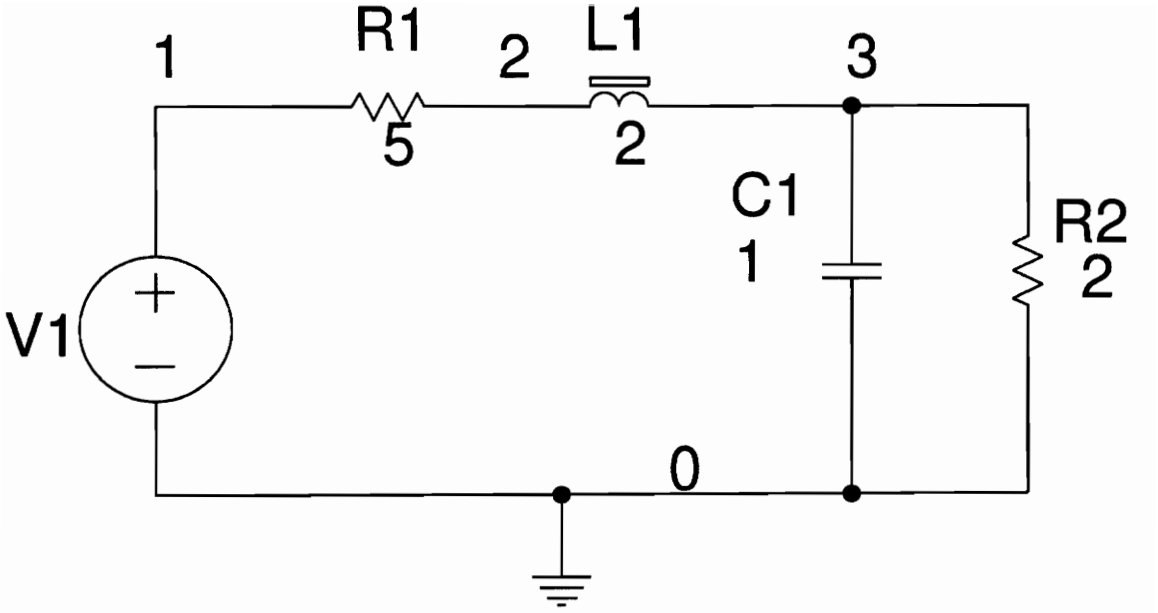

Figure C-1. Example Network

From Figure C-1, we may represent the topology of the circuit by Figure C-2.

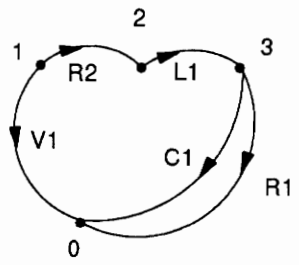

Figure C-2. Topology of Example Network

In the topology drawings, notice how the element type is not included, or the element value. Only the direction of current flow is assigned. The positive and negative nodes may be labelled from knowing the direction of current flow. If the direction of current flow is incorrectly picked, it is not a big problem. When the equations are solved, the currents will come out in the correct direction so long as all of the equations were written consistently.

C.3.2 KCL and KVL

We will use the topology of a circuit in order to write the KCL and KVL equations. We will do this by building a *reduced incident matrix* from the circuit topology, and then showing how KCL and KVL may be written using the incidence matrix.

From [43], a reduced incident matrix may be defined as having entries as follows:

$$A_{kj} = \left\{ \begin{array}{c} -1, \quad \text{if branch j is pointed away from node k} \\ 1, \quad \text{if branch j is pointed towards node k} \\ 0, \quad \text{otherwise} \end{array} \right\} \qquad \text{(C.1)}$$

An exception is made for the case of node *0*, which is considered to be the *ground* node. If the complete incidence matrix is built that includes the ground node, it is easily shown that the matrix is has a row that is linearly dependent on the other rows. So, it is convention to throw out the ground node, since it contains redundant information.

The branches of the circuit are usually ordered in the form:

1. Voltage sources
2. capacitors
3. VCVS
4. CCVS
5. resistors
6. VCCS
7. CCCS
8. inductors
9. current sources

It is shown in [43] and [44] that KCL may be written in matrix form by using the reduced incidence matrix as:

$$A\,i = 0 \tag{C.2}$$

If there are n nodes (plus ground) and b branches, then A will have n rows and b columns. If we require that *hanging nodes* are not allowed, then the number of branches will always exceed the number of nodes.

If we require that the network be *connected*, in other words that there not be two or more completely isolated subnetworks, then it is shown in [44] that the rank of the reduced incidence matrix is n. The reduced incidence matrix may be partitioned into two sections corresponding to the currents in the tree (i_T) and in the cotree (i_L).

We will define that the number of branches contained in the tree is b_T, and the number of branches is b_L. Since any branch is contained in either the tree or else to cotree, we may write an expression for the total number of branches b:

$$b = b_T + b_L \quad . \tag{C.3}$$

The KCL equation, after being rearranged to partition the tree and cotree currents, is written as:

$$\begin{bmatrix} A_T & A_L \end{bmatrix} \begin{bmatrix} i_T \\ i_L \end{bmatrix} = 0 \tag{C.4}$$

The partitioned KCL equation may be premultiplied by A_T^{-1} to give:

$$[I \;\; A_T^{-1}A_L]\begin{bmatrix} i_T \\ i_L \end{bmatrix} = 0 \quad . \tag{C.5}$$

We will define the following variable:

$$D = A_T^{-1}A_L \tag{C.6}$$

so that the partitioned KCL equation may be written as:

$$[I \;\; D]\begin{bmatrix} i_T \\ i_L \end{bmatrix} = 0 \quad . \tag{C.7}$$

We may further subdivide the tree and link partitions into three sub-categories: branches involving inductive or capacitive elements (subscript "x"), branches involving independent current or voltage sources (subscript "u"), and all others (subscript "z"). On this further subdividing, we will define the number of branches contained in each partition as a subscript on b_T and b_L. For instance, the number of independent sources contained in the tree will be defined as b_{Tu}. Since the total number of branches is b, the total number of branches in each partition will sum to give b:

$$b = b_{Tu} + b_{Tx} + b_{Tz} + b_{Lz} + b_{Lx} + b_{Lu} \tag{C.8}$$

These quantities are defined as:

Table C-1. Description of branch quantities

branch	description
b_{Tu}	number of independent voltage sources contained in the tree
b_{Tx}	number of capacitors in the tree
b_{Tz}	number of other components in the tree, consisting of VCVS, CCVS, Resistors, VCCS, and CCCS
b_{Lz}	number of other components in the cotree, consisting of VCVS, CCVS, Resistors, VCCS, and CCCS
b_{Lx}	number of inductors in the cotree
b_{Lu}	number of independent current sources in the cotree

Using this subdivision will give us the following structure for the vector of currents:

$$i = \begin{bmatrix} i_{Tu} \\ i_{Tx} \\ i_{Tz} \\ i_{Lz} \\ i_{Lx} \\ i_{Lu} \end{bmatrix} \tag{C.9}$$

The KCL relationship of equation (C.7), with this partitioning, is described by:

$$\begin{bmatrix} I & 0 & 0 & D_{uz} & D_{ux} & D_{uu} \\ 0 & I & 0 & D_{xz} & D_{xx} & D_{xu} \\ 0 & 0 & I & D_{zz} & D_{zx} & D_{zu} \end{bmatrix} \begin{bmatrix} i_{Tu} \\ i_{Tx} \\ i_{Tz} \\ i_{Lz} \\ i_{Lx} \\ i_{Lu} \end{bmatrix} = 0 \tag{C.10}$$

Using these definitions for the number of branches in each sub-category, we may define the dimensions of each sub-matrix of the D matrix:

Table C-2. Dimensions of D sub-matrices		
sub-matrix	**number of rows**	**number of columns**
D_{uz}	b_{Tu}	b_{Lz}
D_{xz}	b_{Tx}	b_{Lz}
D_{zz}	b_{Tz}	b_{Lz}
D_{ux}	b_{Tu}	b_{Lx}
D_{xx}	b_{Tx}	b_{Lx}
D_{zx}	b_{Tz}	b_{Lx}
D_{uu}	b_{Tu}	b_{Lu}
D_{xu}	b_{Tx}	b_{Lu}
D_{zu}	b_{Tz}	b_{Lu}

It is shown in [43, 44] that KVL may be written in matrix form using the *loop matrix*, B, as:

$$Bv = 0 \tag{C.11}$$

In [43], a relationship is derived between B and A that allows B to be expressed in terms of A:

$$B = \begin{bmatrix} -D^T & I \end{bmatrix} , \tag{C.12}$$

where D was defined in equation (C.6).

This allows us to partition the vector of branch voltages, v, into the similar six categories that we partitioned the branch currents into:

$$v = \begin{bmatrix} v_{Tu} \\ v_{Tx} \\ v_{Tz} \\ v_{Lz} \\ v_{Lx} \\ v_{Lu} \end{bmatrix} \tag{C.13}$$

Using this partitioning, as well as expressing the loop matrix, B, in terms of the incidence matrix, we have:

$$\begin{bmatrix} -D_{uz}{}^T & -D_{xz}{}^T & -D_{zz}{}^T & I & 0 & 0 \\ -D_{ux}{}^T & -D_{xx}{}^T & -D_{zx}{}^T & 0 & I & 0 \\ -D_{uu}{}^T & -D_{xu}{}^T & -D_{zu}{}^T & 0 & 0 & I \end{bmatrix} \begin{bmatrix} v_{Tu} \\ v_{Tx} \\ v_{Tz} \\ v_{Lz} \\ v_{Lx} \\ v_{Lu} \end{bmatrix} = 0 \qquad \text{(C.14)}$$

C.3.3 Component Equations

Each branch, besides contributing to the KVL and KCL equations, also represents an electrical component. For each electrical component there is a *component equation* that describes the relationship between the branch current and voltage. For all components, with the exception of capacitors and inductors, the component equations are simple algebraic equations. For capacitors and inductors the equations are differential equations.

Table C-3 (Page 1 of 2). Elements and Respective Component Equations

Element Name	**SPICE Prefix**	**Component Equation**
Resistor	R	$-v + r\,i = 0$
Voltage Controlled Voltage Source (VCVS)	E	$-v + e\,v_c = 0$
Voltage Controlled Current Source (VCCS)	G	$-i + g\,v_c = 0$
Current Controlled Current Source (CCCS)	F	$-i + f\,i_c = 0$
Current Controlled Voltage Source (CCVS)	H	$-v + h\,i_c = 0$
Capacitors	C	$-i + c\,\frac{dv}{dt} = 0$
Inductors	L	$-v + l\,\frac{di}{dt} = 0$
Independent Voltage Source	V	-v + 'constant' = 0

Independent Current Source	I	-i + 'constant' = 0

Since the Resistor, VCVS, VCCS, CCCS, and CCVS component equations relate branch voltages and currents, each of these equations may be made to fit into a more general matrix form:

$$\begin{bmatrix} F_{v_{Tu}} & F_{v_{Tx}} & F_{v_{Tz}} & F_{v_{Lz}} & F_{v_{Lx}} & F_{v_{Lu}} & F_{i_{Tu}} & F_{i_{Tx}} & F_{i_{Tz}} & F_{i_{Lz}} & F_{i_{Lx}} & F_{i_{Lu}} \end{bmatrix} \begin{bmatrix} v_{Tu} \\ v_{Tx} \\ v_{Tz} \\ v_{Lz} \\ v_{Lx} \\ v_{Lu} \\ i_{Tu} \\ i_{Tx} \\ i_{Tz} \\ i_{Lz} \\ i_{Lx} \\ i_{Lu} \end{bmatrix} = 0 \quad . \qquad \text{(C.15)}$$

The dimensions of each of these component equation sub-matrix is described by the following table:

Table C-4 (Page 1 of 2). Dimensions of component equation sub-matrices

sub-matrix	number of rows	number of columns
$F_{v_{Tu}}$	$b_{Tz} + b_{Lz}$	b_{Tu}
$F_{v_{Tx}}$	$b_{Tz} + b_{Lz}$	b_{Tx}
$F_{v_{Tz}}$	$b_{Tz} + b_{Lz}$	b_{Tz}
$F_{v_{Lz}}$	$b_{Tz} + b_{Lz}$	b_{Lz}
$F_{v_{Lx}}$	$b_{Tz} + b_{Lz}$	b_{Lx}
$F_{v_{Lu}}$	$b_{Tz} + b_{Lz}$	b_{Lu}
$F_{i_{Tu}}$	$b_{Tz} + b_{Lz}$	b_{Tu}
$F_{i_{Tx}}$	$b_{Tz} + b_{Lz}$	b_{Tx}
$F_{i_{Tz}}$	$b_{Tz} + b_{Lz}$	b_{Tz}
$F_{i_{Lz}}$	$b_{Tz} + b_{Lz}$	b_{Lz}
$F_{i_{Lx}}$	$b_{Tz} + b_{Lz}$	b_{Lx}

F_{i_n}	$b_{Tz} + b_{Lz}$	b_{Lu}

The capacitor and inductor branches are described by differential equations of the form

$$i(t) = c\frac{dv}{dt} \tag{C.16}$$

and

$$v(t) = l\frac{di}{dt} \quad . \tag{C.17}$$

If we restrict capacitors to exist only in the tree, and for inductors to exist only in the cotree, then we may combine all of the component equation of the inductors and capacitors into one equation:

$$\begin{bmatrix} i_{Tx} \\ v_{Lx} \end{bmatrix} = \begin{bmatrix} W_c & 0 \\ 0 & W_l \end{bmatrix} \begin{bmatrix} \dot{v}_{Tx} \\ \dot{i}_{Lx} \end{bmatrix} \tag{C.18}$$

C.3.4 Tableau Formulation

In formulating the component equations, we formed a solution vector consisting of all of the branch voltages and currents. Shortly, we will combine equation (C.10), equation (C.14), and equation (C.15) into one large tableau matrix using a similar solution vector. Since equation (C.10) relates the branch currents, equation (C.14) relates the branch voltages, and equation (C.15) relates both the branch voltages and currents, we may do this. First, we will partition the elements of the solution vector to place us in a good position for solving for the state-space matrices with minimum effort. Then, we will form this tableau matrix out of the individual sub-blocks of equation (C.10), equation (C.14), and equation (C.15).

For an initial pass at the selection of state variables, we will choose the capacitive tree branch voltages and the inductive cotree branch currents. In this initial formulation, we are not allowing capacitive cotree elements or inductive tree elements, which come about from capacitive loops and inductive cutsets. It would be easy to modify this formulation to allow these elements.

The initial selection of state variables is then:

$$x = \begin{bmatrix} v_{Tx} \\ i_{Lx} \end{bmatrix} \tag{C.19}$$

In equation (C.18), we see that from knowing i_{Tx} and v_{Lx} we may compute the time-derivatives of the state vector composed of v_{Tx} and i_{Lx}. We will collect i_{Tx} and v_{Lx} into a vector called x':

$$x' = \begin{bmatrix} i_{Tx} \\ v_{Lx} \end{bmatrix} \tag{C.20}$$

The input vector u will be composed of the independent voltage sources and the independent current sources:

$$u = \begin{bmatrix} v_{Tu} \\ i_{Lu} \end{bmatrix} \tag{C.21}$$

The output vector, y, will be composed of everything else:

$$y = \begin{bmatrix} i_{Tu} \\ i_{Tz} \\ i_{Lz} \\ v_{Tz} \\ v_{Lz} \\ v_{Lu} \end{bmatrix} \tag{C.22}$$

We may rewrite the KCL equation (C.10) using this new, larger, solution vector:

$$\begin{bmatrix} I & 0 & D_{uz} & 0 & 0 & 0 & 0 & 0 & 0 & D_{ux} & 0 & D_{uu} \\ 0 & I & D_{zz} & 0 & 0 & 0 & 0 & 0 & 0 & D_{zx} & 0 & D_{zu} \\ 0 & 0 & D_{xz} & 0 & 0 & 0 & I & 0 & 0 & D_{xx} & 0 & D_{xu} \end{bmatrix} \begin{bmatrix} \\ i_{Tu} \\ i_{Tz} \\ i_{Lz} \\ v_{Tz} \\ v_{Lz} \\ v_{Lu} \\ \text{---} \\ i_{Tx} \\ v_{Lx} \\ \text{---} \\ v_{Tx} \\ i_{Lx} \\ \text{---} \\ v_{Tu} \\ i_{Lu} \\ \\ \end{bmatrix} = 0 \qquad \text{(C.23)}$$

Similarly, we may rewrite the KVL equation equation (C.14):

$$\begin{bmatrix} 0 & 0 & 0 & -D_{zx}{}^T & 0 & 0 & 0 & I & -D_{xx}{}^T & 0 & -D_{ux}{}^T & 0 \\ 0 & 0 & 0 & -D_{zz}{}^T & I & 0 & 0 & 0 & -D_{xz}{}^T & 0 & -D_{uz}{}^T & 0 \\ 0 & 0 & 0 & -D_{zu}{}^T & 0 & I & 0 & 0 & -D_{xu}{}^T & 0 & -D_{uu}{}^T & 0 \end{bmatrix} \begin{bmatrix} i_{Tu} \\ i_{Tz} \\ i_{Lz} \\ v_{Tz} \\ v_{Lz} \\ v_{Lu} \\ --- \\ i_{Tx} \\ v_{Lx} \\ --- \\ v_{Tx} \\ i_{Lx} \\ --- \\ v_{Tu} \\ i_{Lu} \end{bmatrix} = 0 \qquad \text{(C.24)}$$

The component equation equation (C.15) needs to be rearranged:

$$\begin{bmatrix} F_{i_{Tu}} & F_{i_{Tz}} & F_{i_{Lz}} & F_{v_{Tz}} & F_{v_{Lz}} & F_{v_{Lu}} & F_{i_{Tx}} & F_{v_{Lx}} & F_{v_{Tx}} & F_{i_{Lx}} & F_{v_{Tu}} & F_{i_{Lu}} \end{bmatrix} \begin{bmatrix} \\ i_{Tu} \\ i_{Tz} \\ i_{Lz} \\ v_{Tz} \\ v_{Lz} \\ v_{Lu} \\ --- \\ i_{Tx} \\ v_{Lx} \\ --- \\ v_{Tx} \\ i_{Lx} \\ --- \\ v_{Tu} \\ i_{Lu} \\ \\ \end{bmatrix} = 0 \quad \text{(C.25)}$$

We may now take the KVL equations equation (C.23), the KVL equations equation (C.24), and the component equations equation (C.25), and merge them together into a large tableau matrix:

$$\begin{bmatrix} I & 0 & D_{uz} & 0 & 0 & 0 & 0 & 0 & 0 & D_{ux} & 0 & D_{uu} \\ 0 & I & D_{zz} & 0 & 0 & 0 & 0 & 0 & 0 & D_{zx} & 0 & D_{zu} \\ 0 & 0 & D_{xz} & 0 & 0 & 0 & I & 0 & 0 & D_{xx} & 0 & D_{xu} \\ 0 & 0 & 0 & -D_{zx}{}^{T} & 0 & 0 & 0 & I & -D_{xx}{}^{T} & 0 & -D_{ux}{}^{T} & 0 \\ 0 & 0 & 0 & -D_{zz}{}^{T} & I & 0 & 0 & 0 & -D_{xz}{}^{T} & 0 & -D_{uz}{}^{T} & 0 \\ 0 & 0 & 0 & -D_{zu}{}^{T} & 0 & I & 0 & 0 & -D_{xu}{}^{T} & 0 & -D_{uu}{}^{T} & 0 \\ F_{i_{Tu}} & F_{i_{Tz}} & F_{i_{Lz}} & F_{v_{Tz}} & F_{v_{Lz}} & F_{v_{Lu}} & F_{i_{Tx}} & F_{v_{Lx}} & F_{v_{Tx}} & F_{i_{Lx}} & F_{v_{Tu}} & F_{i_{Lu}} \end{bmatrix} \begin{bmatrix} i_{Tu} \\ i_{Tz} \\ i_{Lz} \\ v_{Tz} \\ v_{Lz} \\ v_{Lu} \\ --- \\ i_{Tx} \\ v_{Lx} \\ --- \\ v_{Tx} \\ i_{Lx} \\ --- \\ v_{Tu} \\ i_{Lu} \end{bmatrix} = 0 \quad \text{(C.26)}$$

We may use elementary row and column operations to reduce equation (C.26) to echelon form, and then backsolve to form zeros above the main diagonal. After this operation, we will be left with an identity matrix on the main diagonal:

$$\begin{bmatrix} I & 0 & -C & -D \\ 0 & I & -A' & -B' \end{bmatrix} \begin{bmatrix} y \\ x' \\ x \\ u \end{bmatrix} = 0 \tag{C.27}$$

From this equation, we see the following relationship:

$$x' = A'\ x\ + B'\ u \tag{C.28}$$

This can be expanded into:

$$\begin{bmatrix} i_{Tx} \\ v_{Lx} \end{bmatrix} = A' \begin{bmatrix} v_{Tx} \\ i_{Lx} \end{bmatrix} + B' \begin{bmatrix} v_{Tu} \\ i_{Lu} \end{bmatrix} \tag{C.29}$$

We may substitute in equation (C.18), which will enable us to form the desired standard state-formulation:

$$\begin{bmatrix} i_{Tx} \\ v_{Lx} \end{bmatrix} = \begin{bmatrix} W_c & 0 \\ 0 & W_l \end{bmatrix} \begin{bmatrix} \dot{v}_{Tx} \\ \dot{i}_{Lx} \end{bmatrix} = A' \begin{bmatrix} v_{Tx} \\ i_{Lx} \end{bmatrix} + B' \begin{bmatrix} v_{Tu} \\ i_{Lu} \end{bmatrix} \tag{C.30}$$

This is almost in the correct form. By premultiplying by the inverse of the capacitance and inductance matrix, we will be in the right form:

$$\dot{x} = Ax + bu \tag{C.31}$$

where

$$A = \begin{bmatrix} W_c & 0 \\ 0 & W_l \end{bmatrix}^{-1} A' \tag{C.32}$$

and

$$B = \begin{bmatrix} W_c & 0 \\ 0 & W_l \end{bmatrix}^{-1} B' \tag{C.33}$$

Table C-5. Dimensions of State-Space Matrices		
matrix	**number of rows**	**number of columns**
A	$b_{Tx} + b_{Lx}$	$b_{Tx} + b_{Lx}$
B	$b_{Tx} + b_{Lx}$	$b_{Tu} + b_{Lu}$
C	$2b - 2b_{Tx} - 2b_{Lx} - b_{Tu} - b_{Lu}$	$b_{Tx} + b_{Lx}$
D	$2b - 2b_{Tx} - 2b_{Lx} - b_{Tu} - b_{Lu}$	$b_{Tu} + b_{Lu}$

C.4 AN EXAMPLE

This example is a simple, averaging LC-filter. The component values chosen are in Ohms, Farads, and Henries.

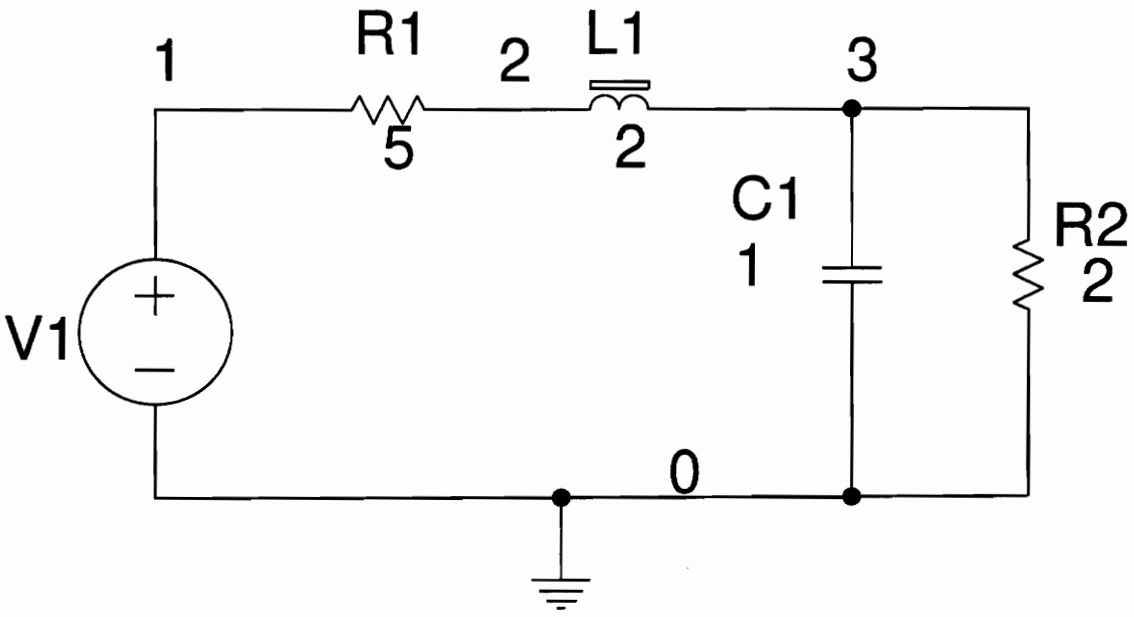

Figure C-3. Example Network

The topology of this circuit is described by Figure C-2. This circuit has five elements and four nodes (including ground). The arrows on the graph indicate the assumed direction of current flow.

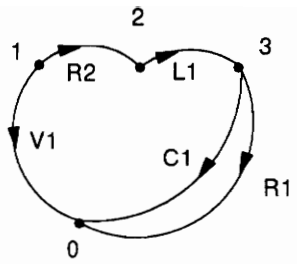

Figure C-4. Topology of Example Network

The following topology graph shows the tree branches highlighted in a darker linestyle. The preference in the selection of tree branches is that voltage sources must be tree branches, capacitors should be tree branches, inductors shouldn't be, and current sources can't be tree branches. With this ordering, the voltage source, resistor R2, and the capacitor were chosen to be tree branches. The inductor was excluded, along with resistor R1.

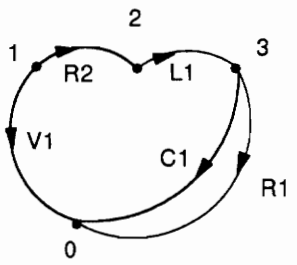

Figure C-5. Tree Structure

The following netlist was automatically generated by the schematic capture program. This netlist is in SPICE2G syntax:

```
CIRCUIT: DSTATE1   DATE: FRI NOV 01 23:42:36 1991
V1 1 0 4.0
R1 1 2 5.0
L1 2 3 2.0
C1 3 0 1.0
R2 3 0 2.0
.END
```

The reduced incidence matrix for this circuit is:

$$\begin{bmatrix} 0 & 1 & 0 & 1 & -1 \\ 0 & 0 & -1 & 0 & 1 \\ 1 & 0 & 1 & 0 & 0 \end{bmatrix} \tag{C.34}$$

After the reduction to row-echelon form and backsolving, the incidence matrix is transformed into the form of equation (C.5):

$$\begin{bmatrix} 1 & 0 & 0 & 0 & 1 \\ 0 & 1 & 0 & 1 & -1 \\ 0 & 0 & 1 & 0 & -1 \end{bmatrix} \tag{C.35}$$

The vector of currents, equation (C.9), is composed of the following elements:

$$i_{Tu} = [i_{V1}] \tag{C.36}$$

$$i_{Tx} = [i_{C1}] \tag{C.37}$$

$$i_{Tz} = [i_{R1}] \tag{C.38}$$

$$i_{Lz} = [i_{R2}] \tag{C.39}$$

$$i_{Lx} = [i_{L1}] \tag{C.40}$$

The number of number of components in each category is:

$$b_{Tu} = 1, \quad b_{Tx} = 1, \quad b_{Tz} = 1, \quad b_{Lz} = 1, \quad b_{Lx} = 1, \quad b_{Lu} = 0 \tag{C.41}$$

We may pick apart equation (C.35) into its individual subsections, using equation (C.10) as a guide:

$$D_{uz} = [0], \quad D_{ux} = [1], \quad D_{xz} = [1], \quad D_{xx} = [-1], \quad D_{zz} = [0], \quad D_{zx} = [-1] \tag{C.42}$$

We may now build a system of equations of the form of equation (C.26) using all of these pieces, as well as the component equations for the two resistors:

$$\begin{bmatrix} 1 & 0 & 0 & 0 & 0 & 0 & 0 & 0 & 1 & 0 \\ 0 & 1 & 0 & 0 & 0 & 0 & 0 & 0 & -1 & 0 \\ 0 & 0 & 1 & 0 & 0 & 1 & 0 & 0 & -1 & 0 \\ 0 & 0 & 0 & 1 & 0 & 0 & 1 & 1 & 0 & -1 \\ 0 & 0 & 0 & 0 & 1 & 0 & 0 & -1 & 0 & 0 \\ 0 & -5 & 0 & 1 & 0 & 0 & 0 & 0 & 0 & 0 \\ 0 & 0 & -2 & 0 & 1 & 0 & 0 & 0 & 0 & 0 \end{bmatrix} \begin{bmatrix} i_{V1} \\ i_{R1} \\ i_{R2} \\ v_{R1} \\ v_{R2} \\ --- \\ i_{C1} \\ v_{L1} \\ --- \\ v_{C1} \\ i_{L1} \\ --- \\ v_{V1} \end{bmatrix} = 0 \qquad \text{(C.43)}$$

After reduction and backsolve, this transforms into:

$$\begin{bmatrix} 1 & 0 & 0 & 0 & 0 & 0 & 0 & 0 & 1 & 0 \\ 0 & 1 & 0 & 0 & 0 & 0 & 0 & 0 & -1 & 0 \\ 0 & 0 & 1 & 0 & 0 & 0 & 0 & -0.5 & 0 & 0 \\ 0 & 0 & 0 & 1 & 0 & 0 & 0 & 0 & -5 & 0 \\ 0 & 0 & 0 & 0 & 1 & 0 & 0 & -1 & 0 & 0 \\ 0 & 0 & 0 & 0 & 0 & 1 & 0 & 0.5 & -1 & 0 \\ 0 & 0 & 0 & 0 & 0 & 0 & 1 & 1 & 5 & -1 \end{bmatrix} \begin{bmatrix} i_{V1} \\ i_{R1} \\ i_{R2} \\ v_{R1} \\ v_{R2} \\ --- \\ i_{C1} \\ v_{L1} \\ --- \\ v_{C1} \\ i_{L1} \\ --- \\ v_{V1} \end{bmatrix} = 0 \qquad \text{(C.44)}$$

From this, we can pick out the equation for the output vector:

$$\begin{bmatrix} i_{V1} \\ i_{R1} \\ i_{R2} \\ v_{R1} \\ v_{R2} \end{bmatrix} = \begin{bmatrix} 0 & -1 \\ 0 & 1 \\ 0.5 & 0 \\ 0 & 5 \\ 1 & 0 \end{bmatrix} \begin{bmatrix} v_{C1} \\ i_{L1} \end{bmatrix} + \begin{bmatrix} 0 \\ 0 \\ 0 \\ 0 \\ 0 \end{bmatrix} [v_{V1}] \qquad \text{(C.45)}$$

We can also pick out the basis for the set of state equations:

$$\begin{bmatrix} i_{C1} \\ v_{L1} \end{bmatrix} = \begin{bmatrix} -0.5 & 1 \\ -1 & -5 \end{bmatrix} \begin{bmatrix} v_{C1} \\ i_{L1} \end{bmatrix} + \begin{bmatrix} 0 \\ 1 \end{bmatrix} [v_{V1}] \tag{C.46}$$

Using the component equations for the capacitor and the inductor, we may pose this equation in the form of equation (C.30):

$$\begin{bmatrix} i_{C1} \\ v_{L1} \end{bmatrix} = \begin{bmatrix} 1 & 0 \\ 0 & 2 \end{bmatrix} \begin{bmatrix} \dot{v}_{C1} \\ \dot{i}_{L1} \end{bmatrix} = \begin{bmatrix} -0.5 & 1 \\ -1 & -5 \end{bmatrix} \begin{bmatrix} v_{C1} \\ i_{L1} \end{bmatrix} + \begin{bmatrix} 0 \\ 1 \end{bmatrix} [v_{V1}] \tag{C.47}$$

This may be easily solved for the desired state formulation:

$$\begin{bmatrix} \dot{v}_{C1} \\ \dot{i}_{L1} \end{bmatrix} = \begin{bmatrix} -0.5 & 1 \\ -0.5 & -2.5 \end{bmatrix} \begin{bmatrix} v_{C1} \\ i_{L1} \end{bmatrix} + \begin{bmatrix} 0 \\ 0.5 \end{bmatrix} [v_{V1}] \tag{C.48}$$

C.5 CONCLUSIONS

In this chapter, it is shown how to create the state-space matrices by transforming from the tableau formulation. This is not the most computationally efficient method for generating the state-space matrices, since the tableau formulation is extremely sparse, and my code takes no advantage of sparsity. However, it was stated in [43] without proof that the state-space

matrices could be generated from the tableau formulation. This chapter represents proof that this is indeed possible.

The state-space formulation is important for theoretical analysis, since many mathematical tools, like eigenvalues, are directly applicable to the state-space formulation. However, most modern general-purpose circuit analysis programs abandon the state-space formulation in favor of the modified-nodal formulation. One of the reasons for this is the state-space formulation does not easily handle nonlinearities, while the modified-nodal analysis does.

The main motivation for this particular work was the need for the generation of the state-space matrices from a netlist that had a syntax similar to that of SPICE. There are very few state-space programs available in the literature, and none that accept SPICE syntax.

Appendix D. STAEQ2 User's Guide

D.1 INVOCATION

The STAEQ2 program is written in Turbo Pascal Version 6.0 for DOS on an IBM-PC compatible system. If another operating system is desirable, it might be possible to translate this to C using a translator program, and then re-compile using a C compiler for the operating system of choice.

The STAEQ2 program is invoked using:

```
staeq2 infile.ext
```

The infile.ext file contains a netlist describing the circuit, written in a modified form of SPICE input syntax. This input syntax is described in the next section.

The STAEQ2 program creates several output files, briefly described below:

- infile.lst - This creates a human readable listing of the state-space matrices if the LIST option has been used on the .OPTIONS card.

- config.ac - this is a small file containing information on the starting frequency, the number of decades of AC analysis, and the number of points per decade.

- input2.dat - this file feeds information into the SIMU program. It contains information on convergence, initial conditions, and the value of the independent current and voltage sources.

- abce2.dat - this file is also for SIMU. It contains the state-space matrices in a one-line per matrix entry form.

D.2 MODIFIED SPICE2 INPUT SYNTAX FOR COSMIR

The input syntax for this simulator is based upon the Spice2 input syntax described in [2]. There are several notable differences since this simulator is based upon a state-space formulation instead of a modified-nodal formulation. Since this formulation does not naturally have node voltages accessable as part of the system of equations, node voltages may be accessed using the branch voltage of an element connected between the desired node and ground.

Nonlinear capacitors and inductors are not allowed, since this simulator assumes a piecewise-linear formulation.

D.2.1 Title, Comment and .END Cards

D.2.1.1 Title Card

Examples:

```
BUCK CONVERTER - CONTINUOUS
TEST OF NEW CIRCUIT
```

This card must be the first card in the input deck. Its contents are printed verbatim as the heading for each section of output.

D.2.1.2 .END Card

Example:

```
.END
```

This card must always be the last card in the input deck. Note that the period is an integral part of the name.

D.2.1.3 Comment Card

General Form:

```
* <any comment>
```

Examples:

```
* RF=1K      GAIN SHOULD BE 100
* MAY THE FORCE BE WITH MY CIRCUIT
```

The asterisk in the first column indicates that this card is a comment card. Comment cards may be placed anywhere in the circuit description.

D.2.2 Element Cards

D.2.2.1 Parameters

General form:

```
PXXXX  value1  value2  value3 ......
```

The parameter statement is used to change the values of components to simulate the switching action in power supply circuits. The maximum number of values contained in any parameter statement determine the number of systems of state space equations that the simulator will generate. For example:

```
PR1  1e-6   1e6   1e-6
PR2  1e6    1e-6
```

In this example, there would be three sets of state space equations generated, the first with PR1=1e-6 and PR2=1e6, the second with PR1=1e6 and PR2=1e-6, and the third with PR1=1e-6 and PR2=1e-6. The last value in a parameter statement will be used over again if the simulator is generating more sets of state space equations than there are values.

The mechanism that causes a transition from one set of state space equations to the next is the boundary condition equation, which is discussed at ta later point.

D.2.2.2 Resistors

General form:

```
RXXXXXXX N1 N2 VALUE
```

Example:

```
R1 1 2 100K
RSWITCH  5  0 PSW
PSW 1E-6   1E6
```

N1 and N2 are the two element nodes. VALUE is the resistance (in ohms) and may be positive or negative but not zero.

VALUE may be assigned a parameter name. The parameter may be defined in another statement. The parameter must start with the letter P. This is the mechanism used for simulating an ideal switch using a resistor whose value changes from a near short to a near open.

In the above example, RSWITCH is a resistor whose value, PSW, changes from 1e-6 to 1e6 Ohms.

D.2.2.3 Capacitors and Inductors

```
General form:

    CXXXXXXX N+ N- VALUE <IC=INCOND>
    LYYYYYYY N+ N- VALUE <IC=INCOND>

Examples:

    CBYP 13 0 1UF
    COSC 17 23 10U IC=3V
    LLINK 42 69 1UH
    LSHUNT 23 51 10U IC=15.7MA
```

N+ and N- are the positive and negative element nodes, respectively. VALUE is the capacitance in Farads or the inductance in Henries.

For the capacitor, the (optional) initial condition is the initial (time-zero) value of capacitor voltage (in Volts). For the inductor, the (optional) initial condition is the initial (time-zero) value of inductor current (in Amps) that flows from N+, through the inductor, to N-.

D.2.2.4 Coupled (Mutual) Inductors

```
General form:

    KXXXXXXX LYYYYYYY LZZZZZZZ VALUE

Examples:

    K43 LAA LBB 0.999
    KXFRMR L1 L2 0.87
```

LYYYYYYY and LZZZZZZZ are the names of the two coupled inductors, and VALUE is the coefficient of coupling, K, which must be greater than 0 and less than or equal to 1. Using the 'dot' convention, place a 'dot' on the first node of each inductor.

D.2.2.5 Linear Dependent Sources

SPICE allows circuits to contain linear dependent sources characterized by any of the four equations

```
i=g*v          v=e*v          i=f*i          v=h*i
```

where g, e, f, and h are constants representing transconductance, voltage gain, current gain, and transresistance, respectively.

Linear Voltage-Controlled Current Sources

General form:

```
GXXXXXXX N+ N- NC+ NC- VALUE
```

Examples:

```
G1 2 0 5 0 0.1MMHO
```

N+ and N- are the positive and negative nodes, respectively. Current flow is from the positive node, through the source, to the negative node. NC+ and NC- are the positive and negative controlling nodes, respectively. VALUE is the transconductance (in mhos).

Since this simulator is branch oriented rather than node oriented, the simulator will insert a zero-valued current source between N+ and N-, and will sense the voltage across this current source. The name of the current source is generated from the name of the G source, prefixed with 'IX_'. An example of the additional component added is:

```
IX_G1 5 0 0.0
```

Linear Voltage-Controlled Voltage Sources

General form:

```
EXXXXXXX N+ N- NC+ NC- VALUE
```

Examples:

```
E1 2 3 14 1 2.0
```

N+ is the positive node, and N- is the negative node. NC+ and NC- are the positive and negative controlling nodes, respectively. VALUE is the voltage gain.

Since this simulator is branch oriented rather than node oriented, the simulator will insert a zero-valued current source between N+ and N-, and will sense the voltage across this current source. The name of the current source is generated from the name of the E source, prefixed with 'IX_'. An example of the additional component added is:

```
IX_E1 14 1 0.0
```

Linear Current-Controlled Current Sources

```
General form:

    FXXXXXXX N+ N- VNAM VALUE

Examples:

    F1 13 5 VSENS 5
```

N+ and N- are the positive and negative nodes, respectively. Current flow is from the positive node, through the source, to the negative node. VNAM is the name of a voltage source through which the controlling current flows. The direction of positive controlling current flow is from the positive node, through the source, to the negative node of VNAM. VALUE is the current gain.

Since the COSMIR program SIMU is limited in the number of independent sources it can handle, if the controlling voltage source is prefixed with 'VX_' it will not show up in the list of independent sources. An example of this is:

```
F2 20 1 VX_CT 3.3
VX_CT 14 3 0.0
```

In the above example, the dependent source F2 is dependent upon the current flowing through VX_CT. The independent voltage source VX_CT has a DC value of zero, and because it is prefixed with 'VX_' it will not show up in the state equations that will be fed on to the SIMU program.

Linear Current-Controlled Voltage Sources

General form:

```
HXXXXXXX N+ N- VNAM VALUE
```

Examples:

```
HX 5 17 VZ 0.5K
```

N+ and N- are the positive and negative nodes, respectively. VNAM is the name of a voltage source through which the controlling current flows. The direction of positive controlling current flow is from the positive node, through the source, to the negative node of VNAM. VALUE is the transresistance (in ohms).

Since the COSMIR program SIMU is limited in the number of independent sources it can handle, if the controlling voltage source is prefixed with 'VX_' it will not show up in the list of independent sources. An example of this is:

```
HCT 20 1 VX_CT 3.3
VX_CT 14 3 0.0
```

In the above example, the dependent source HCT is dependent upon the current flowing through VX_CT. The independent voltage source VX_CT has a DC value of zero, and because it is prefixed with 'VX_' it will not show up in the state equations that will be fed on to the SIMU program.

D.2.2.6 Independent Sources

General form:

```
VXXXXXXX N+ N- <<DC> DC VALUE>
IYYYYYYY N+ N- <<DC> DC VALUE>
```

Examples:

```
VCC 10 0 DC 6
IZZ 13 2 0.001
VMEAS 12 9
```

N+ and N- are the positive and negative nodes, respectively. Note that voltage sources need not be grounded. Positive current is assumed to flow from the positive node, through the source, to the negative node. A current source of positive value, will force current to flow out of the N+ node, through the source, and into the N- node. Voltage sources, in addition to being used for circuit excitation, are the 'ammeters' for SPICE, that is, zero valued voltage sources may be inserted into the circuit for the purpose of measuring current. They will, of course, have no effect on circuit operation since they represent short-circuits.

Since the COSMIR program SIMU is limited in the number of independent sources it can handle, if the controlling voltage source is prefixed with 'VX_' it will not show up in the list of independent sources.

DC is the dc value of the source. If the source value is zero the dc analysis, this value may be omitted. If the source value is time-invariant (e.g., a power supply), then the value may optionally be preceded by the letters DC.

D.2.3 Execution Controls

D.2.3.1 .AC Card

General form:

```
.AC DEC ND FSTART FSTOP
```

Examples:

```
.AC DEC 10 1 10K
.AC DEC 10 1K 100MEG
```

DEC stands for decade variation, and ND is the number of points per decade. FSTART is the starting frequency, and FSTOP is the final frequency. If this card is not included, the default value for ND is 3, FSTART is 10, and FSTOP is 10K. If there is not an integer number of decades between FSTART and FSTOP, the simulator will increase FSTOP so that there is an integer number of decades.

D.2.3.2 .OPTIONS Card

General form:

```
.OPTIONS OPT1 OPT2 ... (or OPT=OPTVAL ...)
```

Examples:

```
.OPTIONS LIST EPS=1.0E-9
```

This card allows the user to reset program control and user options for specific simulation purposes. Any combination of the following options may be included, in any order. 'x' (below) represents some positive number.

option	**effect**
LIST	causes the summary listing of the input data to be print
NSWPT	(2) switching points only, (3) all points - default 2
NIT	max iterations for Newton's method - default 20
MC	number of steps in independent V and I sources - default 1
EPS	tolerance for Phi and D computations - default 1.0D-8
ULIM	upper limit for state variables - default 1.0D20
LLIM	lower limit for state variables - default -1.0D20
BEPS	tolerance for boundary time convergence - default 1.0D-8

D.2.3.3 .PRINT Cards

General form:

```
.PRINT PRTYPE OV1 <OV2 ... OV8>
```

Examples:

```
.PRINT TRAN V(R5) I(VIN)
```

This card defines the contents of the output vector of the system of state space equations that are created by this simulator. PRTYPE is the type of the analysis (TRAN only at this time) for which the specified outputs are desired. The form for voltage or current output variables is as follows:

```
V(element_name)
```

specifies the voltage across the branch named element_name.

```
I(element_name)
```

specifies the current flowing through the branch named element_name.

D.2.3.4 .PLOT Cards

General form:

```
.PLOT PLTYPE OV1 <(PLO1,PHI1)> <OV2 <(PLO2,PHI2)> ... OV8>
```

Examples:

```
.PLOT TRAN V(RX) I(V1)
```

This card defines the contents of one plot of from one to eight output variables. PLTYPE is the type of analysis (TRAN is the only one allowed at this time) for which the specified outputs are desired. The syntax for the OVI is identical to that for the .PRINT card, described above.

D.2.3.5 .TRAN Card

General form:

```
.TRAN TSTEP TSTOP
```

Examples:

```
.TRAN 1NS 100NS
```

TSTEP is the step size within each mode of operation. TSTOP is the final time. A start time of zero is assumed. The transient analysis always begins at time zero.

Appendix E. The ACF Program User's Guide

Once the STAEQ2 program has been used to find the state-space matrices, and the SIMU program has been used to solve for the steady-state operating point, then the ACF program may be used to solve for various small-signal transfer functions.

The ACF program uses the concept of the network analyzer for it's logical operation. It allows any independent voltage or current source to be connected to the small-signal stimulus source. Any voltage or current that was specified as an output using the .PRINT or .PLOT card may be probed to find any desired transfer function.

```
D:\ORCAD\BSTDSC>acf
Version ACF 07/07/93

Enter the number of the stimulus source:
    1     V1
    2     VD
    3     I1
2

Enter the number of the B probe for B/A:
    0     VD
    1     V(RVD)
    2     I(L1)
    3     V(RLOAD)
3

Enter the number of the A probe for B/A:
    0     VD
    1     V(RVD)
    2     I(L1)
    3     V(RLOAD)
0

Enter a value for P >= 0 :
3
```

Figure E-1. User Screen from the ACF Program

Notice that two probes need to be logically connected to the circuit: the 'B' and the 'A' probe. The list of valid connections is made up of all of the output variables from the circuit, as well as including the stimulus. This allows for almost any transfer function to be computed.

Appendix F. The ORCAD/STAEQ/SIMU/ACF Design Environment

The commercially available program 'ORCAD' was used to as a schematic capture program. Once the schematic has been captured, ORCAD may be used to automatically generate a SPICE netlist which may be used as the input to STAEQ2, which creates the state-space matrices.

The opening screen of ORCAD is shown in Figure F-1. We will click the mouse on 'Design Management Tools' and select a particular design. Once a design has been selected, click on 'Schematic Design Tools' to edit that design.

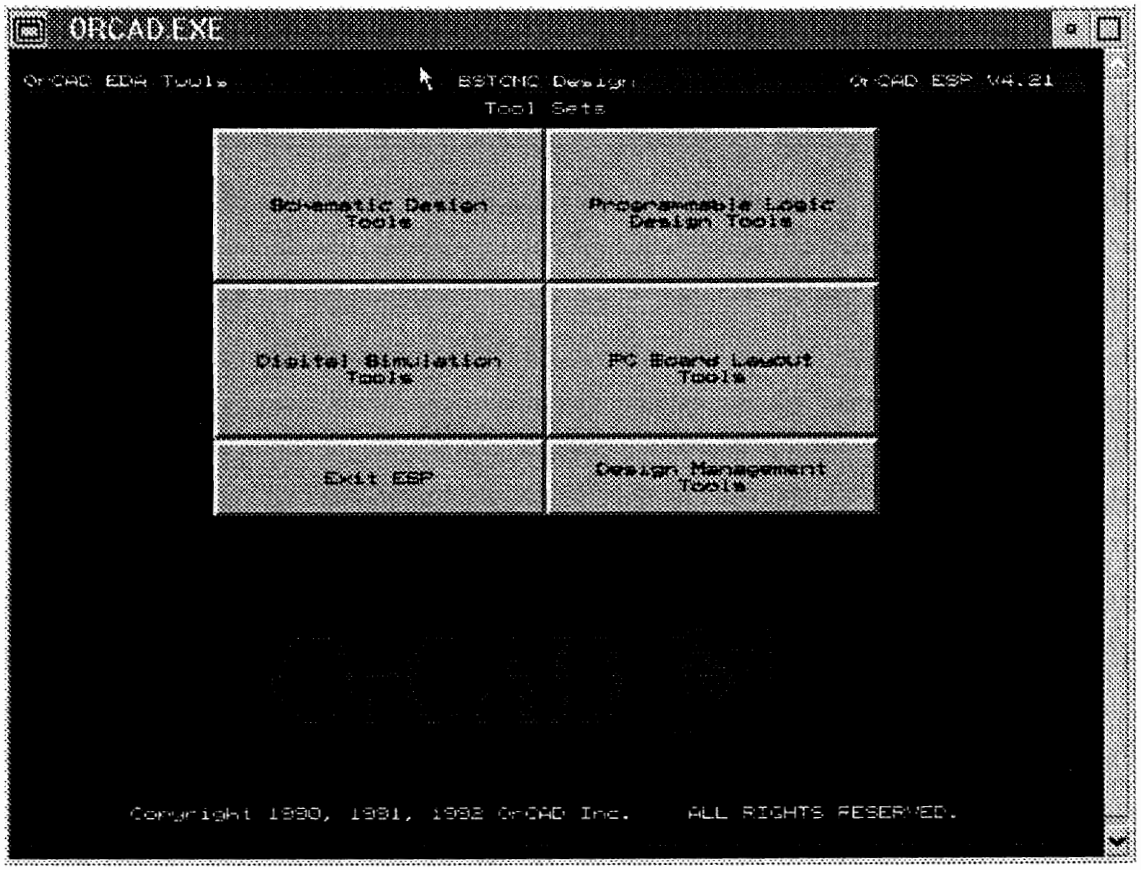

Figure F-1. ORCAD1

Once inside the 'Schematic Design Tools', several options are available. We won't go into a great amount of detail here since that is covered in the product manuals. The schematic is edited using the 'Draft' button. Once the schematic is complete, a netlist from the schematic is created using the 'Create Netlist' button.

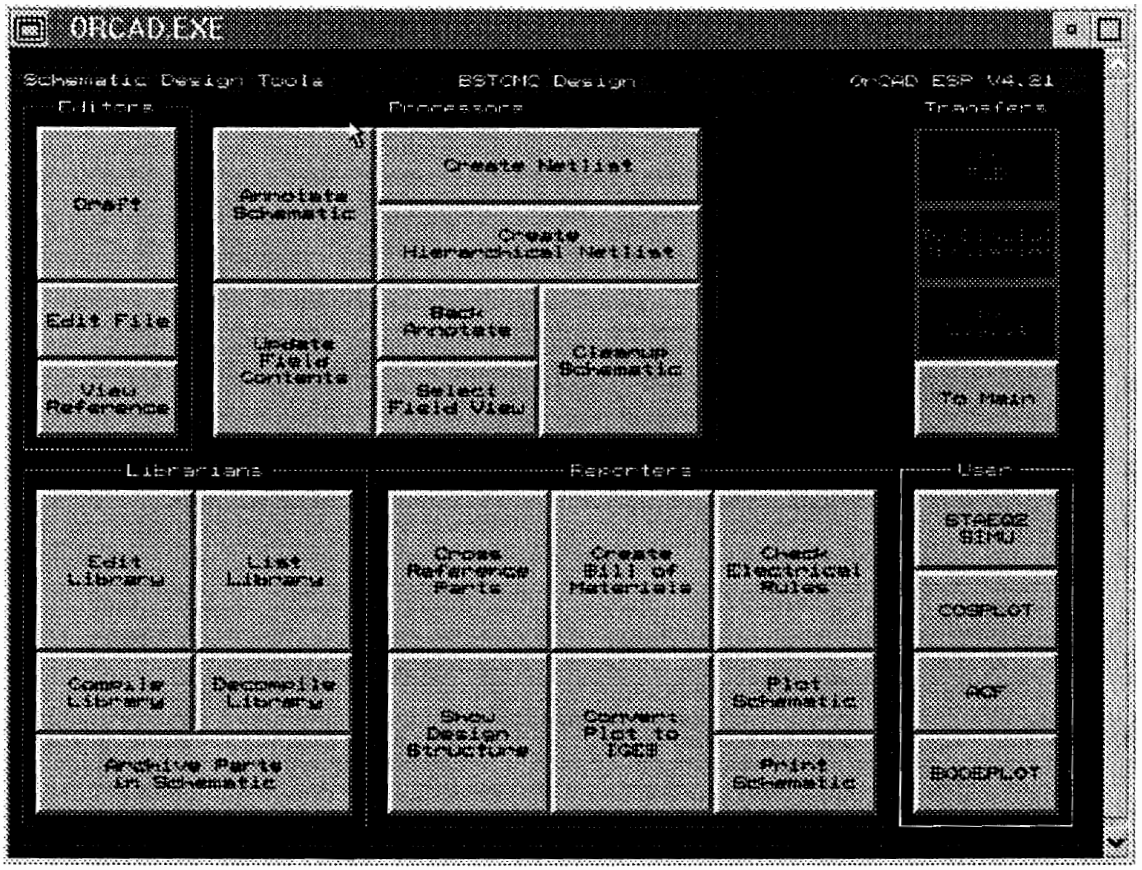

Figure F-2. Schematic Design Tools Menu

Once the netlist has been generated, the STAEQ2 and SIMU programs may be executed by clicking on the STAEQ2/SIMU User button in the lower right side of the screen of Figure F-2. This will swap out the ORCAD program and execute first the STAEQ2 program, then the SIMU program, and then swap back in the ORCAD program. The COSPLOT graphical plotting program may also be executed here.

A screen from STAEQ2 and SIMU is shown in Figure F-3.

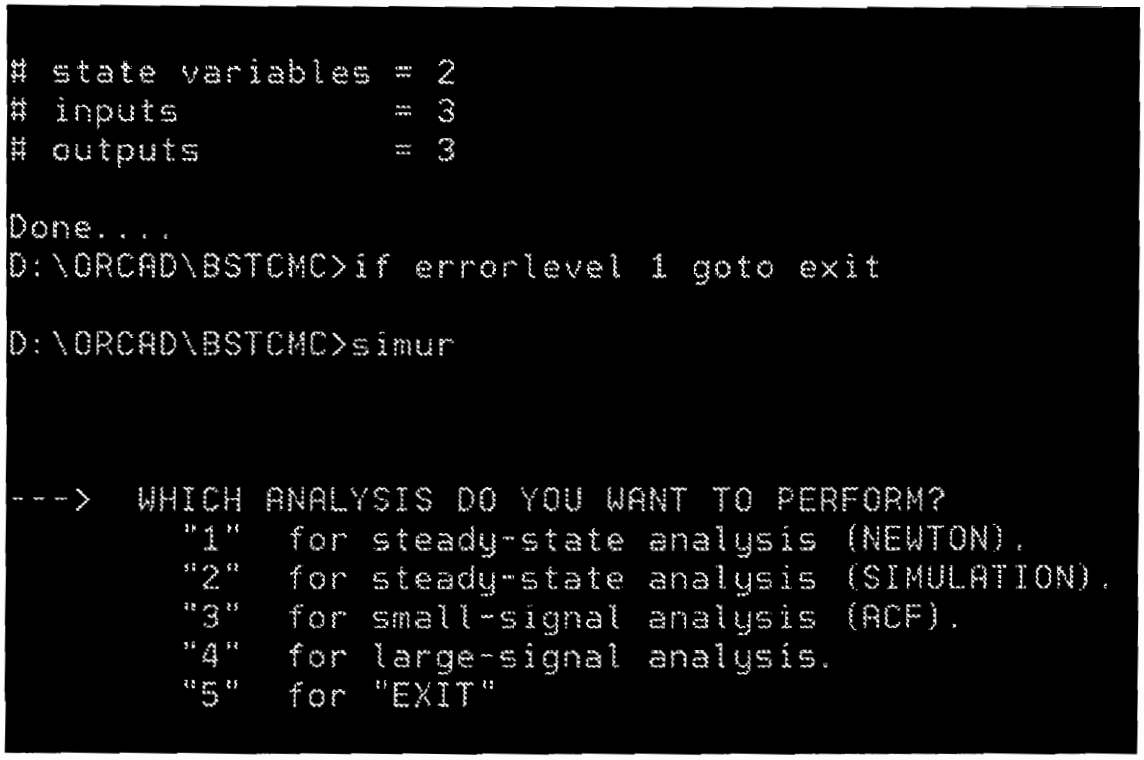

Figure F-3. ORCAD3

Once SIMU has been used to solve for the steady-state, the ACF program may be executed by clicking on 'ACF' from Figure F-2. The output of ACF may be displayed using the BODEPLOT program.

References

[1] C. Hsiao, R. B. Ridley, H. Naitoh, and F. C. Lee, "Circuit-Oriented Discrete-Time Modeling and Simulation for Switching Converters," *IEEE Power Electronics Specialists Conference Record*, 1987.

[2] L. W. Nagel, *SPICE2: A Computer Program to Simulate Semiconductor Circuits.*, PhD thesis, University of California, Berkeley, California, 1975.

[3] Borland, Turbo Pascal Version 6.0 Users' Guide, 1993.

[4] F. C. Lee, Ralph P. Iwens, Yuan Yu, and James E. Triner, "Generalized Computer-Aided Discrete Time-Domain Modeling and Analysis of DC-DC Converters," *IEEE Transactions on Industrial Electronics and Control Instrumentation*, vol. IECI-26, no. 2, pp. 58-69, May 1979.

[5] R. D. Middlebrook, "Input Filter Considerations in Design and Application of Switching Regulators," *IEEE Industry Applications Society Annual Meeting*, pp. 366-382, 1976.

[6] A. Brown and R. D. Middlebrook, "Sampled-Data Modeling of Switching Regulators," *IEEE Power Electronics Specialists Conference Record*, 1981.

[7] OrCAD, ORCAD Schematic Design Tools Reference Guide, 1991.

[8] Microsim, PSPICE User's Guide, 1993.

[9] Jacob Millman and Christos C. Halkias, *Integrated Electronics: Analog and Digital Circuits and Systems*, New York, New York: McGraw-Hill Book Company, 1972.

[10] R. D. Middlebrook and S. Cuk, "A General Unified Approach to Modelling Switching-Converter Power Stages," *IEEE Power Electronics Specialists Conference Record*, 1976.

[11] Arthur R. Brown, *Topics in the Analysis, Measurement, and Design of High-Performance Switching Regulators*, PhD thesis, California Institute of Technology, 1981.

[12] Raymond B. Ridley, *A New Small-Signal Model for Current-Mode Control*, PhD thesis, Virginia Polytechnic Institute and State University, 1990.

[13] S. Cuk and R. D. Middlebrook, "A General Unified Approach to Modelling Switching DC-to-DC Converters in Discontinuous Conduction Mode," *IEEE Power Electronics Specialists Conference Record*, 1977.

[14] V. Vorpérian, "Simplified Analysis of PWM converters Using Model of PWM Switch, Part 1: Discontinuous Conduction Mode," *IEEE Transactions on Aerospace and Electronic Systems*, vol. 26, no. 3, May 1990.

[15] George C. Verghese, Carlos A. Bruzos, and Krishna N. Mahabir, "Averaged and Sampled-Data Models for Current Mode Control: A Reexamination," *IEEE Power Electronics Specialists Conference*, pp. 484-491, 1989.

[16] B. Y. Lau and R. D. Middlebrook, "Small-Signal Frequency Response Theory for Piecewise-Constant Two-Switched-Network DC-to-DC Converter Systems," *IEEE Power Electronics Specialists Conference Record*, 1986.

[17] Billy Lau, "Computer-Aided Design of a DC-DC Switching Converter," *IEEE APEC Conference Proceedings*, pp. 619-628, 1990.

[18] D. J. Shortt and F. C. Lee, "An Improved Switching Converter Model Using Discrete and Average Techniques," *IEEE Transactions on Aerospace and Electronic Systems*, 1983.

[19] D. J. Shortt and F. C. Lee, "Extensions of the Discrete-Average Models for Converter Power Stages," *IEEE Transactions on Aerospace and Electronic Systems*, vol. AES-20, no. 3, pp. 279-289, May 1984.

[20] W. J. Petrowsky and J. O. Groves, Switch-Mode Power Supply Stability, IBM, Technical Report TR 08.219, 1985.

[21] P. T. Krein, J. Bentsman, R. M. Bass, and B. C. Lesieutre, "On the Use of Averaging for the Analysis of Power Electronic Systems," *IEEE Power Electronics Specialists Conference*, pp. 463-467, 1989.

[22] Arthur F. Witulski and Robert W. Erickson, "Extension of State Space Averaging to Resonant Switches - and Beyond," *IEEE Power Electronics Specialists Conference Record*, pp. 476-483, 1989.

[23] Jian Sun and Horst Grotstollen, "Averaged Modelling of Switching Power Converters: Reformulation and Theoretical Basis," *IEEE Power Electronics Specialists Conference*, 1992.

[24] Seth R. Sanders, Mark Noworolski, Xiaojun Z. Liu, and George C. Verghese, "Generalized Averaging Method for Power Conversion Circuits," *IEEE Transactions on Power Electronics*, vol. 6, no. 2, April 1991.

[25] Eric X. Yang, Fred C. Lee, and Milan M. Jovanovic, "Small-Signal Modeling of LCC Resonant Converter," *IEEE Power Electronics Specialists Conference*, 1992.

[26] V. Vorpérian, "Simplified Analysis of PWM converters Using Model of PWM Switch, Part 1: Continuous Conduction Mode," *IEEE Transactions on Aerospace and Electronic Systems*, vol. 26, no. 3, May 1990.

[27] V. Vorpérian, "Analysis of Current-Mode Controlled PWM Converters Using the Model of the Current-Controlled PWM Switch," *PCIM 1990 Proceedings*, pp. 183-195, October 1990.

[28] Richard Tymerski, "Frequency Analysis of Time-Interval-Modulated Switched Networks," *IEEE Power Electronics Specialists Conference Record*, 1990.

[29] J. O. Groves, "Small Small Signal Analysis of Systems With Periodic Operating Trajectories," *IBM Power ITL*, 1988.

[30] J. O. Groves and F. C. Lee, "Small Small Signal Analysis of Systems With Periodic Operating Trajectories," *VPEC PES Proceedings*, 1988.

[31] Kenneth S. Kundert and Alberto Sangiovanni-Vincentelli, "Simulation of Nonlinear Circuits in the Frequency Domain," *IEEE Transactions on Computer-Aided Design*, vol. CAD-5, no. 4, October 1986.

[32] John A. Aseltine, *Transform Method in Linear System Analysis*, New York, New York: McGraw-Hill Book Company, 1958.

[33] Rowan Gilmore, "Nonlinear Circuit Design Using the Modified Harmonic Balance Algorithm," *IEEE Transactions on Microwave Theory and Techniques*, vol. MTT-34, no. 12, December 1986.

[34] Rowan J. Gilmore and Michael B. Steer, "Nonlinear Circuit Analysis Using the Method of Harmonic Balance - A Review of the Art. I. Introductory Concepts," *International Journal of Microwave and Millimeter-Wave Computer-Aided Engineering*, vol. 1, no. 1, pp. 22-37, January 1991.

[35] John W. Bandler, Qi-Jun Zhang, and Radoslaw M. Biernacki, "A Unified Theory for Frequency-Domain Simulation and Sensitivity Analysis of Linear and Nonlinear Circuits," *IEEE Transactions on Microwave Theory and Techniques*, vol. 36, no. 12, December 1988.

[36] John C. Amazigo and Lester A. Rubenfeld, *Advanced Calculus*, New York, New York: John Wiley and Sons, Inc., p. 156, 1980.

[37] Richard Tymerski, "Application of the Time Varying Transfer Function Approach for Exact Small-Signal Analysis," *IEEE Power Electronics Specialists Conference Record*, 1991.

[38] Eric X. Yang, *Extended Describing Function Method for Small-Signal Modeling of Resonant and Multi-Resonant Converters*, PhD thesis, Virginia Polytechnic Institute and State University, Blacksburg, Virginia, 1994.

[39] R. W. Jensen and M. D. Lieberman, *IBM Electronic Circuit Analysis Program*, New York, New York: McGraw-Hill Book Company, 1968.

[40] C. Ho, A. E. Ruehli, and P. A. Brennan, "The Modified Nodal Approach to Network Analysis," *IEEE Transactions on Circuits and Systems*, vol. CAS-22, no. 6, June 1975.

[41] W. T. Weeks, A. J. Jimenez, G. W. Mahoney, D. Mehta, H. H. Qassemzadeh, and T. R. Scott, "Algorithms for ASTAP - A Network-Analysis Program," *IEEE Transactions on Circuit Theory*, vol. CT-20, November 1973.

[42] J. C. Bowers and S. R. Sedore, *SCEPTRE: A Computer Program for Circuit and System Analysis*, Englewood Cliffs, New Jersey: Prentice-Hall, Inc., 1971.

[43] Leon O. Chua and Pen-Min Lin, *Computer-Aided Analysis of Electronic Circuits*, Englewood Cliffs, New Jersey: Prentice-Hall, Inc., 1975.

[44] Norman Balabanian and Theodore A. Bickart, *Linear Network Theory*, Chesterland, Ohio: Matrix Publishers. Inc., 1981.

Vita

The author was born in Nashville, Tennessee on November 20, 1956. Upon graduation from Greenhills High School at Greenhills, Ohio in 1974, the author enrolled in a five year Electrical Engineering program at the University of Cincinnati. Before graduation from UC the author became a member of Eta Kappa Nu, an Electrical Engineering honorary society. While a student at UC the author worked at a co-op assignment at Cincinnati Electronics designing analog integrated circuits. He graduated Cum Laude with a Bachelor of Science degree in Electrical Engineering in June, 1979.

The author joined the International Business Machines Corporation in Lexington, Kentucky in June, 1979. Since that time, he has worked in the Power Products and analog special circuit technology groups at IBM Lexington, and in the IBM Power Systems group at Endicott, New York. He now works for Celestica Corporation, a subsidiary of IBM, in Endicott, New York.

He has two patents in the area of Power Factor Correction and analog IC design, as well as having several articles published in the IBM Technical Disclosure Bulletin. Jim received a Master of Science degree in Electrical Engineering at the University of Kentucky in December of 1986.